Comprehensive Understanding of Archeological Magnetism and Instrumentaion | 2013-10

University of Arkansas

National Park Service
U.S. Department of the Interior

National Center for Preservation Technology and Training

Grant Number: MT-2210-11-NC-13

COMPREHENSIVE UNDERSTANDING OF ARCHAEOLOGICAL MAGNETISM AND INSTRUMENTATION

University of Arkansas

Principal Investigator:
Kenneth L. Kvamme, Professor

Project Team:
Adam S. Wiewel, Doctoral Candidate

Authored by: Kenneth L. Kvamme and Adam S. Wiewel

Department of Anthropology & Archeo-Imaging Lab
Old Main 330
University of Arkansas
Fayetteville, AR 72701 USA
479-575-4130
kkvamme@uark.edu; awiewel@email.uark.edu

September 23, 2013

TABLE OF CONTENTS

page

LIST OF FIGURES…… iv
LIST OF TABLES…… v
EXECUTIVE SUMMARY…… vi

CHAPTER 1: BACKGROUND MATERIAL: ARCHAEOLOGICAL MAGNETISM, RESEARCH QUESTIONS, STUDY SITES, AND INSTRUMENTATION…… 1
- **MAGNETISM AND ARCHAEOLOGY**…… 1
- **STRUCTURE OF REPORT**…… 4
- **THE SITES**…… 5
  - **Fort Clark State Historic Site**…… 5
  - **Double Ditch State Historic Site**…… 6
- **INSTRUMENTATION**…… 7
  - **Single-coil Devices for MS**…… 7
    - *Bartington MS2 with "D" sensor*…… 8
    - *Bartington MS2 with "F" sensor*…… 8
    - *Bartington MS2 with "H" sensor*…… 8
    - *Exploranium KT-P Kappameter*…… 10
  - **Twin-coil Devices for MS**…… 10
    - *Geonics, Ltd, EM38B*…… 10
  - **Magnetic Gradiometry**…… 11
    - *Bartington Grad 601 Dual Fluxgate Magnetic Gradiometer*…… 11
    - *Geoscan Research FM-36 Fluxgate Magnetic Gradiometer*…… 11
- **GIS AND DATA PROCESSING**…… 12
  - **Geographical Information Systems**…… 12
  - **Image processing**…… 12

CHAPTER 2: ACCURACY AND UTILITY OF EMI DEVICES FOR MS MAPPING. 13
- **SURVEY AREAS**…… 13
  - **Area A**…… 14
  - **Area B**…… 14
  - **Area C** …… 14
  - **Area D**…… 14
- **RESULTS: SURVEY AREAS A-C**…… 15
  - **Survey Area A**…… 15
  - **Survey Area B**…… 18
  - **Survey Area C**…… 22
- **REPEATABILITY STUDIES**…… 24
  - **Variations in Repeat Surveys: Geonics EM38B**…… 24
  - **Vegetation Effects: Bartington MS2D**…… 26
- **DISCUSSION AND EVALUATION**…… 28
  - **Data Quality**…… 28
  - **Data Comparability**…… 28
  - **Cost**…… 29
  - **Speed**…… 29

Area……..... 29
Depth……...…….. 30
Data Processing…… 30

CHAPTER 3: UNDERSTANDING MAGNETIC ANOMALY FORMATION…… 31
PRIOR RESEARCH…… 31
ARCHAEOLOGICAL SETTING…….. 34
RE-EXCAVATION……. 35
INSTRUMENTATION……... 36
FIELD METHODS…….. 36
RESULTS……..... 38
Profile A: Subterranean Storage Pit…….. 38
Initial down-hole MS investigation…… 39
Photo-mosaic and profile……... 39
The MS measurements……... 40
Sensor differences…….. 41
Comparison with down-hole results…….. 43
Magnetic gradiometry…… 43
Modeling maximum pit magnetism…… 44
Modeling pit magnetism two-dimensionally…….. 46
Profile B: Fortification Ditch…….. 49
Photo-mosaic and profile……... 50
The MS measurements……... 50
Sensor differences…….. 52
Modeling ditch magnetism two-dimensionally…….. 53
Magnetic gradiometry…… 54
Profile C: House floor…….. 55
Photo-mosaic and profile……... 55
The MS measurements……... 57
Sensor differences…….. 57
Magnetic susceptibility and magnetic gradiometry……... 58
CONCLUSIONS…….. 58

CHAPTER 4: IDENTIFICATION OF REMANENT ANOMALIES…… 60
METHODS……... 60
SURVEY AREAS AND DATA……... 61
Survey Area A…….. 61
Survey Area B …….. 62
Survey Area C ……. 62
Survey Area D…….. 62
RESULTS……. 63
Survey Area A: Shallow Arikara Earthlodge on Village Periphery……... 63
Survey Area B: Buried Mandan Lodge in Village Core……... 68
Survey Area C: Shallow Arikara Log Cabin……. 69
Survey Area D: Double Ditch Village Core……... 72
DISCUSSION……... 76

CHAPTER 5: MAGNETIC VARIATIONS IN HUNTER-GATHERER CAMPS…….. 78
BACKGROUND INFORMATION…… 80
SURVEY AREAS……. 81
Survey A…… 81
Survey B…… 81
Survey C…… 81
Survey D…… 81
Survey E…… 82
RESULTS……. 82
Surveys A and B: Linear MS Transects with Bartington MS2D…… 82
Survey C: Magnetic Gradiometry Transect…….. 84
Survey D: Linear MS Transect with Geonics EM38B…….. 87
Survey E: MS Survey with Geonics EM38B in 30 x 60 m Area…….. 88
DISCUSSION……... 89

CHAPTER 6: CONCLUDING SUMMARY……. 91

ACKNOWLEDGEMENTS……. 92
REFERENCES CITED……... 93

LIST OF FIGURES

page
Figure 1.1. *Instrumentation used in the project*…… 9
Figure 2.1. *Map of Fort Clark showing the locations of MS survey areas*……... 15
Figure 2.2. *MS survey results from an Arikara earthlodge at Fort Clark*…… 16
Figure 2.3. *Scatterplot of MS data yielded by the Bartington MS2D and Geonics EM38B*…. 17
Figure 2.4. *Plots of MS data along four transects*…… 19
Figure 2.5. *MS survey results of a deeply buried earthlodge*…… 20
Figure 2.6. *Scatterplot of MS data yielded by the Bartington MS2D and Geonics EM38B*…. 21
Figure 2.7. *Plots of MS data produced along three transects*……... 22
Figure 2.8. *MS survey results of an earthlodge near the village core*…….. 23
Figure 2.9. *Scatterplot of MS data yielded by the Bartington MS2D and Geonics EM38B*…. 24
Figure 2.10. *EM38B survey results for two areas collected in consecutive years*…… 25
Figure 2.11. *Scatterplot of MS data yielded by the Geonics EM38B in consecutive years*….. 26
Figure 2.12. *MS2D survey results of a 60 x 30 m area near the village plaza*……. 27
Figure 3.1. *Down-hole MS2H survey at Double Ditch*……. 33
Figure 3.2. *Plan of the Double Ditch site showing topography and MG anomalies*…… 35
Figure 3.4. *Field methods for recording MS at Double Ditch*…….. 37
Figure 3.5. *Results of data recording in the subterranean storage pit*……. 38
Figure 3.6. *Storage pit excavation data from 2004*…….. 39
Figure 3.7. *Storage pit profile on east wall excavation*…… 40
Figure 3.8. *MS measurements in the storage pit*……... 41
Figure 3.9. *Graphical data for the MS instrumentation*…… 42
Figure 3.10. *Comparison of two repeated down-hole MS2H profiles*…….. 43
Figure 3.11. *Magnetic gradiometry in vicinity of storage pit*……... 44
Figure 3.12. *Storage pit MS and models*……... 45

Figure 3.13. *Two-dimensional magnetic model by raster GIS*…….. 48
Figure 3.14. *Excavation profile through Ditch 4 showing observed stratigraphy*…… 51
Figure 3.15. *MS mappings of the ditch profile*…….. 52
Figure 3.16. *Scatterplots showing MS response relationships*……. 53
Figure 3.17. *Simple model of two ditch units*…… 54
Figure 3.18. *MG data and mathematically modeled anomaly*…….. 55
Figure 3.19. *Profiles of the house floor excavation*…….. 56
Figure 3.20. *MS mappings and related data of the house excavation profile*……... 57
Figure 3.21. *MG data showing the entire house with the locus of the 2004 excavation*……... 58
Figure 4.1. *Map of Fort Clark showing locations of magnetic gradiometry and MS surveys*.. 62
Figure 4.2. *Shaded digital elevation model of the Double Ditch site*……... 63
Figure 4.3. *Magnetic survey results of a shallow Arikara lodge*…….. 64
Figure 4.4. *Scatterplot illustrating the relationship between MS (EM38B) and MG data*…... 65
Figure 4.5. *Scatterplot showing the relationship between MS (MS2) and MG data*…… 66
Figure 4.6. *Magnetic survey results at the shallow Arikara lodge*……... 67
Figure 4.7. *Scatterplot showing the relationship between MS (EM38B) and MG*…… 68
Figure 4.8. *Magnetic survey results of an earthlodge in area "B"*…….. 69
Figure 4.9. *Magnetic survey results in the vicinity of the Arikara cabin in area "C"*……. 70
Figure 4.10. *Large hearth from an earthlodge underlying the late Arikara log cabin*……. 71
Figure 4.11. *Scatterplot showing the relationship between MS (EM38B) and MG data*…….. 71
Figure 4.12. *The Double Ditch survey area*…….. 73
Figure 4.13. *Scatterplot showing the relationship between MS (EM38B) and MG data*…….. 74
Figure 4.14. *Results of the regression at Double Ditch*…… 75
Figure 4.15. *Data from a single earthlodge at Double Ditch*……... 76
Figure 4.16. *Examples of variations in survey locations at Double Ditch*……... 77
Figure 5.1. *Map of the Fort Clark State Historic Site*……... 79
Figure 5.2. *MS transect data collected by the Bartington MS2D*……. 83
Figure 5.3. *Magnetic gradiometry data along N-S transect*……. 85
Figure 5.4. *Close-up details of the magnetic gradiometry data*…… 86
Figure 5.5. *MS data collected by the Geonics EM38B*…….. 87
Figure 5.6. *MS and magnetic gradiometry*…… 89

LIST OF TABLES

page

Table 3.1. *Descriptive statistics for the raw MS pit measurements*…….. 42
Table 3.2. *Data for storage pit Model 1 based on sphere*……. 45
Table 3.3. *Data for layered storage pit Model 2*……... 46
Table 3.4. *Descriptive statistics for the raw MS ditch measurements*…….. 53

EXECUTIVE SUMMARY

This work attempts to better understand archaeological magnetism, its causes, and how it may be measured to improve interpretations of the magnetic record and the cultural past. It examines four research foci using data gathered at the Double Ditch and Fort Clark State Historic Sites, in North Dakota, and a variety of instruments.

(1) The utility of a twin coil device, the Geonics Ltd. EM38B, is examined for recording magnetic susceptibility (MS), the ability of a material to be magnetized, because these instruments have not been greatly used for this purpose. Results are compared against a well understood single coil instrument, the Bartington MS2D. A variety of archaeological features were surveyed by both instruments, permitting visual and quantitative comparisons of the mapped results. The EM38B parallels or surpasses the MS2D data in quality, and its greater speed of survey and depth penetration often make it preferable as a field instrument.

(2) How subsurface magnetism forms anomalies recorded by magnetometry on the surface is not well understood. Three former excavations were re-opened at Double Ditch that bisect common archaeological features (a storage pit, fortification ditch, and house floor). Magnetic stratigraphy was measured on the exposed profiles with three MS meters: the Exploranium KT-9, the Bartington MS2F, and the MS2D. Mathematical models of the measurements were then compared to the shapes of anomalies recorded at the surface by magnetometry that demonstrate how these surface anomalies are formed.

(3) Anomalies revealed by magnetometry are generally of two types, thermoremanent and induced. The former arise by intense burning, while the latter result from materials of high MS. Both look the same to a magnetometer, which measures the sum of all magnetism. Distinguishing hearths (thermoremanent) from storage pits (induced) is critical to interpretation, but difficult because both generate circular of similar sizes and magnitudes. Magnetometry surveys are used to measure total magnetism followed by MS surveys that measure only induced magnetism. A statistical technique, regression, removes the common correlation between the data sets, exposing the remainder which point to thermoremanent anomalies comprised mainly of hearths.

(4) The presence of such nomadic groups as the Dakota and Crow is well-documented at Fort Clark, yet magnetic surveys have seldom been carried out in hunting-gathering camps. A variety of surveys reveal enhanced MS and magnetic anomalies in areas known to have been occupied by these groups that point to areas of cooking, fire building, food processing, and the accumulation of refuse.

CHAPTER 1: BACKGROUND MATERIAL: ARCHAEOLOGICAL MAGNETISM, RESEARCH QUESTIONS, STUDY SITES, AND INSTRUMENTATION

Magnetic variations in subsurface deposits have been termed "nature's gift to archaeology," because they reflect many anthropogenic activities undertaken in the past (Kvamme 2006a). Consequently, magnetometry surveys have been conducted in hundreds of archaeological sites in the United States because many human activities greatly impact near-surface magnetism. Yet, although great strides have been made in the understanding of archaeological magnetism (Scollar 1990; Kvamme 2006a; Aspinall et al. 2008), there is much that remains not completely understood. Moreover, new instruments for measuring magnetism in the field as well as new field methods constantly arise. This project came about from the need to address a general lack of knowledge, and indeed frustration, in both of these areas: (1) the understanding of archaeological magnetism and (2) abilities of current instrumentation used for the field recording of magnetic properties. Four distinct research foci were developed to address these concerns, and each is explained in a separate chapter of this report.

MAGNETISM AND ARCHAEOLOGY

The detection and mapping of magnetic variations in soils and sediments has proven to be one of the most productive means available for archaeological prospecting. Numerous natural and cultural processes combine to generate magnetic changes that can be recorded by an array of instruments to reveal evidence of past human activities. Magnetic variations are caused by two broad classes of magnetism. One is *induced* magnetism and the other is *remanent* magnetism. The former arises from local variations in soils, sediments, rocks, and other materials that vary in their magnetic susceptibility (MS). MS refers to the ability of a material to be magnetized when subjected to an external magnetic field, such as the Earth's. It is simply the ratio of the magnetism induced in the material to the strength of the magnetizing field. MS varies in soils, sediments, and rocks owing to a large number of factors. Primary among these are iron minerals that are ubiquitous within most soils and sediments and their types, amounts, and densities vary (Linford 2006). Aspinall et al. (2008:24-25) relate several factors that affect soil MS. One, often referred to as the "La Borgne effect," occurs with even moderate heating of the soil through firing, human or natural, creates a reducing atmosphere which causes the iron compound hematite to change to the more magnetic form of magnetite. Later re-oxidization causes magnetite to change to maghemite, also highly magnetic. Human occupation also enhances MS through the introduction of organic waste (e.g., in middens and elsewhere), which promotes bacterial growth, where the bacteria create reducing or oxidizing conditions that lead to magnetic enhancement. Moreover, some bacteria actually crystallize magnetite within their bodies from iron oxides within the soil. Human occupancy further enhances MS in settlement soils through the introduction of magnetic materials such as broken ceramics and bricks (where both were once subjected to heating) or even iron artifacts. Finally, processes of soil formation or pedogenesis enhance MS through the formation of magnetic compounds in the absence of microorganisms. This phenomenon tends to make topsoil exhibit much higher MS than subsoil.

Remanent magnetism, the other broad class, refers to permanent magnetism, which remains in a material even when it is removed from a magnetizing field. While several processes are responsible for remanent magnetism, thermoremanence is of predominant interest in

archaeology because it is caused by intense heating, and many cultural practices cause thermoremanence from cooking fires, to permanent hearths, kilns, or the burning of a structure.

A magnetometer is a device that records variations in the magnetic field caused by local changes in magnetic properties stemming from MS differences in deposits or loci exhibiting remanent magnetism. These changes are referred to as "anomalies" until their sources can be deduced or validated through excavation. Deduction of anomaly causes arise through recognition of patterns in anomaly shapes (e.g., a rectangular anomaly of a certain size may point to the outlines of a buried structure with burned walls) or through knowledge of magnetic theory with respect to local environmental conditions and the form and magnitude the measurements take (Kvamme 2008a).

Most anomalies are generated by magnetism induced from the Earth's magnetic field, and a variety of cultural practices create features in the archaeological record that combine to produce anomalies detectable by a magnetometer, beyond those responsible for MS differences within deposits, described above. These rarely receive emphasis, but include excavations within topsoil, which means that generally higher MS material is *removed*, leading to a lowering of the local magnetic field or a *negative* anomaly. Unfilled ditches, pits, and cellars are common constructions that exhibit negative anomalies. Related are positive magnetic anomalies caused by the mounding of topsoil, be it as spoil next to ditches or pits, mound constructions, or erosion from sod-covered houses. These circumstances, of course, simply increased the volume of high MS material beneath a magnetometer creating *positive* anomalies. People also *import* materials for constructions, whether stone for building or sands, gravel, and clay for floors or roads, and these materials all possess their own levels of MS that add to or detract from the local magnetic field. Finally, while implied as a general cause of increased MS by Aspinall et al. (2008), people build fires for all kinds of purposes in hearths and kilns, and fires occur accidentally or intentionally through warfare. Individually, each fired place will increase MS locally, and if hot enough (beyond the Curie point of about 600° C for many earth materials) will generate thermoremanent anomalies. As the occupancy of a settlement continues, this magnetically enriched material will become dispersed through subsequent constructions or through simple acts of hearth cleaning, which further exacerbates the level of magnetic enrichment in settlement soils (Kvamme 2006a).

Magnetometry surveys today are typically carried out by magnetic gradiometers, which record the *difference* between two sensors separated by a constant vertical distance. The bottom sensor is more sensitive to magnetic changes in near-surface deposits than the top sensor because magnetic field strength falls off with the cube of distance. The top sensor, on the other hand, is more sensitive to constant variations in the Earth’s magnetic field. Differencing the two measurements therefore removes changes in the Earth’s field, leaving what is known as a magnetic gradient measurement. Magnetic gradiometry surveys are extremely fast and efficient, with surveys commonly covering *hectares* per day at sampling densities of 16 measurements per square meter. They have become the workhorse of archaeological geophysics due to this speed, sampling density, and the many magnetic variations they record (Kvamme 2006a). Magnetic field strength is measured in *nanoteslas* (nT, 10^{-9} Tesla, about one part in a half-million of the Earth's magnetic field), and many archaeological anomalies range between 2-20 nT. The exception occurs when iron artifacts lie in the near-surface, because they can generate anomalies of extreme magnitude of many tens to thousands of nT depending on their mass, shape, orientation, and depth below sensors. These robust anomalies are typically *dipolar* in form,

exhibiting closely-spaced positive and negative poles, much like a common bar magnet (Kvamme 2006a).

To magnetometers (or gradiometers), all sources of magnetism look the same, whether induced or remanent. This circumstance often makes interpretation difficult because some anomalies, with similar measurements and which look the same spatially, are generated by very different processes. In the Northern Great Plains, for example, a storage pit (bell-shaped in cross-section, 1.5-2 m deep, with a 1 m diameter orifice) filled and sealed with magnetically enriched settlement soil, will generally yield a positive circular anomaly 1-3 m in diameter. Likewise, a typical auxiliary hearth within a house will yield an anomaly with similar measurements that often looks much the same (statistically, hearth-generated anomalies tend to be larger in magnitude than storage pit-generated anomalies, but there is great variation; Bales and Kvamme 2005). It therefore behooves us to better understand archaeological magnetism, its causes, and how we may measure and explore it in the field in order that we may improve our interpretations not only of the magnetic record, but of our cultural past. These are the underlying purposes of this project.

Unlike magnetometers, MS surveys undertaken with MS meters measure only the *induced* portion of the magnetic signal (in Chapter 4 we make use of this to identify thermoremanent anomalies). Moreover, an MS survey can detect subtle changes in near-surface MS, such as a thin sheet of high MS resulting from the introduction of organic or fired materials caused by a human occupation. This is untrue of a magnetometer, where it is impossible to detect a thin continuous layer which lacks sufficient thickness for a dipole contrast to develop (Clark 2000:101). (We explore this property in Chapter 5 looking for ephemeral evidence of hunter-gatherer occupations.) MS may is quantified in two ways, as a susceptibility per unit volume (κ) or as a mass normalized susceptibility (χ). In this report we are concerned only with the former, which is expressed as a ratio of induced magnetism to that of an inducing magnetic field (Dalan 2006a). In the International System of units (SI), this measurement is dimensionless and typically a small number times 10^{-4}.

Yet, MS meters, which occur in two types, possess severe limitations. Single-coil devices are greatly limited in their depth of penetration, with most instruments penetrating to depths of only 1-10 cm (we make use of this property in Chapter 3 by measuring MS in excavation profiles to better understand how subsurface MS generates anomalies recorded on the surface by a magnetometer). They are also extremely slow to use in the field requiring much time for a single measurement (a half-minute to a minute), making large-area surveys impractical. Surveys that do examine large areas generally do so with extremely coarse sampling intervals on the order of 10 m between sampling points (Payne 1996). Such data, of course, are useful for indicating broad areas of enhanced MS within settlements, but no detail about specific archaeological features and their associated magnetism can be learned. One heroic effort to define King Lobengula's Palace in Zimbabwe managed to utilize a 1 m^2 sampling density in a 54,000 m^2 area, but this survey required many months spaced over several years (Gaffney et al. 2004).

Twin-coil instruments, on the other hand, yield measurements of MS to a depth of a half-meter, and they offer extremely rapid data collection, at rates similar to gradiometers. Many large-area surveys of MS have therefore been performed, including an entire historic Euroamerican village in Kansas (Kvamme 2006c) and much of the native Mandan-Arikara settlement at Fort Clark, North Dakota, which receives focus in this report (Wiewel and Kvamme 2013). Although depth penetration is not good with either MS recording technology, it has been shown that materials of high MS tend to migrate upward through the actions of plowing and

bioturbation through tree-throws, rodents and other burrowing animals, and insect actions, such as earthworms (Clark 2000:110-115). Thus, deeper archaeological deposits beyond the range of MS instrumentation may cause enhancements to overlying deposits that make them detectable.

Yet, MS results with twin-coil instruments have often been poor (Clay 2006) and it has been difficult to relate results to accurate measurements of MS (Dalan 2006a). Moreover, most applications of twin-coil instruments, generally in North America, have focused on *archaeological* indications and findings resulting from the surveys, *not* on an understanding of MS and its properties, which many single-coil studies have pursued (Dalan 2008). A few studies have made comparisons between single- and twin-coil results, but conclusions have been brief, theoretical, and have shown little beyond the fact that twin-coil instruments are faster, penetrate deeper, are less influenced by soil conductivity, and may generally be "preferable for field susceptibility measurements" (Benech and Marmet 1999:31; see also Cole et al. 1995). It is for this reason that in Chapter 2 we specifically investigate and compare, quantitatively, results obtained with single-coil and twin-coil instruments in surveys of identical areas.

STRUCTURE OF REPORT

This report is organized in five chapters. Chapter 2 begins with instrumentation by examining the utility of the two technologies for the field recording of near-surface MS. Twin-coil electromagnetic induction (EMI) devices, such as the EM38 by Geonics Ltd., permit acquisition of in-phase data proportionate to volume MS in the near-surface to a depth of about 50 cm. This rapid survey device permits coverage of very large areas in short spans of time, but with results that have been inconsistent or poor (Clay 2006) and with the difficulty of relating results to accurate measurements of MS obtained with single-coil instruments (Dalan 2006a). We attempt more rigorous examination. Accurate near-surface measurements of volume MS were acquired over contiguous areas at high sampling densities with a single-coil Bartington MS2D field sensor, a long-accepted standard for the field recording of near-surface MS (Dalan 2008), but an instrument that acquires data at a very slow rate and with a very limited penetration depth of less than 10 cm. Multiple surveys of areas and linear transects were undertaken with *both* instruments at the Fort Clark State Historic Site, in central North Dakota, which contains numerous Native and Euroamerican elements (see below), and statistical analyses and comparisons are made on both data sets to yield assessments of the performance of twin-coil EMI instruments in archaeological field contexts.

Chapter 3 attempts to achieve a better understanding of how the archaeological record forms magnetic anomalies that are commonly recorded in magnetometry surveys. It also examines the utility of several hand-held instruments for recording MS in the vertical dimension on bare-earth archaeological profiles or through down-hole sensing. In this study several excavations were made to expose sections, or profiles, across major archaeological feature types that occur in the Northern Great Plains (and elsewhere): a subterranean storage pit, a fortification ditch, and a house floor. To reduce project costs, previously excavated trenches across the feature types of interest were re-opened in the Double Ditch State Historic Site, in central North Dakota (see below for a site description; Kvamme and Ahler 2007). MS was recorded across the faces of the profiles every 5-10 cm (depending on the sizes of the profiles), and the resultant data were then compared against magnetometry findings previously recorded at the surface. Visual and quantitative comparisons, through mathematical modeling, are made to better realize how subsurface magnetic variations cumulate to generate magnetic anomalies recorded at the surface.

Chapter 4 investigates a radical approach to confront a common problem in the interpretation of magnetometry data resulting from large surveys. Anomalies in these surveys are often highly interpretable when they form regular shapes (e.g., circles, squares) that point to the loci of former houses, for example. Yet, thousands of anomalies in magnetometry do not give such clues. As noted earlier, many measure 1-3 meters in diameter with roughly circular shapes, and excavations reveal they are typically generated by two cultural processes. One is by hearths, which form thermoremanent anomalies, and the other occurs when a cache pit is abandoned and filled with magnetically enriched soils that cause induced anomalies. Both feature types look the same to a magnetometer and therefore make site interpretation difficult. Distinguishing between hearths and storage pits is critical to understanding site structure and organization in any region. In this study, carried out over a variety of house features at the Fort Clark and Double Ditch State Historic Sites, magnetometry and MS field surveys were conducted. As magnetometry quantifies the *sum* of remanent and induced magnetism while MS surveys are sensitive only to the latter, regression methods are employed where regression residuals are argued to show magnetic anomalies resulting primarily from remanent magnetism, generally hearths. The remainder point to induced anomalies that most often represent storage pits. Validation is offered because in many instances hearth versus storage pit locations are known or can be strongly assumed.

Chapter 5 presents the final case study which addresses yet another shortcoming in archeo-geophysics. It focuses on hunter-gatherer camps, something rarely undertaken owing to a general lack of subsurface architecture and other major ground disturbances that are the primary targets of geophysical surveys. Moreover, this study is designed to address a specific shortcoming in our knowledge of early Native interactions with fur trading centers in Northern Plains history, specifically at the historically well-documented Fort Clark State Historic Site (see Wood 1993). Historically, nomadic Dakota and Crow groups visited Fort Clark for purposes of trade. A likely camping spot was along nearby Chardon Creek, some distance away from the Mandan-Arikara village (the major historical feature in the park, see below), but within the current park boundary. Eye-witness accounts also relate nomadic camps much closer to the Mandan-Arikara village. These camps form a crucial aspect of the history of the site that is not well understood and archaeological investigation has been nearly absent. MS and magnetometry surveys were performed to locate hearths and anthropogenic enhancements to the soil from cooking fires, food waste, and other occupational activities. These results give a fuller idea of spatial and organizational aspects of the site's history.

THE SITES

Two archaeological sites were employed in this project to address the foregoing research questions. Both are located in central North Dakota, in prominent archaeological and historical state parks, and each hold a wide variety of archaeological features of relevance to the research.

Fort Clark State Historic Site

Fort Clark State Historic Site (32ME2) is located on the west bank of the Missouri River in central North Dakota, approximately 60 km northwest of present-day Bismarck. It contains the remains of two fur trading posts, Fort Clark (operated by the Upper Missouri Outfit [American Fur Company] between 1830-1860) and Fort Primeau (constructed by the St. Louis Fur Company in approximately 1846 and operated until 1861). It was also the location of a large

Mandan-Arikara earthlodge village. The village was constructed by the Mandan in 1822; the tribe occupied the village until 1837 when they were decimated by a smallpox outbreak. The following year the village was appropriated by the Arikara, who remained there until 1861. In the mid-nineteenth century, Fort Clark was a significant place in the Northern Plains for trade between various Native American groups and Euroamericans. Moreover, Fort Clark was visited by such notables as Prince Maximilian of Wied, artists George Catlin and Karl Bodmer, naturalist John James Audubon, and anthropologist Lewis Henry Morgan, who each left invaluable accounts or depictions of the site (Wood et al. 2011).

The site contains numerous cultural features with archaeological components. Primary among these is the village itself, with nearly a hundred earthlodge locations (a hemispherical structure covered with earth), as well as the footprints of several very late Euroamerican-style log cabins occupied by Native Arikara, the village plaza, a fortification ditch, and countless storage pits and hearths. A burial ground, two large pony corrals, borrow pits, and numerous trails are also associated with the village. The two fur-trading posts are large, and one is associated with an interpreter's earthlodge and garden space, a midden-dumping ground, cemetery, and perhaps outbuildings. Most of these features have been mapped by Wood (1993), who documented nearly 1,800 small surface depressions (i.e., collapsed storage pits and graves), 86 earthlodges, corrals, trails, borrows, and the two trading posts.

In 2000-2001, the Fort Clark Interpretation Project was established, a program involving the State Historical Society of North Dakota, PaleoCultural Research Group, the University of Arkansas' Archeo-Imaging Lab, and field schools from the University of Missouri-Columbia and University of Kansas. This two-year program involved geophysical surveys, microtopographic mapping, soil coring, and test excavations within the Mandan-Arikara village and both trading post areas (Ahler 2003; Hunt 2003). In 2000 Kvamme (2007) surveyed a 20 m wide transect across 400 m of the village area, using magnetic gradiometry, electrical resistance, electromagnetic induction, and ground-penetrating radar instruments. Although the surveys were limited in coverage, several findings were significant, including the identification of a buried and previously unknown circular earthlodge. Based on these results, Wiewel and Kvamme (2013) undertook more extensive investigations of the Mandan-Arikara village in 2011 and 2012. Magnetic gradiometry and electrical resistance surveys covered the greatest areas, approximately 12 and 7.9 ha, respectively. Smaller areas within the village core were surveyed by electromagnetic induction, magnetic susceptibility, and ground-penetrating radar. These data have been combined in a GIS along with aerial color and thermal infrared imagery, collected by Tommy Hailey in 2004 (Heller 2009), and airborne lidar, obtained in 2012. The overarching goals of these investigations were to document additional unknown structures and other features to gain a better understanding of the village's content and layout and to address questions related to this research project.

Double Ditch State Historic Site

Double Ditch village (32BL2) lies on a high terrace about 20 m above the Missouri River and 15 km north of Bismarck, North Dakota. It was one of several traditional Mandan settlements near the mouth of the Heart River that were occupied for many generations. The region was abandoned due to pressure from the Sioux after the devastating smallpox epidemic of AD 1781-82 (Bowers 1949:138-146). Double Ditch is one of the most impressive archaeological sites in the Great Plains owing to its large size (about 9 ha), many internal features, dynamic setting overlooking the river, and the fact that few other such settlements yet exist in a relatively

intact state owing to modern development, agricultural encroachment, and inundation by Missouri River reservoirs. Double Ditch contains numerous lodge depressions, tall mounds (up to 3 m) that mostly represent middens, and two prominent fortification ditches.

In 2001 the State Historical Society of North Dakota initiated a four-year project to upgrade public interpretation and education at several publicly owned sites, including Double Ditch. This program utilized state-of-the-art geophysical surveys and aerial remote sensing carried out by the University of Arkansas Archeo-Imaging Lab, combined with traditional excavation. The results of this work have been documented in a large series of reports, with geophysical and aerial remote sensing results summarized in Kvamme and Ahler (2007). At the time, Double Ditch represented the most intensively and extensively surveyed site by multiple remote sensing methods in the Americas. Magnetic gradiometry surveys of the entire village plus a significant surrounding area (11.6 ha) reveal countless subterranean food storage pits, hearths, large and small middens, trails, and *two previously unknown fortification ditch and bastion systems* (beyond those seen in the site's surface) that vastly increase the settlement's area. Electrical resistivity surveys of the village (9.3 ha) help define middens and other depositional areas, as well as the loci of houses (earthlodges) and earth-borrowing pits. EMI surveys of the village core offered insights into differences between induced and thermoremanent magnetic features. Ground-penetrating radar yielded details about ditch, house, and mounded midden interior forms. Aerial methods permitted thermal infrared imagery of the entire site and its environs that distinguished houses, borrow pits, and ditches from mounded middens and fill areas through temperature variations. The remote sensing program reduced excavation costs by targeting features of interest with high accuracy. Thirty-four excavations confirmed anomaly identifications and establish a chronology for the site that documents its late-fifteenth century origins (linked with outer Ditch 4) to its contraction in the eighteenth century (inside Ditch 1) and ultimate abandonment about AD 1782. The complete magnetic gradiometry survey of the entire village, the EMI survey of several houses within the village core, and the 34 excavations across a wide sample of archaeological features all contribute to the present study.

INSTRUMENTATION

A variety of geophysical devices were employed in this project. All measure archaeological magnetism in some way. Our great focus was on magnetic susceptibility and so several types of MS meters and sensors were investigated.

Single-coil Devices for MS

Several single-coil devices, popular in European archaeological investigations of MS, were utilized (Gaffney and Gater 2003; Dalan 2008). All of these instruments are subject to drift owing to temperature influences, so they first require an "air" reading. The sensor head is placed well away from the influence of magnetically susceptible material (i.e., in the air) and a "zeroing" key is pressed, which effectively zeros the instrument. Following this, a measurement is immediately made with the sensor in contact with a target. In general, two such reading cycles are made at each measurement station and the two measurements are averaged. This process, of course, is very slow, and for this reason surveys of large areas with these instruments require a great amount of time and are rarely undertaken except under very coarse sampling intervals. While digital storage is possible permitting measurements to be later downloaded, we recorded measurements on paper and later entered the information into a computer. This avoided the

necessity of a field computer, which we felt would not save time owing to the slowness of the data collection process. The exception to some of the forgoing occurs with the down-hole MS2H sensor, which requires a field computer and a variation on the zeroing process, described below. Data from the following single-coil MS devices were utilized.

Bartington MS2 with "D" sensor

The MS2 meter is a portable instrument for measuring MS with a variety of sensor heads, each designed for different tasks and settings (Figure 1.1a). The MS2 generates a low intensity alternating magnetic field in the sensor coil. Material within the influence range of this signal will change the frequency in proportion to its MS (Clark 2000:102). The MS2D sensor is circular and measures 185 mm in diameter. It is connected to a handle with an integrated electronics unit and an extension tube (Figure 1.1b). It is designed to read volume MS on a flat ground surface, such as lightly vegetated ground. Reliable readings demand firm and close contact with the surface. Uneven or undulating ground, or thick vegetation that introduces void space beneath the sensor head, lowers the accuracy of the readings. It is with this sensor that most of the surface work in MS was conducted. During fieldwork at Fort Clark, which contains many iron trade artifacts due to the two trading forts, extremely high measurements were regularly encountered during the surveys owing to proximity to these artifacts. At these locations alternative measurement loci were measured to obtain "clean" measurements of soil MS, unbiased by the presence of ferrous metals. This typically required moving the instrument only 10-15 cm to the left or right to obtain readings at "normal" levels.

Although it is not commonly employed for wall profiling, we nevertheless chose the MS2D sensor to investigate comparability with the other sensors in one of the wall profile studies of Chapter 3. Its depth response rapidly falls away to 50% at a distance of 15 mm and only 10% at 60 mm from a surface. This instrument requires calibration by a factor of 2.0 on rough surfaces and 1.333 on smooth surfaces (Bartington Industries 2013). Measurements are volume susceptibilities to a resolution of 10^{-5} SI.

Bartington MS2 with "F" sensor

The MS2F sensor is designed to read volume MS on a flat surface, such as a profile wall. Its sensor face measures only 15 mm in diameter which is connected to a handle with an integrated electronics unit and an extension tube (Figure 1.1c, d). Its depth response rapidly falls away to only 10% at a distance of 6 mm from the tip. Tip contact measurements must be calibrated by multiplying the observed readings by 2.0 (Bartington Industries 2013). This instrument was used exclusively in the study of profile walls in Chapter 3. All measurements were made with direct contact. Measurements are volume susceptibilities to a resolution of 10^{-5} SI.

Bartington MS2 with "H" sensor

The MS2H sensor was not physically employed in this project, but we did have access to published data from use of this instrument at the Double Ditch site in 2004 (Ahler 2005a; Dalan 2008; Kvamme and Ahler 2007), so we incorporated comparisons with these data sets in our profile studies of Chapter 3. The MS2H is designed for the subsurface measurement of MS through use of a down-hole probe. Its diameter is 21.5 m, which is suitable for use in holes 22-25.4 mm in diameter. The sensor is connected to a 5 m cable, permitting deep holes to be explored (Figure 1.1e shows use of a stiff aluminum tube for down-hole insertion). Vertical

resolution is 12.5 mm within the hole and horizontal sensitivity falls to 50% at 2 mm. The speed at which down-hole readings are made requires a field computer with software. Readings are automatically or manually recorded as the probe is lowered into the hole, with measurements commonly acquired every 20 mm. Like the other sensors, this instrument requires a zeroing step (air reading) before measurements are acquired. After a full data sequence is obtained within a hole a second air reading is made, and changes from the first air reading permit computation of instrument drift and a linear correction may be applied to the data (Bartington Instruments 2013). Measurements are volume susceptibilities to a resolution of 10^{-5} SI.

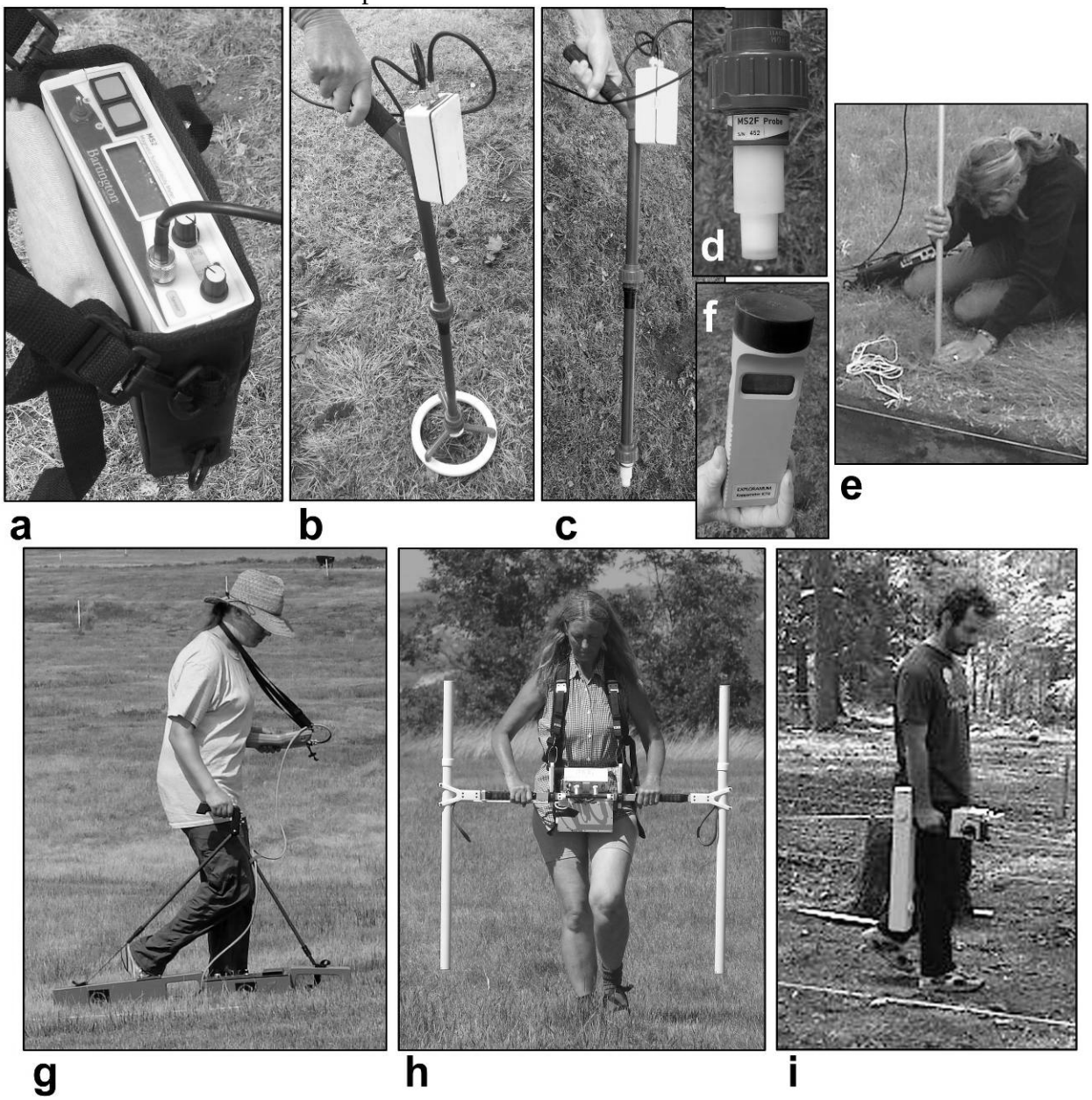

Figure 1.1. *Instrumentation used in the project: a) Bartington MS2 control unit, b) field handle with MS2D sensor head, c) field handle with MS2F sensor head, d) close-up, MS2F sensor, e) MS2 unit with MS2H down-hole sensor probe being inserted, f) Exploranium KT-9 Kappameter, d) Geonics Ltd. EM38-B connected to portable data logger, h) Bartington Grad 601 dual fluxgate magnetic gradiometer system, i) Geoscan Research FM-36 fluxgate gradiometer.*

Exploranium KT-P Kappameter

This device is designed for measuring volume MS on rocks, drill cores, or directly on soils and soil profiles. It is self-contained within a small hand-held package, with a sensor face measuring 65 mm in diameter (Figure 1.1f). Although it offers several sensing configurations for rough or smooth surfaces, we elected to use the button-less sensor face designed for smooth surfaces or flat profiles. In this mode the KT-9 is calibrated for the sensor head to be placed on a smooth plane, such as a profile wall, where 90% of its depth response is derived with 20 mm of its face. The instrument yields a resolution of 10^{-5} SI (Exploranium 1997).

Twin-coil Devices for MS

In North America, magnetic susceptibility surveys have been rare until recently, and they have generally been carried out with twin-coil instruments. Geonics, Ltd, a Canadian company, is the primary manufacturer of these devices, and several models have been employed by archaeologists. One of the most popular is the EM38 series in several models, which permit recording of ground conductivity and MS, simultaneously in some instruments. Unlike the previous single-coil instruments, designed for "spot" readings at specific points and requiring significant time for each reading, these instruments are designed for rapid, continuous data collection along large transects or over broad areas in lateral surveys. Dalan (2008:4) notes that most investigators have focused only on the conductivity data generated by these devices, and interest has grown only recently in their capabilities for recording MS, a consequent focus of this project.

Geonics, Ltd, EM38B

This device is a non-contact "slingram type" instrument that may be carried above the ground (with reduced penetration depth) or dragged on the ground. It permits the simultaneous acquisition of ground conductivity and MS data. A transmitting coil sends low-frequency electromagnetic (radio band) energy that induces eddy currents in conductive earth, which in turn generate a weak secondary electromagnetic field recorded by a receiver within the instrument. One component is made up of electromagnetic energy 90° out of phase with the transmitted signal, known as the quadrature phase and related to the conductivity of the soil. A second component is in-phase with the primary signal and is related to MS. It represents the ratio in strength of the induced to transmitted signals, generally quantified in “parts per thousand” (ppt). These measurements were converted to volume susceptibilities in SI units using:
$K = 2 \times 10^{-3} \Delta I/P$, where $\Delta\ I/P$ is the difference in the in-phase reading (set at 1.45 ppt at 1.5 m above the ground) and the in-phase reading on the ground (Geonics Ltd 2003:14).

Prospecting depth is related to transmitter frequency, the separation distance between transmitting and receiving coils, and by coil orientation, which is usually kept with dipoles vertical. The EM38B operates at a frequency of 14.6 kHz with a coil separation of 1 m. It is connected by cable to a non-integrated data logging device (Figure 1.1g). The in-phase MS component, of sole interest in this project, permits investigation of MS to a depth of 50 cm, with peak sensitivity at 20 cm (Dalan 2008:4), considerably deeper than the single-coil instruments reviewed above. Yet, given this limited prospecting depth, the instrument must be maintained at a constant height (Clay 2006:93) by dragging it on the surface (as height variations strongly influence measurements), and tilting of the instrument during survey must be avoided to

maintain the vertical dipole mode of the coils, otherwise measurement variations will be introduced.

The EM38B, which reads continuously, is extremely fast. At Fort Clark measurements were sampled at a density of 2 per meter, with 1 m separation between transects, while 4 measurements per meter were acquired at Double Ditch, with transects separated by a half-meter. The measurements are recorded automatically by the data-logging device. It sounds a "beep" once per second at which time the operator must insure the instrument is aligned with meter marks on an adjacent tape to insure correct spatial positioning of the measurements. This instrument, particularly in the in-phase mode, is subject to drift caused primarily by temperature changes. It therefore needs to be “tuned” or zeroed periodically, and requires data processing to reduce or eliminate drift effects in large surveys.

Magnetic Gradiometry

In many sections we also utilize magnetic gradiometry (MG) data. Unlike the previous instruments which transmit *active* signals to record near-surface responses, gradiometers are *passive* devices that record native levels of remanent and induced magnetism as the instrument passes over the surface. Two such instruments were employed.

Bartington Grad 601 Dual Fluxgate Magnetic Gradiometer

This instrument supports two fluxgate gradiometers in narrow tubes, with sensor separations of 1 m (Figure 1.1h). This permits data collection in two transects while the operator walks only one, doubling survey speed. It supports very stable electronics that minimize sensor drift, automatic tuning or zeroing, high capacity memory for surveys of large areas, and resolution to 0.1 nT. Surveys with the 601 can be walked rapidly at a meter or more per second while collecting 8 measurements per meter with each sensor. An audible signal permits alignment of the instrument with each meter mark on adjacent tapes for control of spatial positioning. All MG data collection at Fort Clark from 2011-2012 was accomplished with this instrument.

Geoscan Research FM-36 Fluxgate Magnetic Gradiometer

This device, used from 2001-2004 to acquire magnetic gradiometry data at the Double Ditch site (utilized in Chapters 3 and 4), is now an older, obsolescent instrument, that has been superseded by the FM-256 by the same manufacturer. It nonetheless permitted rapid, high-density data acquisition over broad areas to a resolution of 0.1 nT. This instrument has top and bottom sensors with a vertical separation of only 0.5 m (Figure 1.1i), somewhat reducing sensitivity compared to the Bartington 601 (with a 1 m sensor separation). The FM-36 was typically placed in an automatic recording mode that could acquire up to 8 measurements per unit time (usually 1-1.5 seconds, depending on operator speed). An audible signal, with each unit of time, permitted alignment of the instrument with meter marks on adjacent tapes for control of spatial positioning. Owing to this instrument's limited memory, however, surveys at Double Ditch obtained only 4 measurements per meter along transects. The quality of information acquired was partially a function of how well the instrument was "tuned" (it must be zeroed frequently to minimize instrument noise and drift) and how steadily the instrument’s heading was maintained through a transect—any wobbling or wiggling by the operator introduced errors. For this reason, this instrument required significant data processing to remove the effects of drift and operator errors (see below).

GIS AND DATA PROCESSING

Geographical Information Systems

Geographical Information Systems (GIS) were used extensively for data management, analysis, and display in this project. GIS are complex software systems that enable one to encode, manage, and display information that has a spatial component, and they offer tools for data editing, manipulation, spatial analysis and modeling (Kvamme 1999). All of these capabilities were employed here. Specifically, raster GIS were employed because geophysical measurements acquired across an area or a profile occur systematically in a matrix composed of rows and columns. Location is controlled by row and column position where each cell is linked with real world spatial coordinates. The attribute held in a particular cell of a raster grid represents the measurement corresponding to a specific area. In image or picture data, cells in a raster are frequently referred to as “pixels" (for “picture elements”). Rasters are well-suited for representing phenomena that vary continuously across an area, such as magnetic fields. Displays simply color-code or grayscale each cell. In this project each data set from each instrument was held in a separate raster. These rasters then could be overlaid, manipulated, and "dressed up" with scales and grids to generate cartographic products for this report. The raster capability of "map algebra" was used extensively to mathematically manipulate the data. The Idrisi GIS (v. 17, "Selva"; Clark University 2013) was uniformly employed.

Image processing

Image processing methods were used routinely to enhance contrast and brightness of the magnetic imagery. Additionally, interpolation was consistently employed throughout to increase apparent resolution and image continuity while reducing pixelation at the same time. All of these tactics were employed to improve visualization of the continuous magnetic fields.

Special-purpose geophysical software in the form of Geoplot 3, by Geoscan Research, was also employed for the removal of survey defects in some of the geophysical data. Magnetic gradiometry data sets required "zeroing" of transects, a technique that normalizes the data in each transect to a mean of zero which eliminates "heading errors" that arise in fluxgate gradiometry surveys from changes in direction during zigzag surveys. A "de-staggering" algorithm was also applied to these data to correct staggered or "herringbone" edges along anomaly boundaries caused by slight timing errors during zigzag surveys (see Kvamme 2006b for fuller descriptions of these defects). "De-spiking" or removal or extreme measurements caused by the presence of iron artifacts was sometimes employed.

EMI data seldom required such post-processing because these data were collected using unidirectional or "parallel" survey methods, although "de-spiking" to remove extreme measurements caused by metals was often employed. The study areas examined in this project were generally small, confined to blocks generally of 20 x 20 m, which enabled rapid surveys minimizing instrument drift effects (systematic increases and decreases in measurement values typically caused by temperature variations). However, a larger block of EMI data measuring 20 x 60 m was acquired at Double Ditch, and in this survey instrument drift was apparent. This required balancing or "edge-matching" the 6 individual 20 x 20 m sub-blocks (tiles) so that measurements would "match" across tile edges. The procedure here simply balances or matches the mean measurements at tile edges to remove apparent discontinuities that result from instrument drift (see Kvamme 2006b for more details).

CHAPTER 2: ACCURACY AND UTILITY OF EMI DEVICES FOR MS MAPPING

Despite the many benefits of magnetic susceptibility (MS) surveys for exploring and understanding the archaeological record, only a small number of instruments are currently available for near-surface explorations, as outlined in the Chapter 1. As noted there, most popular are the MS2 instruments and associated field sensors manufactured by Bartington of the United Kingdom. They are hand-held and designed for accurate "spot" measurements of volume MS taken at specific sample points. A number of EMI instruments by Geonics, Ltd., manufactured in Canada, are designed for rapid data collection over large areas. These instruments differ in several fundamental ways. Most importantly, Geonics instruments, such as their popular EM38 series, are twin-coil devices that acquire data proportionate to volume MS through a 50 cm depth as well as soil conductivity. Some models permit both to be obtained simultaneously. MS surveys with this instrument are capable of rapidly covering large areas with high sampling rates, but results have often been inconsistent and difficult to relate to accurate measurements of MS, leading some to avoid MS surveys completely, focusing only on the conductivity component (Clay 2006; Dalan 2006a). On the other hand, the Bartington MS2's field sensors are single-coil instruments that accurately measure near-surface volume MS. Regardless of their accuracy they too pose limitations, such as shallow measurement depths (less than 10 cm) and much slower survey speeds. Given the limitations of these instruments archaeological studies of MS using various instruments have infrequently been compared.

Although archaeologists acknowledge these shortcomings, they may be outweighed by the potential benefit of MS studies for mapping human occupations and delineating activity areas within sites. Although Dalan (2006a, 2006b) has examined in detail the performance of the MS2 in vertical or down-hole settings (using the "H" sensor package; Bartington 2013), absent thus far is an assessment of the performance of MS instrumentation in lateral surveys across areas. To assess the utility, quality, and accuracy of MS data in these contexts, we compared the results of field surveys with the Geonics EM38B, an instrument capable of recording MS data simultaneously with soil conductivity, to that of the Bartington MS2 with the "D" sensor head, appropriate for recording MS data on a natural ground surface (Bartington 2013). Furthermore, along with presenting the results of these surveys we give consideration to other advantages and disadvantages of each instrument. These include factors like ease of use, survey and data processing time, and survey repeatability.

SURVEY AREAS

To make assessments of these instruments we surveyed four areas of the nineteenth century Mandan-Arikara village within the Fort Clark State Historic Site using the Geonics EM38B and the Bartington MS2D meters and these areas were also surveyed by magnetic gradiometry (Figure 2.1). These areas contain many archaeological features, including the most common types encountered at this site. EM38B surveys were actually carried out throughout the entire village core (Wiewel 2014) with 2 samples/m with 1 m separation distances between transects (for 2 measurements/m^2). Data were extracted from this corpus for each of the survey areas below. Owing to their slowness, MS2D surveys were conducted with various sample densities taken every 1, 2, or 3 meters. Magnetic gradiometry (MG) surveys, which were also conducted throughout the village, acquired 8 samples/m with one-half meter distances between

transects (for 16 measurements/m^2), and these data are also examined for comparative information and detail.

Area A

This 20 x 20 m survey plot lies west of the village fortification ditch and contains an Arikara earthlodge from the site's later occupation (Figure 2.1). This lodge is evidenced topographically by a slightly elevated earthen berm marking its perimeter and subtle hints of other possible features. A MG survey in 2011 revealed the presence of a central hearth, a possible auxiliary hearth, and storage pits. It also indicated a near-absence of ferrous metal artifacts compared to lodges closer to the village core, making this survey area ideal because much less "noise" would be introduced from the extreme measurements that such objects cause in MS surveys. Consequently, EM38B and MS2D surveys were also conducted in this area in 2012 with the latter at one sample per meter (Wiewel and Kvamme 2013).

Area B

This 20 x 20 m plot is in the village core and includes an earthlodge, although it is not visible on the ground surface today (Figure 2.1). Instead, its location was discovered by ground-penetrating radar, electrical resistance, MG, and EM38 surveys conducted in 2000 (Kvamme 2001; see also Kvamme 2007:214-215). These surveys, and the lack of a surface indication, point to the lodge's greater depth and suggest its association with the early Mandan occupation of the site. This survey area therefore offered an opportunity to evaluate measurement depth capabilities. The area was resurveyed with MG in 2011, and EM38B and MS2D surveys were conducted in 2012 with the last at one sample per meter.

Area C

This plot includes a 16 x 30 m area in the village core that was surveyed specifically to investigate MS associated with an earthlodge and an adjacent area free of a lodge. EM38B data were acquired in 2012 as part of the village survey. The MS2D survey was performed in 2011with sampling every 2 m owing to time constraints.

Area D

This large plot of 30 x 60 m was utilized to examine the effects of vegetation thickness on the Bartington MS2D sensor system and repeatability of the data by survey and re-survey under long and short-grass conditions. Sampling was undertaken every 3 m owing to the size of the area.

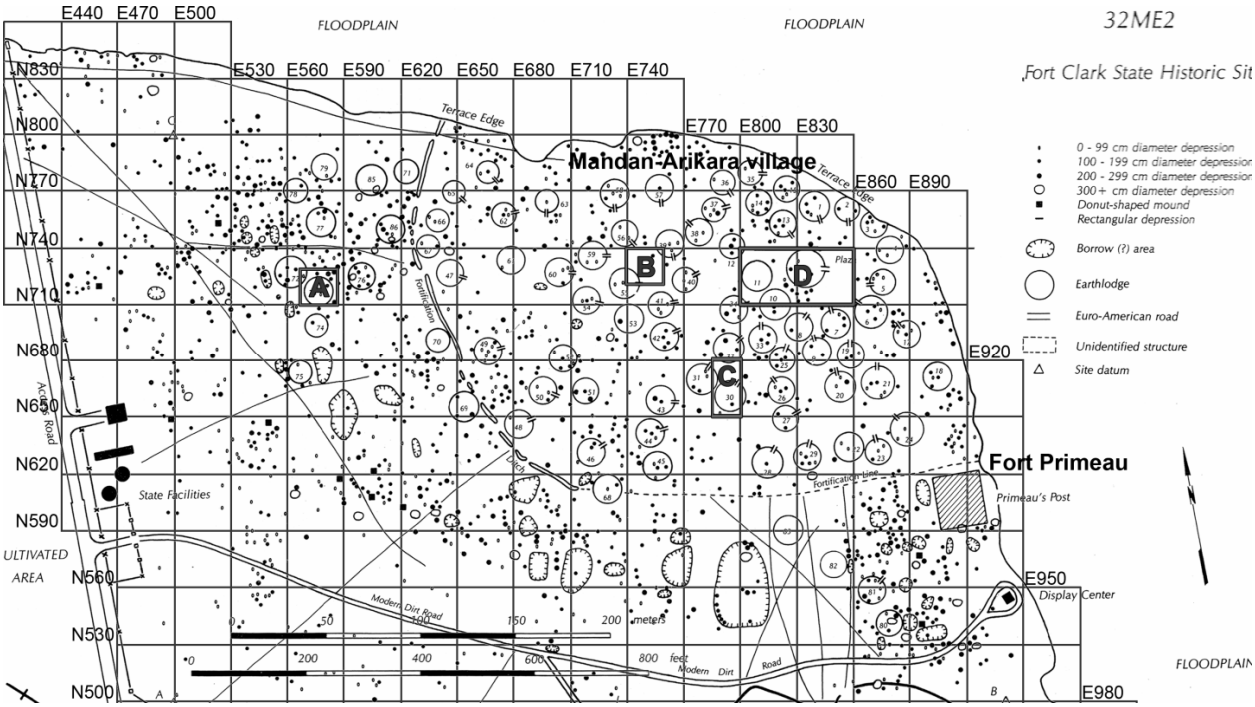

Figure 2.1. *Map of Fort Clark showing the locations of MS survey areas A-D (adapted from Wood 1993: Figure 3). A 30 m grid with the local coordinate system is shown.*

RESULTS: SURVEY AREAS A-C

In the following sections we explore the performance of the twin-coil EM38B and correspondences between its data and results from the MS2D in several ways. Most simply, plan view maps from each data set are examined visually for similarities and differences. The presence or absence of anomalies is noted and discussed, often with reference to background MG data. Pearson's *r* is employed to quantify the strengths of relationships between the data sets. Additionally, individual profiles are examined to better illustrate the extent to which these data sets correspond. Since different sampling strategies were employed for each instrument, the two data sets were made equivalent for some of the analyses (such as correlations studies) by de-sampling the EM38B measurements to the same density as the MS2D data, with one sample every meter ($1/m^2$) or every two meters (1 per 4 m^2). The EM38B data were also subjected to a "de-spiking" algorithm (see Chapter 1) to remove extreme measurements caused by highly conductive metals in order to make these data sets more comparable to those collected with the MS2D, where large measurements caused by near-surface iron artifacts were avoided in the field. Finally, to enhance visualization of anomalies, data sets were subjected to interpolation to reduce the pixelation of the imagery resulting from the coarse field sampling. These data are shown side-by-side below with the data at native spatial resolutions used in the analyses.

Survey Area A

Visually, the MS data from the two instruments acquired from the shallow, late Arikara earthlodge at the site's western periphery look rather similar (Figure 2.2). For instance, the lodge perimeter is indicated by a ring of slightly enhanced magnetism. This enhanced area corresponds to topsoil which is mounded due to its erosion off the top of the former lodge that stood in this space. Although this feature looks similar in each data set, its magnitude is somewhat higher in

the EM38B data (which gives an average of approximately 6 x 10^{-4} SI compared to 4.5 x 10^{-4} SI for the MS2D). This variation could be due to the different volumes evaluated by each instrument or to calibration and measurement issues discussed in the Chapter 1 and elsewhere (see below for an examination of vegetation thickness on MS2D measurements, for example). Near the center of the lodge both MS data sets reveal an anomaly interpreted as a food processing and cooking activity area because it is large and surrounds the central hearth (visible in the MG image, Figure 2.2c). Its magnitude is once again higher in the EM38B data. This area of enhanced MS probably arises from intensive and repeated firing of the hearth, which increases MS, from hearth cleanings, which disperses materials of high MS, and the introduction of organic materials to the sediments around the hearth from food preparation and cooking.

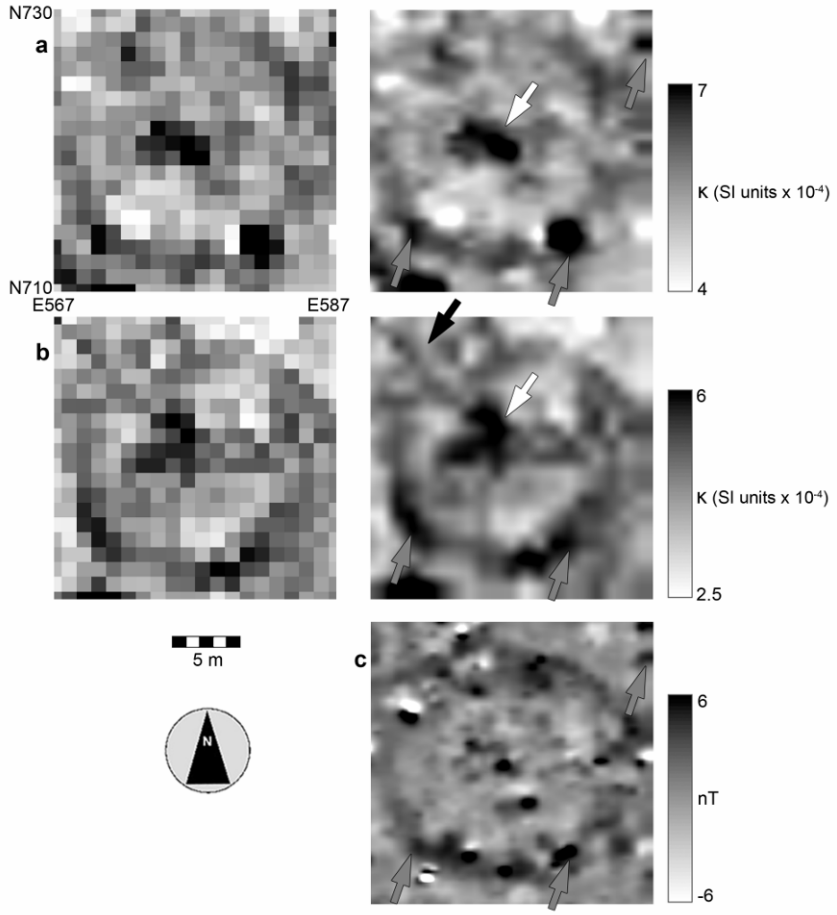

Figure 2.2. *MS survey results from an Arikara earthlodge at Fort Clark: a) Geonics EM38B, b) Bartington MS2D, and c) MG data shown for comparison. The left column in the a and b rows shows the 1 m spatial resolution data used for quantitative comparisons. The right column shows the datasets after interpolation (smoothing). A white arrow points to a likely activity area that includes a central hearth. Gray arrows point to possible storage pits. A black arrow indicates a linear feature, possibly an entryway.*

On the south side of the lodge, near its perimeter, are multiple anomalies of higher magnetism believed to represent the loci of storage pits (Figure 2.2). These anomalies are clearly evident in the MG image with roughly circular shapes. In the EM38B data they also appear circular, but they are somewhat elongated in the MS2D imagery. The latter result may be due to

the lower sampling density of the MS2D survey. Moreover, storage pits are deep features, occasionally reaching depths of 1.5-2 m. The greater depth response of the EM38B (about 50 cm) may improve detection while the MS2D, with its 10 cm depth response, can only detect the high susceptibility of materials that happen to migrate upwards from rodent and insect activities, and the shape of the result can be much less patterned (see Chapter 1).

Another likely storage pit, located outside of the lodge on its northeast edge, is noticeable in the MG and EM38B data, but is absent in the MS2D image. This absence might be explained simply by the lack of depth sensitivity of the MS2D and the coarser sampling employed. Thus, the MS2D's shallow depth response may be a significant limitation in cases of deeper features, like subterranean storage pits.

Other circular anomalies, located around the perimeter of the lodge, are clearly visible in the MG data but are absent from the MS images. Although this result may be due to their depth, it is more likely a function of the lower MS sampling densities. An unexpected linear anomaly extending through the lodge perimeter toward the northwest, is visible in the MS2D dataset (Figure 2.2b). This anomaly perhaps indicates the location of the lodge entryway, although robust indication does not appear in the EM38B or gradiometry image. It is emphasized that with the coarse one meter spatial resolution of these surveys that it is difficult to reliably examine shape characteristics of small features.

Although the MS data yielded by each instrument appear similar, a correlation coefficient (Pearson's *r*) indicates only moderate correlation, with *r*=0.49 (Figure 2.3). This result is explained by a number of factors. Primary among these is the different depth or volume sensitivities of the two instruments. Differences in the exact locus at which measurements are recorded also introduce surprisingly large variations to this relationship, a circumstance more fully explored in a repeatability study below. An examination of individual transects across the 20 x 20 m survey area reveals additional complexities to this relationship.

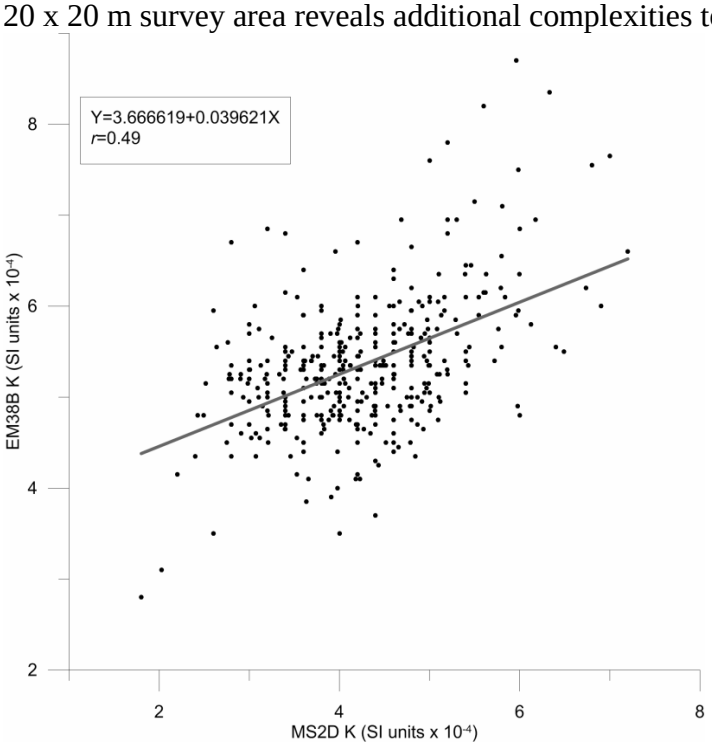

Figure 2.3. *Scatterplot of MS data yielded by the Bartington MS2D and Geonics EM38B showing a moderate correlation.*

The relationships between four transects that cross-cut many of the anomalies discussed previously are shown in Figure 2.4. The first, third, and fourth transects show moderately strongly correlations. The third reveals similarities between the two instruments most clearly because anomalies arising from the lodge perimeter and the central hearth region are well indicated. Although transects 1, 3 and 4 appear similar in form they consistently differ in magnitude, as noted previously. Although most transects exhibit moderate to strong relationships, about one-quarter are only weakly correlated. This is exemplified in the second transect which exhibits a very low correlation. Although this line plot shows some shared anomalies like the cooking area near the lodge center, it otherwise indicates few similarities.

In general, this dataset demonstrates that twin-coil data from the EM38B parallels well results gained from the Bartington MS2D. In other words, EM38 results tend to reproduce measurements of the MS2D. Anomalies seem largely in parallel spatially, graphically along transects, and statistically, as revealed by Pearson's *r*. The minor differences in MS values between the instruments are likely explained by small variations in measurement loci as well as the aforementioned differences in depth or volume responses peculiar to each instrument. Despite the fact that the surveys were conducted along transects marked with surveyors tapes, the rapid pace of the EM38B survey at a rate of one meter per second causes small variations in the placement (on the order of 10-20 cm) of this instrument compared to the more carefully controlled MS2D, contributing to differences in results. It is also quite possible that in some transects MS varies little in the top half-meter, yielding similar measurements and strong correlations between the instruments, while in other transects large depth variations may exist between the near-surface where the MS2D is most sensitive and the greater depths at which the EM38B is sensitive, causing divergent measurements.

Survey Area B

Survey Area B was placed over a deeply buried lodge discovered by a 2000 geophysical survey (Kvamme 2001), evidently from the site's early Mandan occupation (Figure 2.1). In this case, comparisons between the MS surveys by the EM38B and MS2D show fewer correspondences. Visually, a plan view indicates little resemblance between the data obtained from the EM38B and the MS2D (Figure 2.5). In the EM38B data the lodge perimeter is weakly visible, but it is nearly impossible to discern in the MS2D image. The perimeter is only slightly more apparent in the MG image. Several anomalies of elevated MS are apparent in the EM38B data set. One near the lodge center probably indicates an activity area near the central hearth, where the hearth, food wastes and cooking would have enhanced MS. The lodge’s central hearth, confirmed by coring, is clearly indicated by MG and the EM38B. Along the lodge perimeter, multiple circular anomalies of increased MS likely indicate the locations of storage pits (Figure 2.5a), some of which have been confirmed by coring (Ahler 2003:52-55). Two closely correspond to anomalies visible in the MG data (Figure 2.5c).

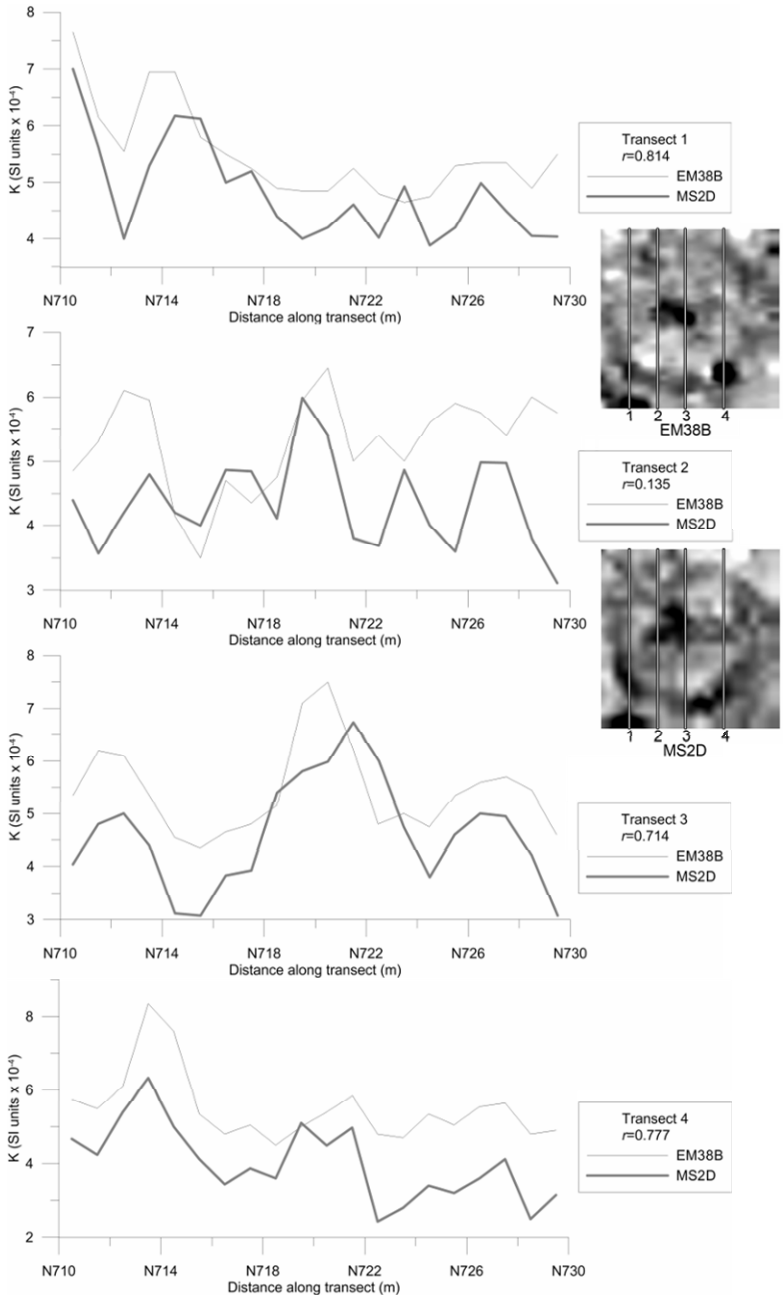

Figure 2.4. *Plots of MS data along four transects showing the relationship between Geonics EM38B and Bartington MS2 results. Location of transects are shown on MS maps to right.*

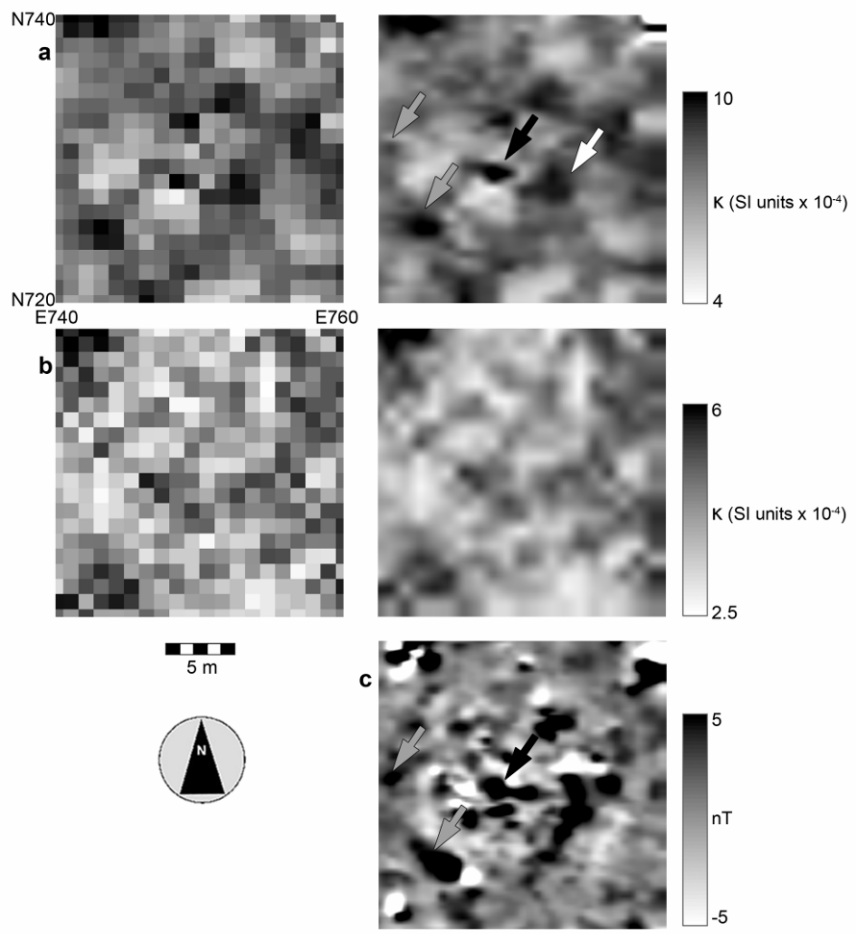

Figure 2.5. *MS survey results of a deeply buried earthlodge near the village core at Fort Clark: a) Geonics EM38B, b) Bartington MS2D, and c) MG shown for comparison. The left column in a-b shows the data at a 1 m spatial resolution. The right column shows interpolated data sets for reduced pixelation. A white arrow points to a possible activity area near the lodge's central hearth (black arrow). Gray arrows indicate confirmed storage pits.*

Parallel anomalies do not appear to occur in the MS2D data set (Figure 2.5b). In fact, the MS2 data appear to lack strong spatial patterning indicative of a lodge, suggesting the MS2D's depth response is too shallow for this survey area and that magnetic enhancements simply do not reach the surface (from rodent or insect action) in this area. Coring indicates this lodge is filled with refuse and that its floor lies nearly a half-meter below the ground surface (Ahler 2003:52-55), beyond the range of the MS2D and at the limits of the EM38B. Nevertheless, the EM38B does offer subtle and strong hints of various house features. Pearson's *r* confirms these observations, showing a weak relationship between the two MS datasets (r=0.34, with only a single extreme outlier removed [likely due to metal]; Figure 2.6). Given the different depth sensitivities of the two MS instruments, these findings are not surprising.

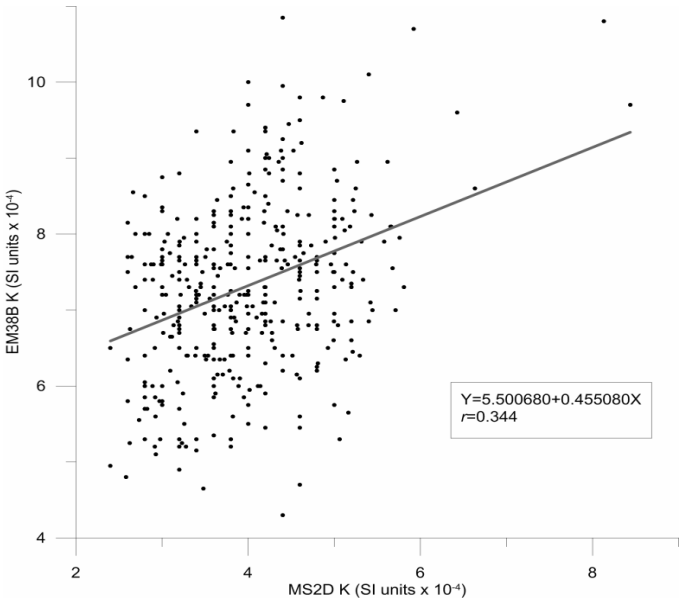

Figure 2.6. *Scatterplot of MS data yielded by the Bartington MS2D and Geonics EM38B showing weak correlation between the two.*

As noted in Survey Area A (see also the repeatability study below), slight placement differences between the two instruments during the surveys also contribute to a reduced correlation. Additionally, as the MG data indicates (Figure 2.5c), this area contains numerous iron artifacts (indicated by dipolar anomalies). In the MS2D survey, whenever extreme measurements were recorded due to iron, data were acquired at adjacent iron-free locations (see Chapter 1), further exacerbating placement differences and contributing to reduced correlation.

Comparisons along individual transects yield further insights and some surprising results, however (Figure 2.7). Although a global correlation reveals only a moderately weak relationship between the two MS data sets (r=0.34), transect-by-transect comparisons indicate moderate to strong relationships along nearly two-thirds of them. To illustrate, three transects are examined that cross-cut prevalent anomalies (Figure 2.7). In the first transect, anomalies revealed by the EM38B exhibit a strong response, and although their magnitudes are weaker, similar anomalous areas are also indicated by the MS2D. The third transect offers the clearest example of similarities, with two anomalies of high MS evident in both data sets. This outcome is surprising given the different depth sensitivities of the instruments, especially the MS2D where the depths to the sources of these anomalies are greater than the instrument's maximum measurement depth of 10 cm. Evidently, in some instances, bioturbation agents like earthworms and rodents may have migrated MS enhanced deposits upwards. The second transect in Figure 2.7 is also characteristic because it illustrates a result common to about one-third of the transects. It exhibits little relationship between the two data sets and visually their plots look quite different. Yet, the single central anomaly, interpreted as representing a cooking and hearth area near the lodge center, does appear in both data sets.

The lesson of Survey Area B is that the EM38B is able to produce moderate to good responses even at the limits of its purported sensitivity range of a half-meter. Major and minor anomalies, that are known to exist by MG, are also seen in the EM38B data. This circumstance is not true for the MS2D survey although some subtle correspondences are noted. The EM38 shows greater utility in this deeper context.

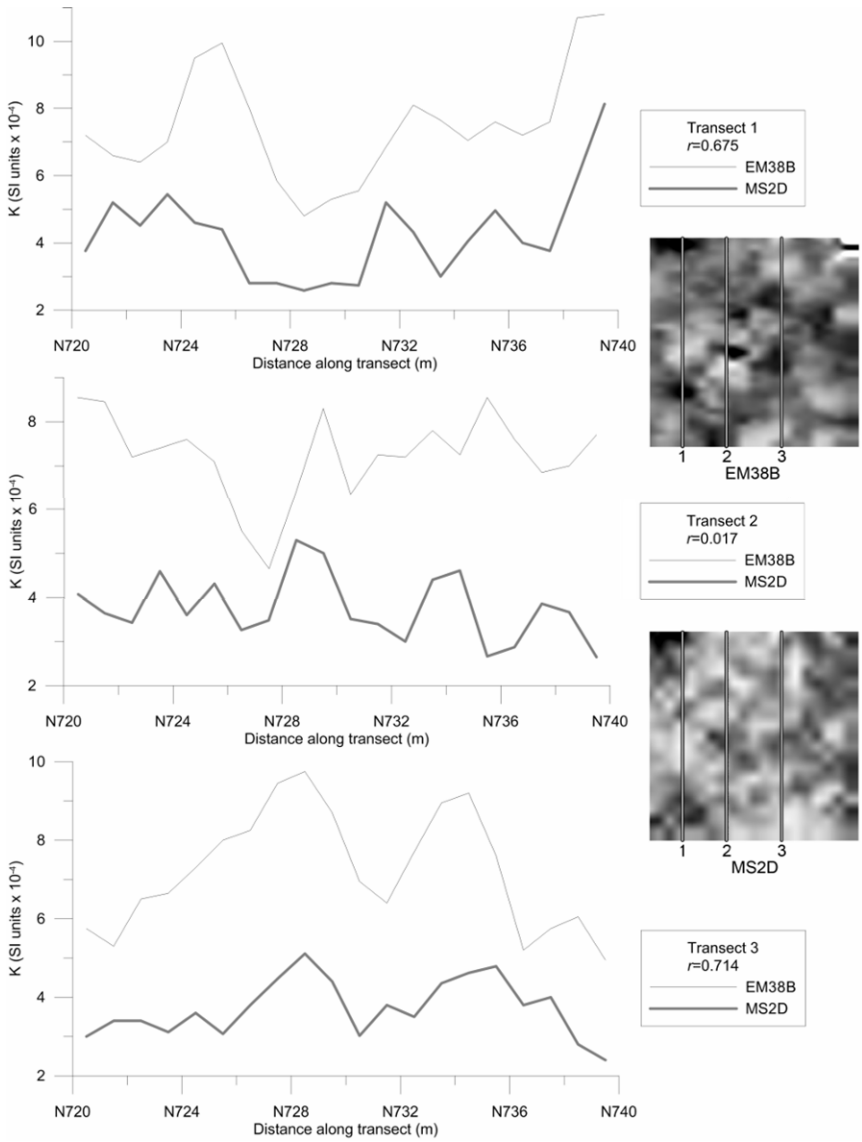

Figure 2.7. *Plots of MS data produced along three transects showing relationships between Geonics EM38B and Bartington MS2 results. Location of transects are shown on MS maps to the right.*

Survey Area C

This area includes a lodge in the village core and an "empty" space immediately to the north as indicated by surface conditions (Figure 2.1) and a MG mapping (Figure 2.8c). The MG data show the outline of a lodge with a centrally located hearth, a number of storage pits, and many iron artifacts indicated by dipolar anomalies. This survey clearly shows parallels between the EM38B data and the MG survey where the perimeter of the earthlodge, multiple storage pits, and other anomalous areas closely correspond. Two anomalies marked with gray arrows in the EM38B and MG data indicate likely locations of storage pits (Figure 2.8). The MS2D data, however, only poorly reproduce the spatial patterns of these features seen in the other data sets (Figure 2.8a, b), although multiple, roughly circular anomalies do appear near a portion of the lodge's perimeter. Although the lodge's outline is vaguely perceptible in the MS2D data, few

other similarities are apparent, a circumstance echoed by Pearson's *r* which reveals a very weak relationship of *r*=0.123 (Figure 2.9).

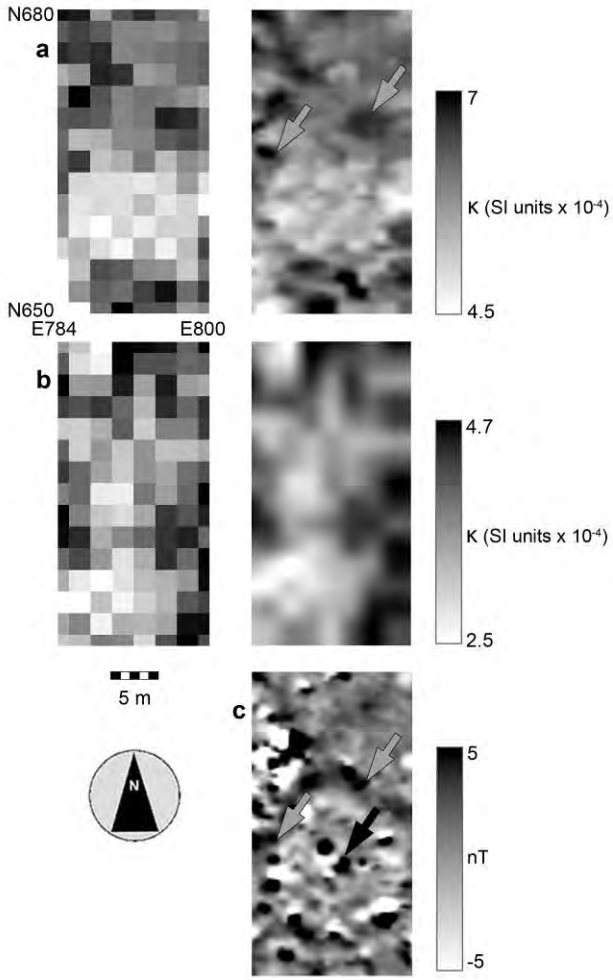

Figure 2.8. *MS survey results of an earthlodge near the village core at Fort Clark: a) Geonics EM38B, b) Bartington MS2D, and c) MG data shown for comparison. The left column in a-b shows the data at 2 m spatial resolution (the native resolution of the MS2D survey). The right column shows interpolated data sets. A black arrow points to a hearth, and possible storage pits are indicated by gray arrows.*

In this instance, the MS2's lack of corresponding anomalies is most likely due to the coarse sampling strategy employed in this survey area rather than measurement depth issues, as a clear depression pointing to this earthlodge is visible on the surface. MS2D measurements were collected every two meters rather than one meter as in previous examples owing to time limitations. The coarse sampling means that many principal anomalies indicated by the other methods may have simply been missed, causing obvious correspondences to be absent in the data set. Moreover, the plethora of iron artifacts indicated by the MG means that the MS2D data were sampled in adjacent locations to avoid the extreme measurements (see Chapter 1), further reducing correspondences with EM38 measurement stations and thereby reducing the correlation.

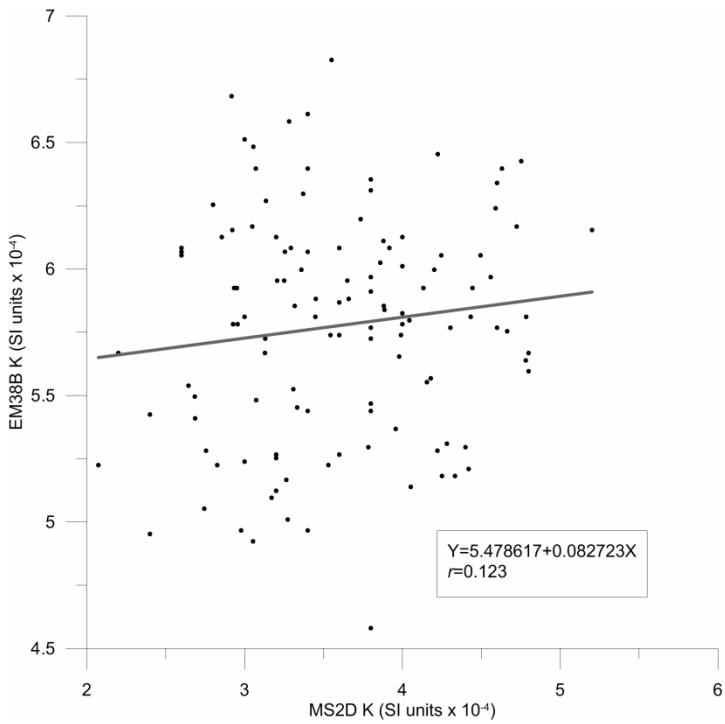

Figure 2.9. *Scatterplot of MS data yielded by the Bartington MS2D and Geonics EM38B in Survey Area C showing a weak correlation.*

REPEATABILITY STUDIES

Another factor that must be considered with geophysical instruments is survey repeatability. In some of the foregoing discussions we argued that small variations between measurement loci probably contribute to discrepancies and reduced associations between data sets. But just how "bad" can this effect be? We decided to investigate this question with a repeat survey of a region. We also developed concerns during field tests with the Bartington MS2D in areas with surface vegetation of variable thickness, where we observed large measurement differences. We wondered to what extent does vegetation thickness affect measurements with this instrument? This section investigates these questions.

Variations in Repeat Surveys: Geonics EM38B

Geonics EM38B data were collected in two of the survey areas, A and B, twice, during the consecutive summers of 2011-2012, which allows consideration of measurement repeatability. Visually, the MS data collected in the two years looks quite similar in both areas, although minor and subtle differences are apparent (Figure 2.10).

In Survey Area A, the near-surface Arikara lodge, MS anomalies indicating possible activity areas and a central hearth are visible in both plan views, although in 2011 distinct anomalies are indicated (Figure 2.10a). Moreover, several anomalies roughly circular in shape and indicating likely storage pits, are located around the lodge’s perimeter. Matching anomalies can be seen in the data sets from consecutive years, but their sizes and magnitudes differ.

Many corresponding anomalies are also visible in Survey Area B, the deeply buried lodge from the site's early occupation (Figure 2.10b). One prominent anomaly, likely a storage pit due to its location near the lodge’s perimeter, is indicated in the 2012 dataset but is absent in the 2011 image (gray arrow). The many small differences between the two data sets are most likely due primarily to small variations in instrument placement during the surveys. It demonstrates

how this simple factor can alter results, and sometimes strongly. In both cases the spatial differences in measurement loci between the two surveys were probably less than 15 cm most of the time, and nowhere should they have exceeded a quarter meter.

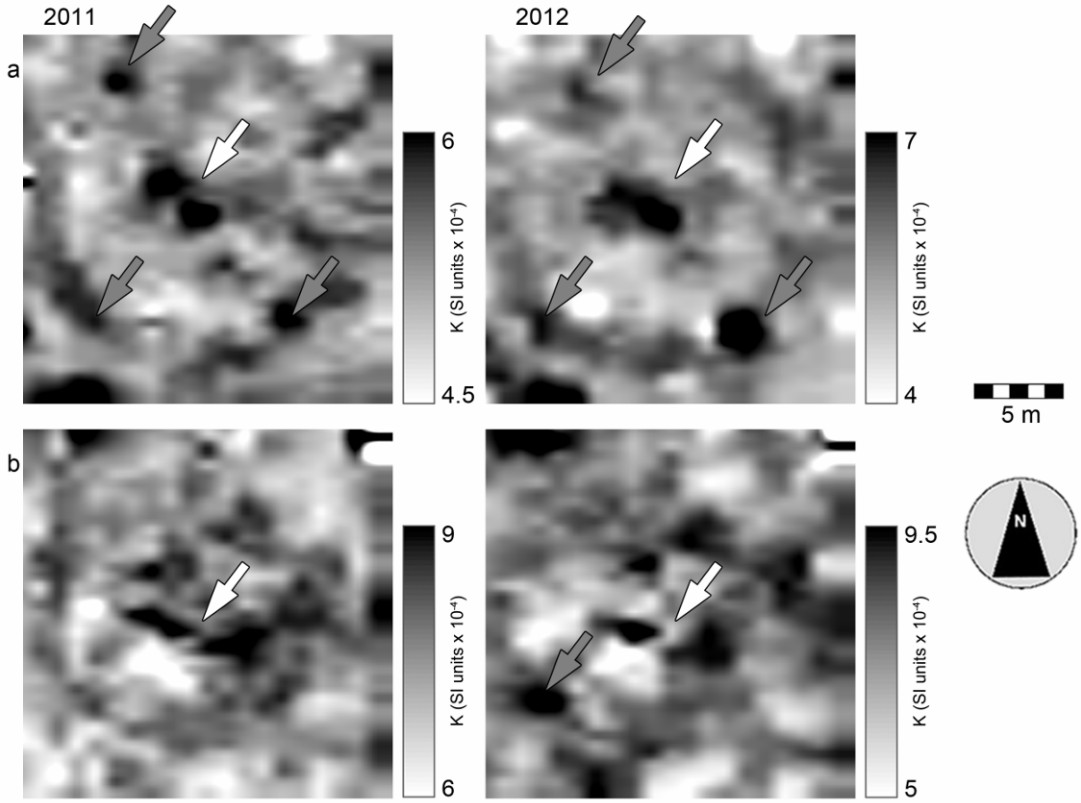

Figure 2.10. *EM38B survey results for two areas collected in consecutive years: a) Survey Area A, and b) Survey Area B. White arrows indicate activity areas and the locations of central hearths. Gray arrows indicate likely storage pits.*

The small apparent differences in Figure 2.10 suggest less than perfect correlations, and this is true quantitatively. Pearson's correlation coefficient reveals only moderate relationships between the data sets, with r=0.54 and r=0.56 in Survey Areas A and B, respectively (Figure 2.11). Paired-difference t-tests (with $H_0{:}\mu_D=0$ *and* $H_1{:}\mu_D\neq 0$), however, indicate no significant difference in mean MS response between the consecutive years in either survey area (Survey Area A: t=0.00015; df=799; p > .5; Survey Area B: t=0.00014; df=795; p > .5), so the data are stable and there is no bias from year to year. This is further supported by the regression where, effectively, the functions are: Y = X (Figure 2.11).

We find the foregoing results surprising because it indicates that only about 25 percent ($100*r^2$) of the variation in these data sets seems to be reproducible by subsequent surveys! Although we believe that the measurement differences and moderate correlations are likely a consequence of minor instrument placement variations between the two years, another factor may also contribute. Twin-coil instruments like the EM38B are affected by moisture which impacts soil conductivity (Clay 2006), and a small correlation exists between the quadrature (conductivity) and in-phase (MS) components. It was very wet in 2011 and much drier in 2012, which possibly may have contributed to some of the differences seen here.

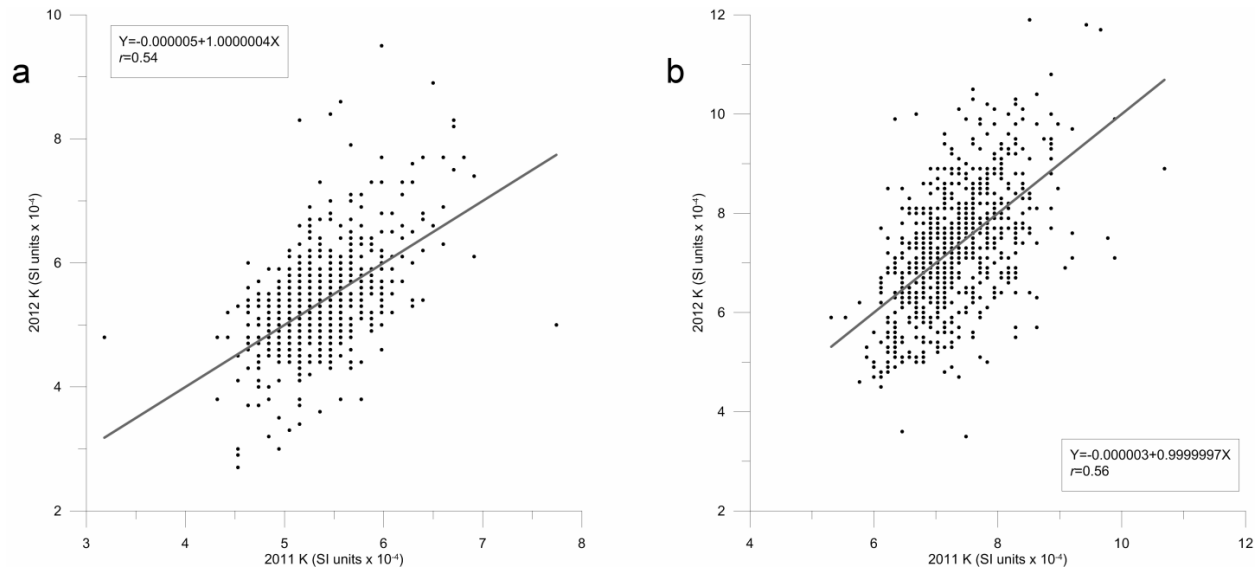

Figure 2.11. *Scatterplot of MS data yielded by the Geonics EM38B in consecutive years in a) Survey Area A, and b) Survey Area B.*

Vegetation Effects: Bartington MS2D

According to its specifications, the MS2D is sensitive to a depth of perhaps 10 cm, although the response falls to 50 percent at a depth of only 1.5 cm and 10 percent at 6 cm (see Chapter 1; Bartington 2013). Given the instrument's limited depth sensitivity and rapid decline in strength of response with depth, vegetation thickness is an issue, especially when it varies in thickness over a survey area. To evaluate this potential problem, surveys of a 60 x 30 m region in Area D were performed (Figure 2.1). This area borders the village plaza and contains multiple earthlodges, including the larger Arikara ceremonial lodge near the survey area's center. In this area the grass was un-mowed and averaged 15 cm in height. In our initial survey the un-mowed grass was compressed to a height of approximately 2-3 cm by pressing the "D" coil firmly to the ground surface. In a subsequent repeat survey the grass was shortened to a height of less than 1 cm with a weed trimmer. In both surveys a coarse sampling strategy was employed owing to time limitations, with samples collected every three meters (for 200 total measurements). This sampling density precludes discussion of small anomalies, although larger anomalies and broad changes in MS are evident (Figure 2.12).

The two MS2 data sets yield a moderately high correlation of r=.683 and visually they appear quite similar (Figure 2.12). For instance, a large area of low MS is evident in both images in the central and western parts of the survey area. Surprisingly, this area includes two earthlodges, as clearly revealed by MG (Figure 2.12d). The eastern perimeter of the Arikara ceremonial lodge, however, does indicate a large anomalous area of enhanced MS in both data sets. Most of the village plaza to the east of that lodge exhibits low MS, which is likely due to its use for public ceremonial activities where constructions were prohibited.

The MS2 measurements following the trimming of the grass are, as expected, greater in magnitude (Figure 2.12a). More importantly, differencing the two MS data sets reveals that small and moderate measurements changed only slightly, but anomalies of high MS increased in strength after trimming. Furthermore, a paired-difference t-test (with $H_0{:}\mu_D=0$ *and* $H_1{:}\mu_D>0$) indicates the difference between the MS measurements before and after trimming the grass is highly significant statistically (t=29.6; df=199; one-tailed p<0.0001). Although the two datasets

appear similar visually, MS values measured in shorter grass are significantly greater, a factor to consider when performing surveys in areas with different vegetation heights and thicknesses. This finding has bearing in Chapter 5 where MS evaluated under tall grass is compared against similar measurements acquired under mowed conditions.

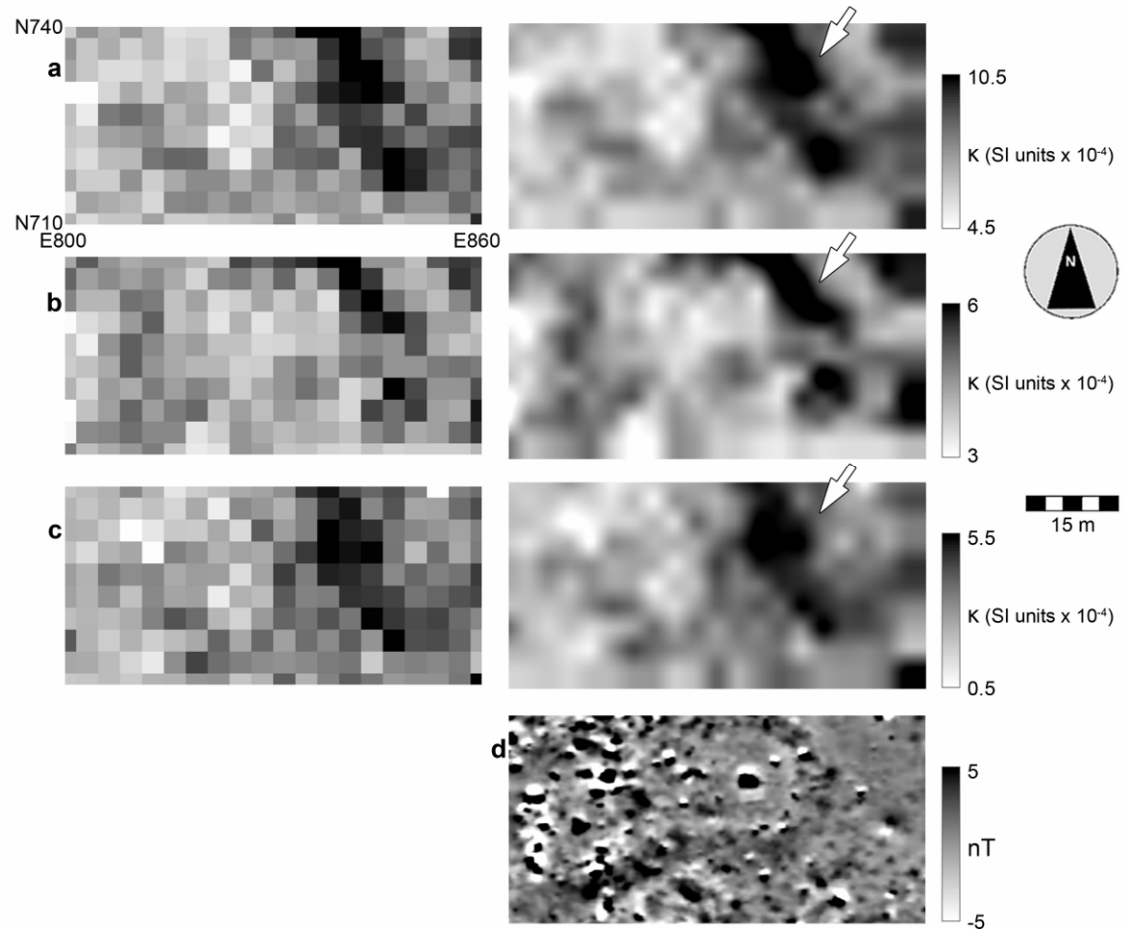

Figure 2.12. *MS2D survey results of a 60 x 30 m area near the village plaza at Fort Clark: a) results after trimming grass, b) results with un-mowed grass, c) difference between a and b, d) MG data showing two lodge circles for comparison. The left column in a-c shows the data at a 3 m spatial resolution. The right column shows interpolated or smoothed datasets to improve visualization. A white arrow points to an anomaly with elevated MS which appears to correspond to the perimeter of the Arikara ceremonial lodge.*

These results present concerns because it seems evident that some of the variation in MS2D measurements is surely a result of vegetation thickness, and many sites contain variable thicknesses of vegetation, as occurs at Fort Clark. Similar concerns are reported in plowed fields where rough soil surfaces can introduce voids beneath the sensor that may also introduce measurement variations (Clark 1990:104). It seems apparent, then, that some of the discrepancies and reduced correlations between the EM38B and the MS2D seen here are merely the result of this phenomenon.

DISCUSSION AND EVALUATION

The purpose of this study was to compare the utility of a popular EMI twin-coil device, the Geonics EM38B, against a standard, the single-coil Bartington MS2 with the "D" field sensor head, for recording MS data in archaeological contexts. The MS2D has long been held as a standard for the field evaluation of MS, while questions and uncertainty exist concerning the use of a twin-coil system like the EM38 for the same purpose (Clay 2006). Evaluations of the EM38B against the MS2D and comparison MG datasets were made in shallow, moderate, and "deep" archaeological settings, and a data repeatability study was carried out. An evaluation of the EM38 requires consideration along several dimensions.

Data Quality

Two EM38B repeatability studies indicate that data may be replicated with good accuracy, even from year-to-year. Our repeat data were unbiased from one year to the next and indicated moderately good correlations (r=.54 and r=.56). Measurement variation is thought to be largely due to inconsistencies in instrument placement at identical loci.

Repeatability of measurements with the MS2D is known to be good, and is something we experienced because at each station we acquired at least two measurements which were averaged. Frequently, individual measurements were identical or very close. More worrisome is our repeatability study under conditions of long and short vegetation, which demonstrated a large and statistically significant difference. This result implies that in vegetated sites, with different forms of vegetation or different states of mowing (as occurs at Fort Clark), a large amount of the variation in MS measurements may simply be due to vegetation thickness. In these contexts this raises the question of the utility of the MS2D as a standard for comparison.

Another dimension of data quality lies in the precision with which MS can be measured at a specific locus. With the 18.5 cm diameter of the "D" sensor, the Bartington MS2 holds an advantage here as it is easy to target the same spot again and again. Yet, variation may exist in the presence of vegetation or an uneven surface, where a different downward pressure will compress the vegetation or soil, and cause different readings as the sensor closes with the target material. For more precise MS measurement at particular points on "bare" soil surfaces, rocks, ceramics, or other materials, the "F" sensor head (described in Chapter 1; Bartington 2013) offers clear advantages as it is designed for these contexts.

The EM38 and similar twin-coil instruments offer no advantages in this regard. A meter long and unwieldy, the measurement point is taken to be at the center of the device, and a valid reading is obtained when the instrument is absolutely vertical in the vertical dipole mode (see Chapter 1). Height above the surface also impacts this instrument, but with its greater depth sensitivity it is a lesser factor. The greatest impediment to this instrument's repeatability lies in the common practice that most surveys are conducted "on the fly" while walking transects at a rate of a meter per second while data are recorded with an automatic data logger (see Chapter 1). This makes exact placement along a line at specific intervals impossible to achieve, although our experience suggests location precision within about 15-20 cm.

Data Comparability

Our in-phase measurements with the Geonics EM38B reveal results that parallel those obtained with the Bartington MS2D. This is particularly true in a setting where targets are shallow (Survey Area A), but a moderate correlation was shown even in a "deep" setting (Survey

Area B). Many anomalies are indicated by both instruments with similar forms and placements, although the EM38B consistently yielded MS values of somewhat higher magnitude. Statistically, the relationship between the EM38B and the MS2D in the shallow survey area yielded r=.49. This relationship is almost identical to the EM38 year-to-year repeat study which yielded r=.54 and r=.56. The lack of a perfect correlation in the latter was explained by small measurement placement differences, and the same argument may therefore be made for the former relationship. In other words, the EM38B replicates the MS2D measurements as closely as it is able to repeat its own measurements. Even in the deep Survey Area B, below the supposed prospecting depth of the MS2D, a correlation of r=.34 was achieved between the two devices.In Survey Area C little correspondence was seen between the EM38B and MS2D (r=.12) which may have been due to the coarse sampling interval of 2 m or the presence of large amounts of iron artifacts which caused more varied measurements.

Cost

A significant consideration in instrument choice is cost. Although the EM38 is now offered by Geonics in an upgraded format (i.e., EM38-MK2), the meter and a data logger used here sold for approximately $15,000 in 2002. In contrast, the MS2 meter and probe handle currently retails for nearly $4,500, and the "D" surface scanning sensor costs an additional $1,200. Thus, the Bartington instrument costs nearly one-third the price of the Geonics EMI instrument. Yet, costs must be weighed against benefits, so other dimensions of value must also be considered.

Speed

The speed of the EM38 is very fast. We routinely sample 2 measurements per meter, and have often sampled 4 per meter in 12 years of experience with this instrument. Survey speed of our EM38B system is consistently one meter per second, regardless of sampling rate, so a 20 m transect requires 20 seconds, and a 30 m transect a half-minute. With the need for zeroing and line set-up additional time is required, of course, but a 20 x 20 m block is commonly surveyed in about a half-hour (with 1 m transect separation or 20 lines) or an hour (with a half-meter transect separation or 40 lines).

Surveys with the MS2 are much slower. In fact, we found that complete survey of a 20 x 20 m block with two people requires nearly an hour and a half, and at only half the sampling density (i.e., one measurement per meter). Several factors slow the survey speed of the MS2 instrument. The instrument must be zeroed prior to each measurement, it must be pressed to make firm contact with the ground, and multiple measurements are typically averaged together at each measurement station. Furthermore, the MS2 lacks a data logger and instead requires measurements to be manually recorded. We note that it is possible to log data with a field computer and appropriate software, but the extra weight and difficulties of handling a computer, versus a paper notepad, argued for the latter, as we felt little increase in speed would be realized.

Area

The phenomenal speed of the EM38B means that long transects and vast area surveys may rapidly be undertaken in short spans of time. In the past dozen years of use of this instrument, we have conducted numerous area surveys exceeding a half-hectare, and many over a full hectare, including a 2012 survey at Fort Clark (Wiewel 2014). The benefits of large area surveys have long been touted (Kvamme 2003a). By surveying and creating imagery of large

areas it becomes easier to understand and interpret the meaning of the many anomalies encountered owing to the spatial patterns and organization they illustrate. A simple linear anomaly in a small area survey is difficult to interpret specifically, for example, because it may represent a trail, a boundary, or the wall of a house. A larger view of a region, however, can remove this ambiguity by showing three other connected walls that make it a house.

Due to its slower speed of data acquisition, the Bartington instrument is better suited for "spot" checking MS measurements at specific places. Large scale MS2D surveys are possible, of course, and many have been undertaken (see Gaffney et al. 2004), but generally with lower sampling densities (e.g., samples taken every 5 or 10 m; Payne 1996). Surveys of small areas under high sampling densities are also possible with this instrument, as we demonstrate, but they require significantly more time than the EM38.

Depth

As has been mentioned repeatedly, the in-phase component of the EM38B measures to a depth of approximately 50 cm, although it is most sensitive at 20 cm below surface, with rapid fall-off of response below and above 20 cm. A measurement with this device is therefore an average MS through the 50 cm "depth," but one that is non-linearly weighted as a function of depth, with peak response at 20 cm. Dalan (2006a:172) presents the full response curve.

The MS2D, on the other hand, measures to perhaps 10 cm, although its sensitivity falls to 50 percent at a depth of only 1.5 cm and 10 percent at 6 cm. It is therefore very sensitive to variations in surface vegetation thickness, as our foregoing study shows. Since most archaeological features worldwide are buried much deeper than 10 cm, one might question why this instrument is at all useful. The answer is that magnetically susceptible material is able to migrate upward, the chief vehicle being repeated plowing. Other processes that contribute in the same way include bioturbation, such as rodent work, insects (earthworms), and tree throws (Clark 1990; see Chapter 1). Thus, the MS2D can suggest the presence of more deeply buried features, although only indirectly through these processes, as has been indicated in foregoing sections. Yet, detecting a magnetically susceptible feature directly through a deeper sensing instrument like the EM38B yields a more robust indication than through a process where more dispersed and ephemeral magnetic material has simply migrated from its original source locus. This was indicated by clearer anomaly forms and shapes in some of the foregoing analyses.

Survey Area B clearly revealed the advantage of the EM38B with its deeper response. In the buried earthlodge in this area, with its floor about 50 cm beneath the surface, this instrument gave clear anomalies representing such features as hearths, storage pits, and iron artifacts, and even suggested weakly the house's perimeter outline, as revealed by comparisons against MG data and the results of a coring program. Corresponding data from the MS2D poorly represented these features and yielded a moderately low correlation of r=.34 with these data.

Data Processing

Processing in-phase EM38 data may be slightly complicated in that it can require detrending to remove instrument drift, "matching" of data from grid-to-grid to remove edge imbalances (see Kvamme 2006b; Chapter 1), and perhaps de-spiking to remove extreme measurements caused by metal artifacts (if so desired). Since the MS2 is zeroed before each measurement, drift is less of a problem. Yet, this advantage is negated by the need to manually input each of the handwritten measurements prior to processing MS2 data, unless one makes use of a field computer.

CHAPTER 3: UNDERSTANDING MAGNETIC ANOMALY FORMATION

Enormous numbers of magnetometry or magnetic gradiometry (MG) surveys have been carried out in archaeological sites in recent decades (Aspinall et al. 2008). Far more magnetometry surveys have been conducted in archaeology than probably all other geophysical surveys combined, and for good reason. Compared to other types of geophysical surveys, magnetometry has consistently proven to be one of the most productive in terms of the nature and detail of typical findings (Kvamme 2006a). Additionally, fast instrumentation permits rapid surveys enabling larger areas to be examined. In the Northern Great Plains, MG surveys have completely revolutionized the conduct of archaeology and understanding of the archaeological record. These surveys permit subterranean storage pits, hearths and other subsurface features to be accurately located. Prior to magnetometry locating storage pits was extremely difficult (their orifices are only a meter in diameter), requiring pure luck, and they are extremely important to archaeologists because of the wealth of artifacts, faunal, and environmental data they offer. MG surveys have generated many new insights into the layout and organization of prehistoric villages by revealing lodge numbers, sizes, and shapes, a new level of agricultural production and village population by the vast numbers of storage pits encountered (used primarily for maize), and even forced recognition of new ideas as in the discovery that the Double Ditch site in North Dakota actually contains *four* defensive ditches and a larger population than anyone dreamed (Kvamme and Ahler 2007).

Surface surveys by MG have often been followed by subsequent excavations which frequently yield insights into the nature of archaeological features that cause MG anomalies. One might witness how a former ditch completely filled with settlement soils yields a strong positive anomaly along its length, and surmise that this phenomenon occurs because settlement soils tend to be magnetically enriched from human occupational activities (i.e., possess high levels of magnetic susceptibility or MS). Likewise, a two meter deep storage pit filled with layers of midden-like deposits commonly yields large anomalies as well. How and why does this occur? What exactly is the nature and distribution of subsurface magnetism within specific types of archaeological features, how does magnetism correlate with observable stratigraphic layers, and how do the effects of subsurface magnetism cumulate to be recorded at the surface as an anomaly in the MG data? These are the sorts of questions that are frequently asked, but rarely investigated.

A chief reason for our general lack of knowledge of subsurface magnetism and anomaly formation is that although it is very easy to acquire magnetic measurements at the surface with a variety of devices, it is much more difficult to do so beneath the ground. In recent years this limitation has begun to change with the advent of new instrumentation and approaches to get at the subsurface.

PRIOR RESEARCH

One of the first breakthroughs in permitting study of subsurface magnetism was a down-hole magnetic susceptibility sensor developed by Rinita Dalan and Bartington Instruments (Dalan 2006b). Prototypes have been available since the early 2000s, so a rapidly developing knowledge base is being acquired in a variety of settings (see Dalan 2006a; Dalan and Goodman 2007). This sensor, now available through Bartington as the "H" sensor in the MS2 system (i.e., the MS2H), requires a small diameter (22-25 mm) hole to be bored into the earth, which may be

undertaken with an Oakfield corer or similar hand-push device. The sensor head, 21.5 mm in diameter and connected to a long cable, is lowered into the hole where volume MS is recorded through its walls. The cable is connected to the MS2 and a laptop with Bartington software that permits rapid data capture and recording (Dalan 2006b). MS measurements are commonly recorded at 2 cm intervals down the hole, permitting high resolution logging and the ability to detect magnetic variations in thin deposits. Measurements up to 3 m below the surface have been recorded. Drift resulting from temperature changes down the hole can be a problem, so the instrument is zeroed in the air prior to the first reading and an air reading is taken after the last; the difference indicates the amount of drift and a linear correction can then be applied to the data (Dalan 2006b:186; see Chapter 1).

Early archaeological tests with the MS2H were made at the Double Ditch site in North Dakota (Dalan 2008; Kvamme and Ahler 2007), which are particularly relevant here (Figure 3.1). A site-wide MG survey (Kvamme and Ahler 2007) discovered numerous storage pits, and several were selected for excavation (Figure 3.1b). One was bisected by excavation, giving an excellent profile that revealed the many deposits that made up its fill (Figure 3.1c). A core-hole was placed in the unexcavated portion of the pit several centimeters beyond the excavated face, and MS2H readings were recorded every 2 cm through the bottom of the pit to a sterile deposit at a depth of 1.6 m. A second core-hole was made immediately adjacent to the pit, but clearly outside of it and a second set of readings was made to the same depth. A comparison of the MS measurements was extremely insightful (Figure 3.1c), because it gave one of the first glimpses of subsurface magnetism in the Northern Plains and provided data that helped to form explanations for the great magnetism of these features. The contrast between the two data curves was stunning, with the background reference outside of the pit illustrating uniformly low MS. Within the pit large changes in magnetism were indicated, much correlated with the stratigraphy, suggesting that some of the fill represented only common settlement soils (slightly more magnetic), while others were highly magnetic, apparently taken from hearth cleanings or more magnetic midden materials according to the corresponding stratigraphic record. This study therefore provided convincing evidence that further research into subsurface magnetism is warranted (a second down-hole magnetism study at Double Ditch with the MS2H is described in a section below).

Subsequent to this work, Dalan and Goodman (2007) pursued the next logical step. Recognizing that a single core-hole yields information at only a point, they developed the tactic of placing core-holes throughout a region to investigate subsurface magnetism in an archaeological *volume*. Core-holes were placed systematically every 10 m in a 40 x 50 m region of the Dahnke-Reinke site, a multicomponent Woodland-Archaic site in North Dakota. With MS recorded every 2 cm in 30 core holes, three-dimensional visualization software designed for ground-penetrating radar (GPR) surveys was employed to better understand magnetic characteristics in this region. Specifically, the software permitted interpolation of MS information *between* the individual core-holes through the 30 x 50 m region, to a depth of 1.3 m. This volume could then be rotated, sliced, and diced to examine specific features, characteristics, and changes in the subsurface MS. The study revealed a number of continuous and discontinuous buried soil horizons across the region and the loci of several of zones of enhanced MS related to various occupations.

This approach was carried a step further by Fogel (2005; see also Dalan 2008:18-20) when he employed a 1 m sampling interval in a 9 x 9 m space to explore magnetic variations through the volume of a Mississippian mound-top structure in the Parchman site, in Mississippi.

Based on full knowledge derived from subsequent excavation, enhanced MS correctly defined the floor area, the vertical extent of the structure, a portion of it that was no longer intact, and fired daub from the structure's burned walls.

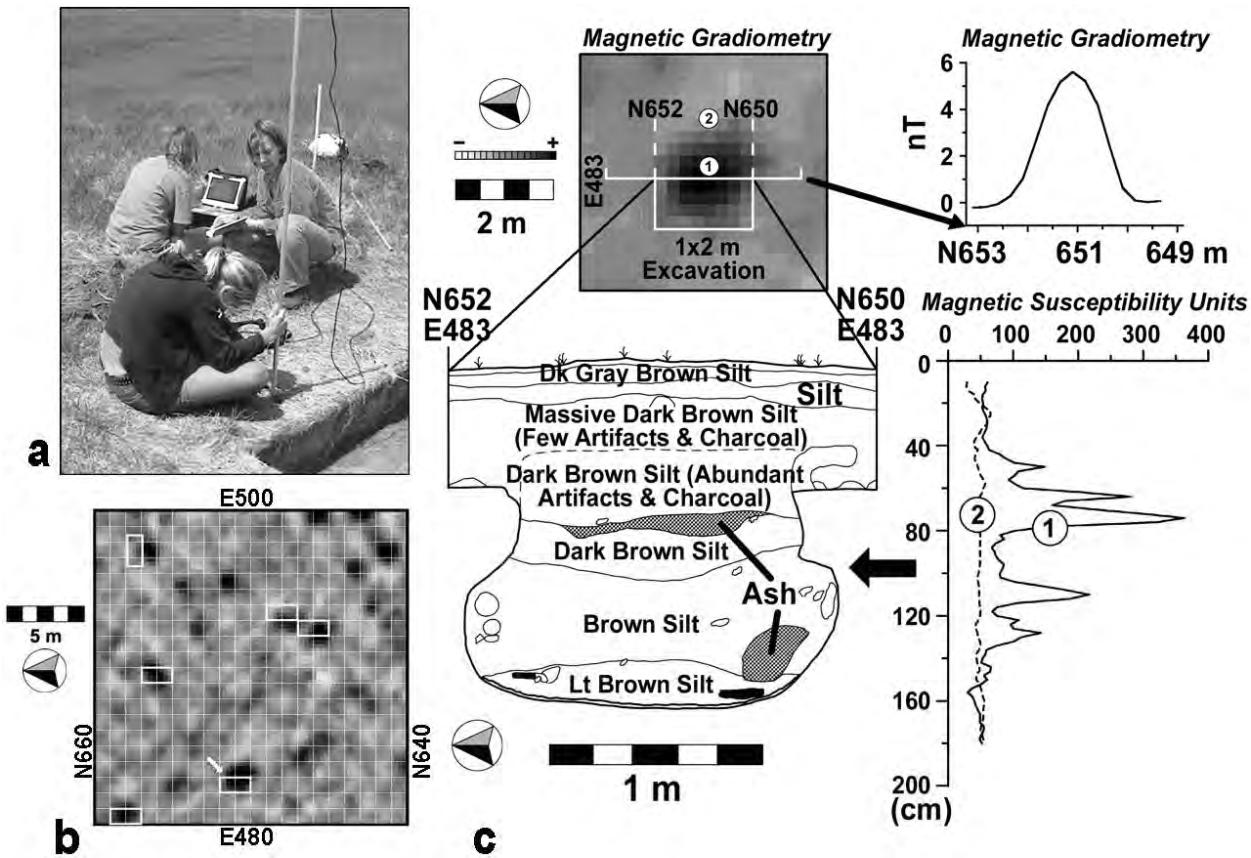

Figure 3.1. *Down-hole MS2H survey at Double Ditch: a) MS2H in action, b) 1 x 2 m excavation units over MG anomalies representing storage pits (MS tested pit indicated by arrow), c) excavation profile of storage pit with corresponding MS profiles inside and outside pit (labeled "1" and "2," respectively, graph at right). The MG plan and profile recorded at surface given at top. Note that the MS measurements were recorded in arbitrary uncalibrated instrument units.*

Although the advances offered by the MS2H are groundbreaking by permitting visualization and analysis of the magnetic subsurface, the foregoing studies suffer from a uniform deficiency. They offer only a low resolution examination of horizontal or lateral changes in magnetic characteristics, although the vertical resolution is very high indeed. Ten meter or even 1 m lateral sampling does not permit detailed examination of horizontal magnetic variations that contribute to the formation of specific anomalies in MG datasets.

In an Austrian publication (in German), Neubauer (2001:91-92) illustrates a method for high spatial resolution investigations of subsurface magnetism. This was accomplished by utilizing *excavation profiles* across archaeological features and the systematic recording of MS every .2 m or .1 m across the profile faces using the MS2F sensor system (see Chapter 1; Bartington Instruments 2013). The results illustrated not only detailed changes in MS with depth,

but also lateral variations for many meters across ditches and other archaeological features, imparting a greater understanding of anomaly formation as recorded on the surface.

It is this last approach that is pursued here. In sections below we similarly undertake high spatial resolution measurements of MS on excavated archaeological profiles in a North American setting. We examine several archaeological features of known type in an earthlodge village setting in North Dakota in an effort to improve understanding of magnetic anomaly formation recorded by surface sensors.

ARCHAEOLOGICAL SETTING

To reduce the costs and the time required to perform excavations, and to eliminate the need for artifact analyses and reporting on excavated materials, we decided to reinvestigate a previously excavated site and reopen excavation units that had been placed within archaeological features of interest. We selected the Double Ditch site, in North Dakota (see Chapter 1), because 34 excavation units were placed within this site from 2002-2004 in a large archaeological project that combined geophysics and aerial remote sensing methods with traditional excavations (Kvamme and Ahler 2007). Both authors had worked on this project and were therefore familiar with the site. Importantly, prior excavations had been placed in a variety of archaeological feature types including middens, bastions, fortification ditches, storage pits, and house floors. This enabled us to pick and choose particular features best suited for this project. We selected for our investigation three archaeological features common to the Northern Plains.

- *Subterranean storage pit*. Subterranean storage pits are ubiquitous in the Northern Plains Village tradition, with hundreds or even thousands common throughout villages. A 1 x 2 m excavation unit cut 2 meters deep that revealed a full storage pit in profile was selected ("A" in Figure 3.2). This storage pit happens to be the same one investigated with the down-hole data logger by Dalan (2008), permitting comparison (Figure 3.1).

- *Fortification ditch*. With several trenches cut across the site's four fortification ditches we selected a 2 x 5 m trench that was placed across the outer Ditch 4 in a perpendicular direction ("B" in Figure 3.2). This unit reached 2 m in depth.

- *House floor*. A 1 x 2 m excavation unit was selected that cut through a house floor ("C" in Figure 3.2). This unit reached 50 cm in depth.

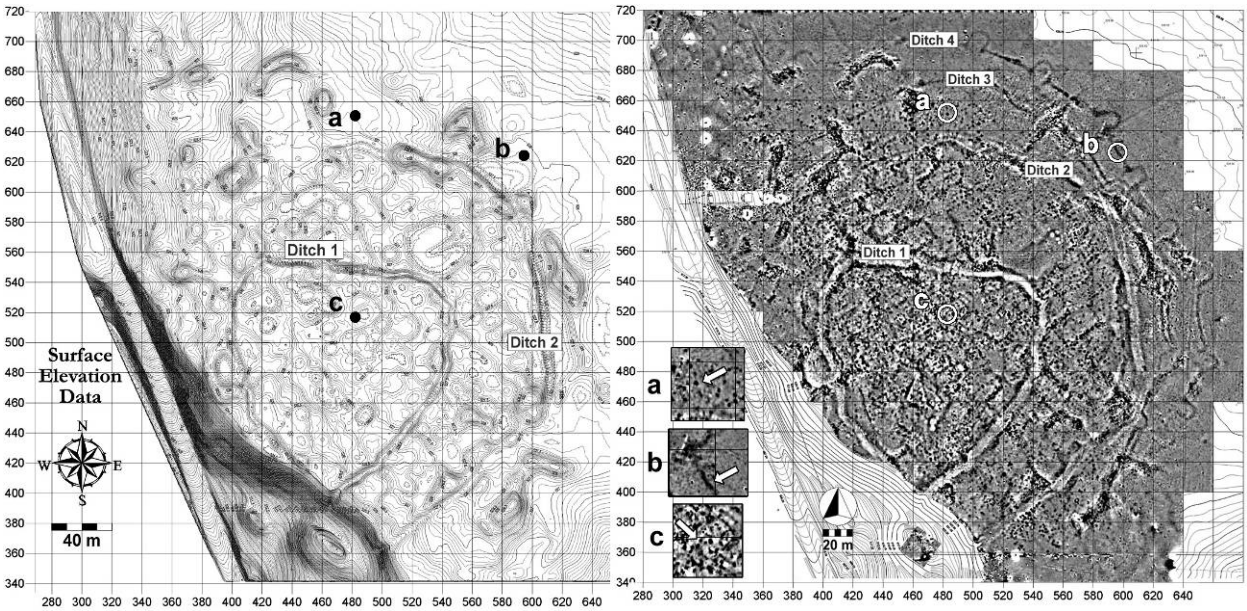

Figure 3.2. *Plan of the Double Ditch site showing topography (left) and MG anomalies (right) and the locations of the three excavation units where magnetic profiling was undertaken: a) storage pit, b) fortification ditch, c) house floor.*

RE-EXCAVATION

The locations of the Double Ditch excavations that were made between 2002-2004 were relocated by the State Historical Society of North Dakota (SHSND) through use of maps, recognition of their shapes (as small depressions in the surface), the presence of pea gravel that was used for fill, and in one case through use of a total station. The fill of the two deep units was removed by a "mini"-backhoe (provided by the SHSND) followed by shoveling and trowel work, while the matrix in the single shallow unit was removed entirely by hand. (Figure 3.3).

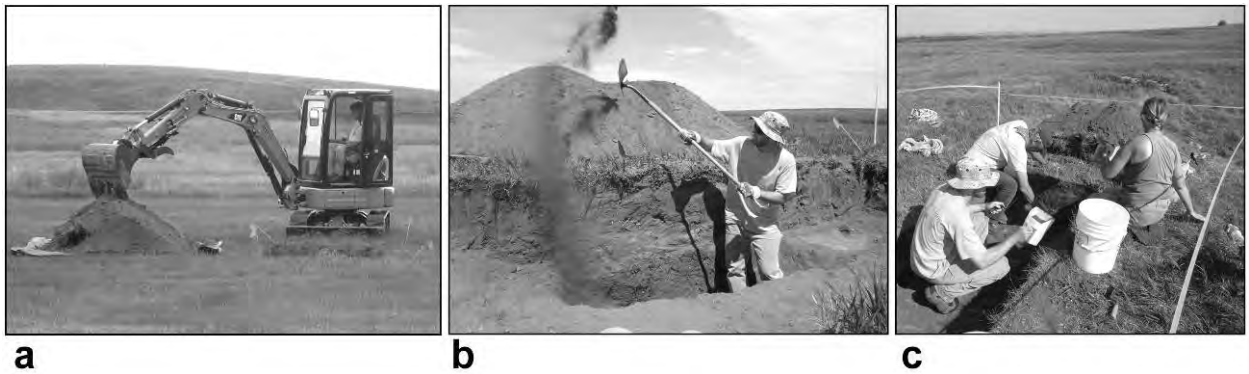

Figure 3.3. *Opening of old excavation pits at Double Ditch: a) power excavations, b) shoveling, and c) hand excavations.*

INSTRUMENTATION

Three devices were utilized to record MS on the profile walls. Each was described in detail in Chapter 1.

- *Bartington MS2F*. The 15 mm diameter "F" sensor head is designed to read volume MS on a flat surface, such as a profile wall. Ninety percent of its depth response lies within 6 mm of the flat sensor face (Bartington Instruments 2013).
- *Bartington MS2D*. The 185 mm diameter "D" sensor head is designed to read volume MS on a normal vegetated surface. It is with this sensor that much of the surface work in MS was conducted in this project, as described in other chapters; it is not normally employed for wall profiling. We nevertheless chose this sensor to investigate comparability with the other sensors in one of the profiles. Its response is excellent when in contact with a flat surface (such as a wall profile), with 90% of its depth response within 60 mm (Bartington Instruments 2013).
- *Exploranium KT-9 Kappameter*. This device is designed for measuring MS on rocks, drill cores, or directly on soils and soil profiles. It is calibrated for the sensor's 65 mm diameter head to be placed on an absolutely smooth plane, such as a profile wall where 90% of its depth response is derived with 20 mm (Exploranium 1997).

FIELD METHODS

Following removal of the artificial matrix in each of the excavated units (a sandy gravel was employed for fill after the 2002-2004 excavations), the wall selected for magnetic measurements was carefully scraped with a trowel and cut back 2-5 cm to provide a fresh surface for the mapping and a "clean" one for the MS measurements (to avoid contaminants from the fill matrix and variations in MS they might introduce). Next, each profile was carefully photographed digitally at high resolution. Photo-mosaics were then created by "stitching" together multiple individual photos using Adobe Photoshop®. In the case of the subterranean pit, some of the photos were taken at extreme oblique angles owing to the depth and narrowness of the pit. They had to be corrected spatially through use of "perspective" functions, and attempts were made to brighten images near the dark bottom of the pit using "brightness" functions in Photoshop. After the photography, the profiles were carefully examined visually, and observable stratigraphy was then "drawn" onto the profiles with the point of a trowel. The stratigraphy was then mapped onto graph paper through use of meter tapes, line levels, and plumb bobs

To obtain MS measurements on the profile faces metal tapes and pins could not be employed because they would interact with the instrumentation. Instead, string, wood, and plastic materials were utilized to guide data collection. Parallel strings, made horizontal with line levels, were first affixed to each wall from top to bottom, every 10 cm or 20 cm, depending on the wall's size. They were to guide the vertical placement, or "rows," of the MS measurements (Figure 3.4). The strings were held in place by wooden golf tees pressed into the walls, on the advice of Rinita Dalan (personal communication). Horizontal control of the measurement loci was realized through use of a plastic stadia rod placed adjacent to the excavation at the surface. A plumb bob was dropped from this rod when necessary for horizontal alignment.

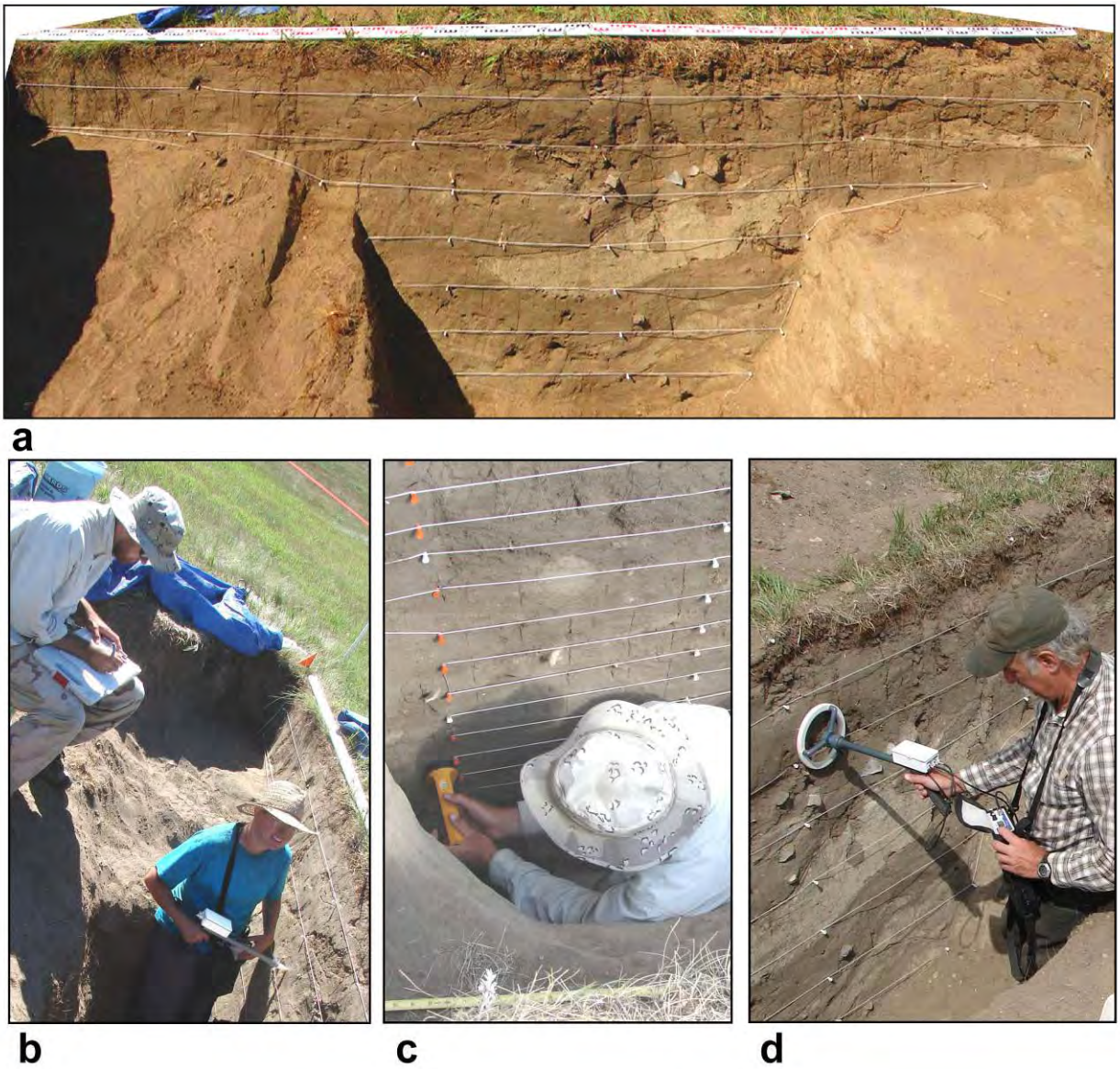

Figure 3.4. *Field methods for recording MS at Double Ditch: a) cleaned and scraped profile of fortification ditch (Study "B") with parallel strings placed 20 cm apart, b) recording MS with the MS2F, c) recording with the KT-9, and d) recording with the MS2D.*

The MS measurements were then obtained systematically, row-by-row on each profile. This was accomplished simply by placing each instrument firmly on the flat face of the wall. It was frequently difficult to place the unwieldy, 18.7 cm long KT-9 within the tight confines of the pit and a number of measurements could not be taken. The 7.2 mm long sensor head of the MS2F could easily be unscrewed from its field handle, however, facilitating placement. This made its use much easier as did its smaller diameter, and measurements could be acquired in even the most confined locations. Each measurement was read twice and averaged. One person operated each instrument, with a second person recording the measurements onto graph paper, where a grid was established to coincide with that of the profile (Figure 3.4). In this manner, measurements could be written on the paper row-by-row to coincide with the surveys as they

took place. Sampling was performed every 5 cm or every 10 cm, depending on the size of the profile (Figure 3.5).

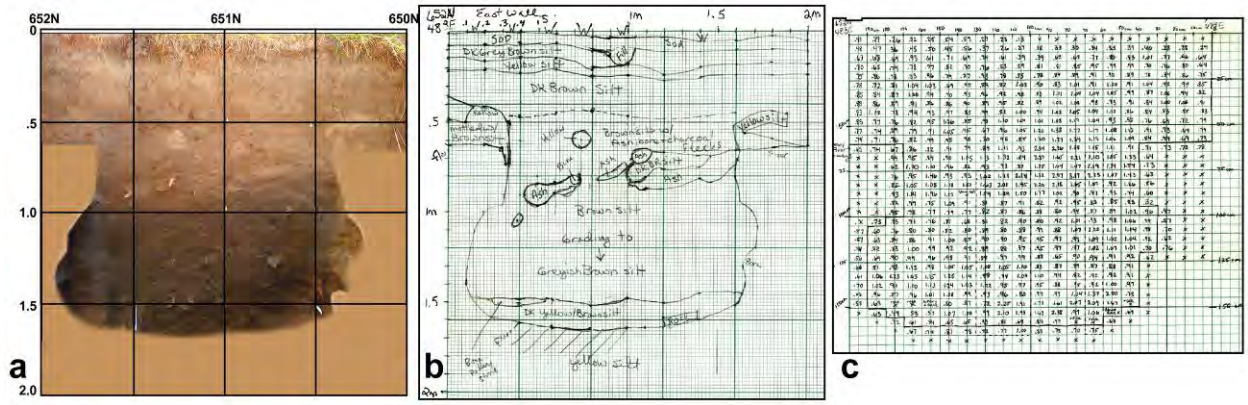

Figure 3.5. *Results of data recording in the subterranean storage pit: a) composite photograph of profile, b) profile map, and c) hand-written MS2F measurements. Poor lighting near the bottom of the pit degraded the quality of the photographic imaging.*

After fieldwork, the data on the graph paper sheets were entered into a spreadsheet (MS Excel) and then read into a GIS (Idrisi) for processing, analysis, and display.

RESULTS

In this section, the results of the profile MS mapping are given for each archaeological feature investigated. Comparisons are made of MS against observed stratigraphy and MG findings previously recorded at the surface from 2001-2004 (Kvamme and Ahler 2007), and against theoretical expectations achieved through mathematical modeling. Additionally, comparisons are made between the data from the various MS instruments employed in the profile mapping.

Profile A: Subterranean Storage Pit

This storage pit was initially discovered through a marked anomaly in a MG survey conducted in 2001 (Figure 3.1b; Kvamme and Ahler 2007). Half of it was subsequently excavated in 2004 and designated as Feature 701. Ahler's (2005a:84-89) original summary of the excavation reveals a sod layer followed by a dark gray-brown silt layer and a lighter gray-brown silt layer, each about 10 cm thick and representing the A horizon and A-B transition (Figure 3.6a). This is followed by a 40 cm thick unit common to the region consisting of homogenized brown silt with dispersed artifacts and little structure. This unit includes the lower part of the natural B horizon which transitions to the C horizon at a depth of 60 cm. At a depth of about 50 cm, however, hints of the pit orifice could be vaguely discerned by a fill of darker sediments containing artifacts. Excavation of the pit, as a designated feature, began at a depth of 60 cm and continued through to its bottom at a depth of 1.6 m. Its minimum diameter at the orifice is 1.3 m and its maximum diameter of 1.75 m occurs at a depth of 1.2 m below the surface. Ahler (2005a:84) estimated a total storage volume of about 1.4 m^3. This pit is jug-shaped with its greatest diameter well above the floor, which is concave in form (Figures 3.6a). Sediments with many artifacts filled the pit, particularly near the bottom where much bone occurred. Culturally introduced materials include pottery, bone, fire-cracked rock, charcoal, ash, shell, and lithics

(flakes and bifaces), deposited in many episodes, few of which are visible stratigraphically. A concentration of bone and ash near the bottom suggest a distinct dumping episode, but thick strata within the pit indicates large amounts of sediment were dumped in relatively few episodes. The walls of the pit itself show no indications of erosion, suggesting it was filled rapidly. An ashy layer at about 80 cm below the surface could indicate household hearth-cleaning activities deposited in one or more episodes. Significant rodent disturbances occur throughout the pit.

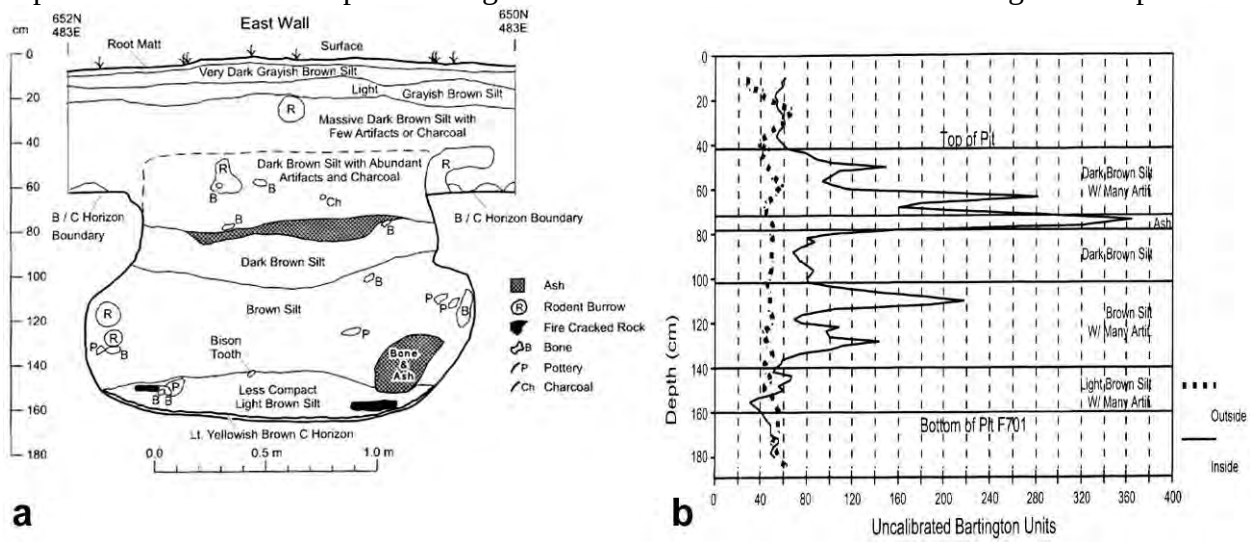

Figure 3.6. *Storage pit excavation data from 2004: a) profile map, and b) MS2H core-hole data plotted against depth and stratigraphic units (after Ahler 2005a:Figure 38). The locus of the core-hole was approximately down the center of the pit.*

Initial down-hole MS investigation

Initial MS measurements were acquired in this storage pit in 2004 by Rinita Dalan (2008; see also Ahler 2005a:86-89) in a single 2.5 cm diameter hole down its center, but 30 cm beyond its face, using the down-hole MS2H instrument. These results indicated high levels of MS compared to in-situ deposits outside of the pit that explained the formation of the large MG anomaly (Figure 3.6b; see also Figure 3.1b). Moreover, complex variation in MS down the length of the hole appeared to correlate well with observed stratigraphic changes, particularly with the layer of ash and the dark brown silt with many artifacts (Figure 3.6b). These data, along with dumping episodes visible in the profile, suggest individual deposits of materials possessing varied levels of MS, representing individual basket loads of material as the pit was filled from various sources, including ash from a hearth cleaning and associated sediments of high MS. These MS data offer a good complement to the traditional stratigraphic profile in their general agreement, but also in the additional information they offer. They give (1) a clear indication of the beginning depth of the pit by the sudden rise in MS at a depth of about 42 cm, and (2) evidence of individual sediment packets, perhaps dumping episodes, that possess very high or very low MS (the various "peaks and valleys" in the graph in Figure 3.6b). Many of these episodes are not seen visually in the stratigraphic profile.

Photo-mosaic and profile

Our profile photography and stratigraphic mapping yield similar views of the storage pit that compare well against the 2004 data, but with some minor differences owing to the profile being cut back about 5 cm to achieve a fresh face for the magnetic measurements. In general,

individual basket loads of deposits are not visible in the profile, with the exception of the pockets of ash and the associated lens of very dark brown silt, which was packed with charcoal and appeared to be composed largely of burned earth (Figure 3.7a, b). The photo composite reveals numerous pieces of rock, bone, and occasional ceramic sherds in the profile wall which were not mapped. We did not distinguish a sharp boundary between the lower dark brown silt and brown silt units as was observed in 2004, but rather saw it as an indistinct gradation. Additionally, we saw no strong evidence of the lower ash pocket mapped in 2004 (compare Figures 3.6a, 3.7), but it may indeed have been a small pocket that was removed by our excavations.

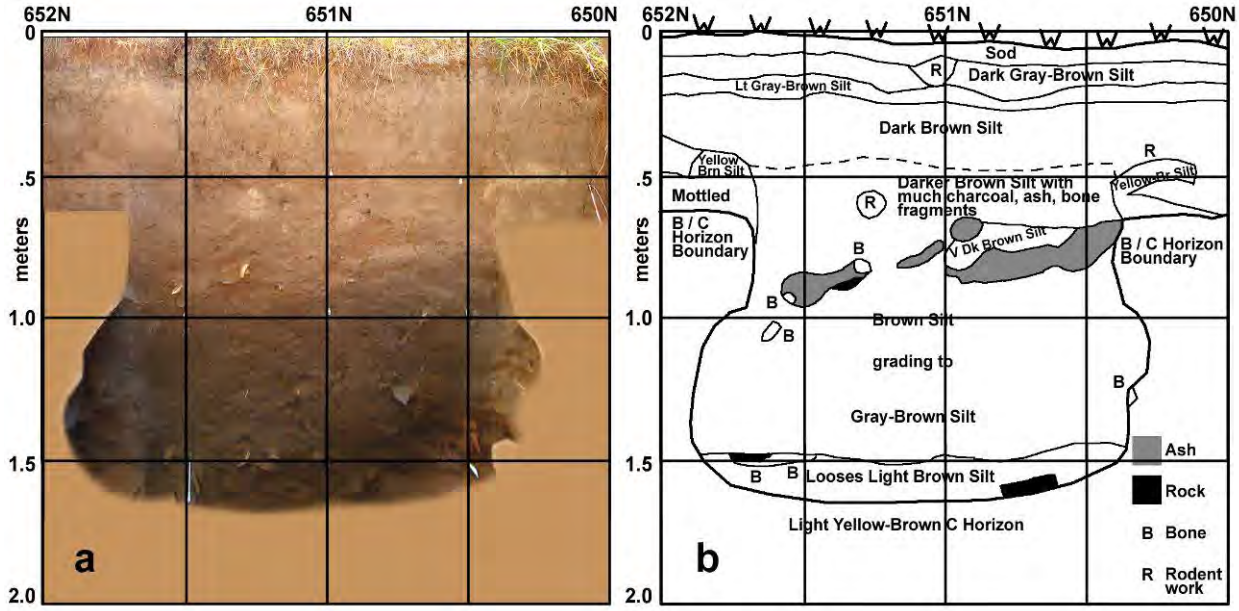

Figure 3.7. *Storage pit profile on east wall excavation: a) photomosaic, and b) drawn profile. The 2x2 m profile lies on the east wall of the excavation at E483 in the Double Ditch local coordinate system, with north coordinates indicated. North is to the left.*

The MS measurements

MS measurements were acquired with the MS2F and KT-9 every 5 cm in the vertical direction and every 10 cm horizontally. This permitted 519 measurements with the MS2F and 503 with the KT-9, a somewhat smaller number because this larger instrument made it difficult to acquire data in tight places within the constricted pit. Results are given in Figure 3.8a, b, color-coded by MS. For comparison against the visual record, interpreted profile lines are superimposed. Additionally, to reduce pixelation and better approximate the continuous nature of MS, the data were resampled to a resolution of 2.5 x 2.5 cm by GIS methods (Figure 3.8e, f).

Comparisons of the MS maps to the photomosaic and the drawn profile (Figures 3.7-3.8) reveal many similarities and differences. Large parallels are immediately obvious in the locus of the large ash lenses and burned earth midway down the profiles and the multiple regions of high MS that correspond well. High MS also occurs near the bottom of the pit near the loci of several rocks that illustrate high MS, possibly signifying fire-cracked rock with elevated MS and associated sediments of high MS from a hearth cleaning. The prominent rodent burrows in the top third of the pit (Figure 3.7b) indicate low MS owing to different fills, some composed of C-horizon materials of low MS or less compact low-density fills, causing reduced MS. Significantly, the top of the pit at the level of its orifice, between .4-.5 m deep, shows a mild jump in MS that probably corresponds with the darker matrix that the excavators observed

(Ahler 2005a:84-85; arrows, Figure 3.8c). While the stratigraphic profile suggests uniformity with each stratum, the MS data clearly indicate this is not the case, as measurements vary horizontally at each elevation. This is particularly true in the lower half of the pit where there appears to be many pockets of high and low MS, probably direct evidence of individual fill episodes composed of sediment loads with differing levels of MS.

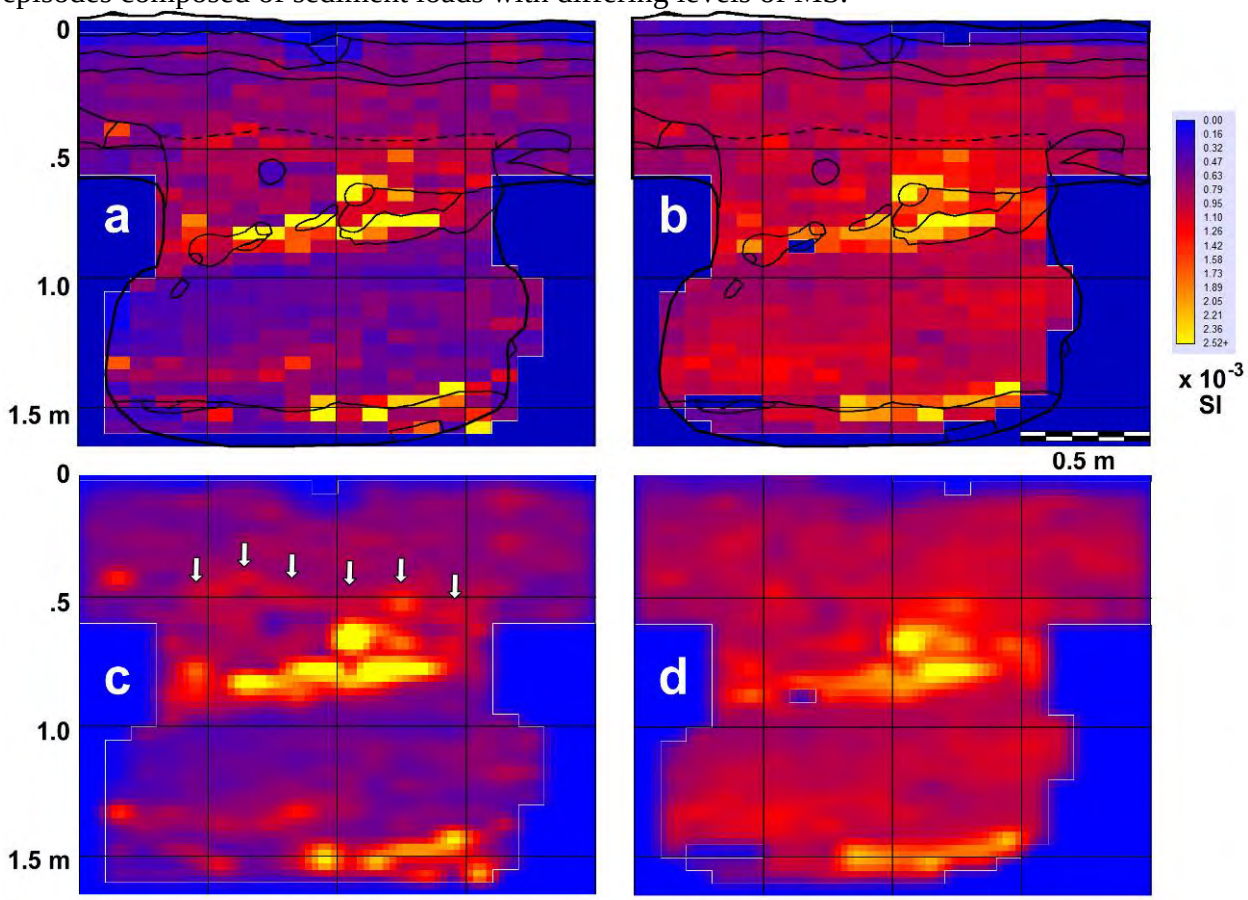

Figure 3.8. *MS measurements in the storage pit: a) MS2F, b) KT-9, c) resampled MS2F, and d) resampled KT-9. The raw data in a-b occur at a resolution of 5x10 cm; the resampled imagery in c-d is at a spatial resolution of 2.5x2.5 cm.*

Sensor differences

A principal difference between the two instruments is that the measurements from the MS2F appear to generally be lower than those from the KT-9 (Figure 3.8), and this is borne out statistically (Table 3.1). The MS2F yields a mean of $.744 \times 10^{-3}$ SI while the KT-9 gives a mean of $.966 \times 10^{-3}$ SI for the more than 500 measurements. A paired-difference test (Hays 1988) was conducted not on the full sample, but on a systematic unaligned random sample composed of $n=35$ measurements taken from the pit. This was undertaken to reduce the apparent spatial autocorrelation inherent in these data and more closely approximate statistical independence (a requirement of the test). The results yield a mean difference of $.27 \times 10^{-3}$ SI with s.d.=$.173 \times 10^{-3}$ SI, yielding t=9.23 and pointing to a highly significant difference (p<.0001). This difference can also be seen visually in a comparison of the histograms (Figure 3.9a, b).

Table 3.1. *Descriptive statistics for the raw MS pit measurements. All measurements x 10^{-3} SI.*					
Instrument	*N*	*Mean*	*s.d.*	*Min*	*Max*
MS2F	519	.744	.519	.04	4.66
KT-9	503	.966	.383	.13	3.70

At the same time, the MS2F yields more extreme measurements, with many that far surpass the maximum value obtained by the KT-9 (Figure 3.9a, b). This circumstance is reflected by the much higher s.d. of the MS2F data (Table 3.1) and can be seen visually in the magnetic profiles of Figure 3.8. Nevertheless, spatial patterns in the data sets do parallel each other well, and this correspondence is indicated by a Pearson's correlation coefficient between the redundant raw measurements of *r*=.82 (Figure 3.9c). A logarithmic plot was also examined owing to the skewness of the data which better indicates the relationship (but with *r*=.78; Figure 3.9d).

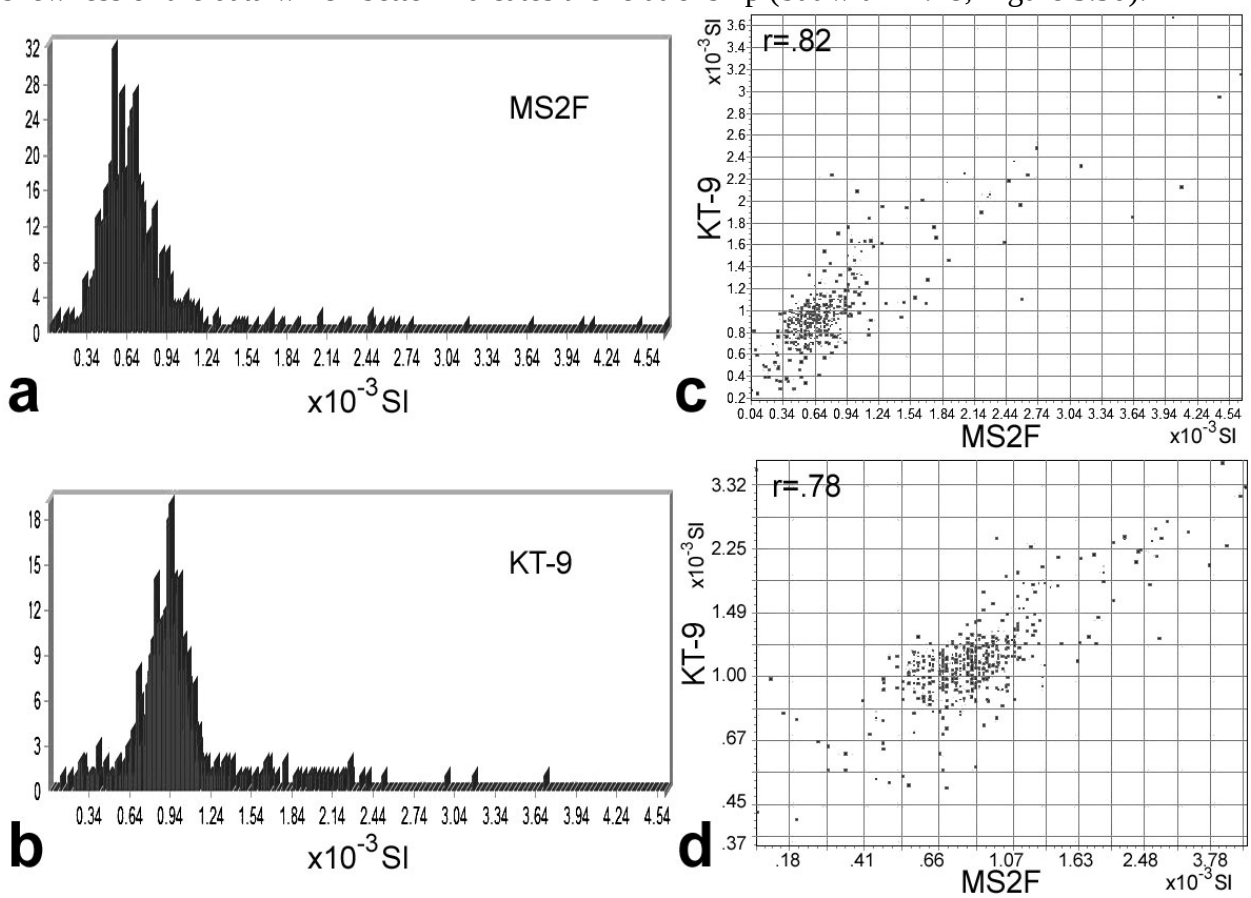

Figure 3.9. *Graphical data for the MS instrumentation: a) MS2F, b) KT-9. c) raw plot of data correspondences, and d) logarithmic plot*

The differences and variation between the two datasets are explained by a number of factors, chief of which are differences in lateral and depth sensitivities. The MS2F sensor head is only 15 mm in diameter and 90% of the measured signal is derived within 6 mm of its face (Bartington Instruments 2013). The KT-9 sensor diameter is 65 mm and 90% of the signal arrives within 20 mm of its face (Exploranium 1997), so this instrument has a much wider and deeper sensitivity than the former. The effect of the latter is like an averaging or low-pass filter where MS is smoothed over a broader and deeper region, and this agrees with the graphical

results in Figure 3.8. It is also certainly the case that small variations in the placement of the instruments while recording the data contributed to the observed differences (Figure 3.9).

Comparison with down-hole results

A comparison between our profile MS results with those of Dalan's (2008) MS2H work of 2004 can be accomplished by extracting the central column of data from our MS wall profile. The comparison is not perfect because Dalan's down-hole profile was taken 30 cm *behind* our profile face where somewhat different deposits are likely to occur. Moreover, our data were sampled every 5 cm vertically, while Dalan's were sampled every 2 cm. In addition, her data were presented in arbitrary (uncalibrated) "Bartington units" while ours are quantified in SI units. Nevertheless, the shapes of the curves may be compared. The data indicate interesting parallels (Figure 3.10) with similar peaks and valleys indicating high and low MS, respectively, at broadly similar depths. Yet, off-sets between the various local maxima are apparent and point to differences in depths and deposits between the loci of these vertical profiles, only 25-30 cm apart.

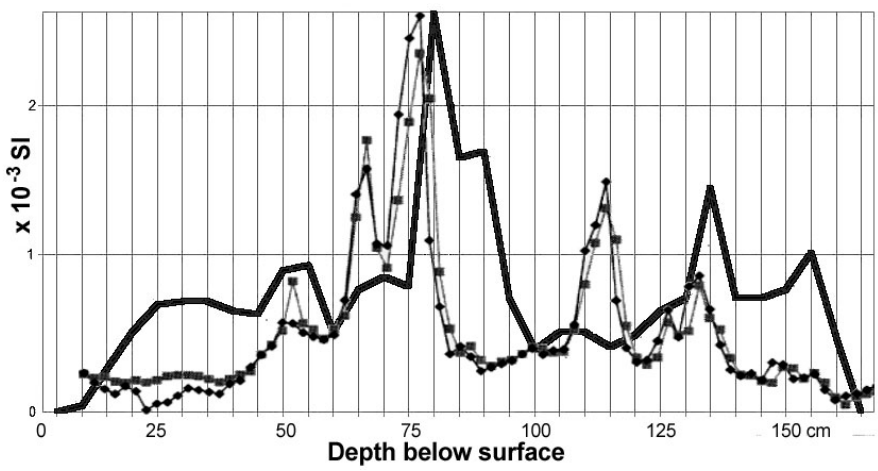

Figure 3.10. *Comparison of two repeated down-hole MS2H profiles (dotted lines) with equivalent MS2F profile (bold line) taken from pit centerline. Note that vertical scale of MS2H data is approximate.*

Magnetic gradiometry

The foregoing has illustrated the nature of magnetic variation within a typical storage pit through a detailed mapping of MS through its entire cross-section. But how is this variation expressed on the surface and what is recorded by a MG that passes over that surface? The raw measurements recorded by a MG (the Geoscan Research FM-36; see Chapter 1) in the vicinity of the pit in 2001 are illustrated in Figure 3.11a. North-south transects were separated by .5 m and measurements were recorded every .25 m. Evidence of the pit in the form of strong positive magnetic anomalies were recorded in at least 4 transects, with minor anomalies expressed in two others. A profile view of the transect most closely coincident with our profile face (at coordinate 483E) is illustrated in Figure 3.11b. It reveals the maximum anomaly strength of 5.19 nT near the center of the pit, with rapid fall-off to neutral, near-zero measurements to the left and right. It is obvious that the minor lateral sensitivity of the instrument detects the pit's enhanced magnetism beyond the actual extent of the pit.

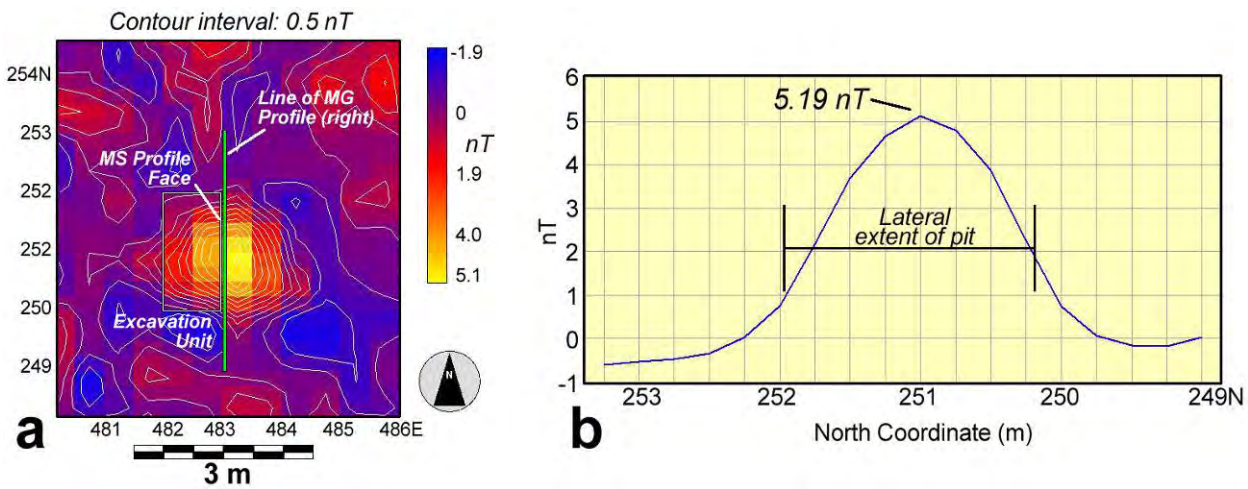

Figure 3.11. *Magnetic gradiometry in vicinity of storage pit in a) plan, and b) profile views.*

Modeling maximum pit magnetism

Breiner (1973:24), Burger et al. (2006:444), and others give equations for modeling the maximum value of a dipole source based solely on the induced magnetic component, which gives a simple start-point. Scollar (1990: 428) notes that "since the remanent magnetism of any buried structure is nearly never known, [its] formulation is not of practical importance." With the high magnetic latitude of North Dakota vertical magnetization may initially be assumed, so:

$$F = (2M)/(4\pi d^{3}) \qquad \text{Eq. 1.}$$

The magnetic moment $M=\Delta kHV$, where k is the MS contrast between the dipole source and its surroundings, H is the ambient field strength, and V is the volume of the source. The parameter d is the distance between the center of the dipole source and the sensor. When working with gradiometry data the equation must be solved twice, once for each sensor, and a difference between bottom and top sensors computed.

<u>*Model 1*</u>. The MS2F measurements in the pit are again illustrated in Figure 3.12a, with a number of simple geometrical models of the pit superimposed. In both models, the top magnetic unit is ignored because it is considered a uniform stratum that covers much of this region of the site and therefore produces a constant anomaly. In the first model, the geometry was modeled as a sphere with radius r=.7 m, which yields a volume of $V=4/3\pi r^3=1.44$ m^3. Note that this value is extremely close to the volume of 1.4 m^3 estimated by Ahler (2005a:84). GIS methods were used to compute the average MS within the sphere (the target), which was $k_T=.844\text{x}10^{-3}$ SI. Background MS measured on the excavation walls outside of the pit gave $k_B=.450\text{x}10^{-3}$ SI, so the magnetic contrast is $\Delta k=.844\text{x}10^{-3}-.450\text{x}10^{-3}=.394\text{ x}10^{-3}$ SI. The Fort Clark State Historic Site is located at: 47.2519° N, 101.2753°. The National Geophysical Data Center on-line magnetic field calculator (<u>http://www.ngdc.noaa.gov/geomag-web/#igrfwmm</u>) indicates that on July 1, 2012 (about the time of our fieldwork), the total magnetic field strength was H=56,503 nT (with an inclination angle I=72.79^o). The center of the sphere lies at a depth of approximately d_0=1.05 m below the surface. The original MG survey was carried out with a FM-36 by Geoscan Research (see Chapter 1), which has two sensors, so the anomaly strength, F, must be computed twice and differenced. The FM-36 has a bottom sensor typically carried about .3 m above the surface and a

top sensor a half-meter higher, at about .8 m. This gives $d_1=d_0+.3=1.35$ and $d_2=d_0+.8=d_1+.5=1.85$ m. These relevant data are summarized in Table 3.2.

Table 3.2. *Data for storage pit Model 1 based on sphere.*
k_T=.844x10^{-3} SI; k_B=.450x10^{-3} SI; Δk=.394 x10^{-3} SI
H=56,503; I=72.79^o; V=1.44 m^3; d_1=1.35 m; d_2=1.85 m

Solving for d_1 gives:

$$F_1 = (2 \times .000394 \times 56{,}503 \times 1.44)/(4\pi 1.35^3) = 2.07 \text{ nT}$$

for d_2:

$$F_2 = (2 \times .000394 \times 56{,}503 \times 1.44)/(4\pi 1.85^3) = 0.81 \text{ nT}$$

and

$$F=F_1-F_2=1.26 \text{ nT}.$$

Incidentally, considering the inclination angle at this far northern magnetic latitude gives little difference using sin(I)F, since: sin(72.79^o)1.26 nT=1.20 nT. This model considers only the induced magnetic component, so the result is likely a little low as materials with remanent magnetism likely occur in some of the hearth-cleaning deposits (Figure 3.7). Yet, it is obvious that this model is unsatisfactory, with the MG survey giving 5.19 nT as the anomaly maximum (Figure 3.11b).

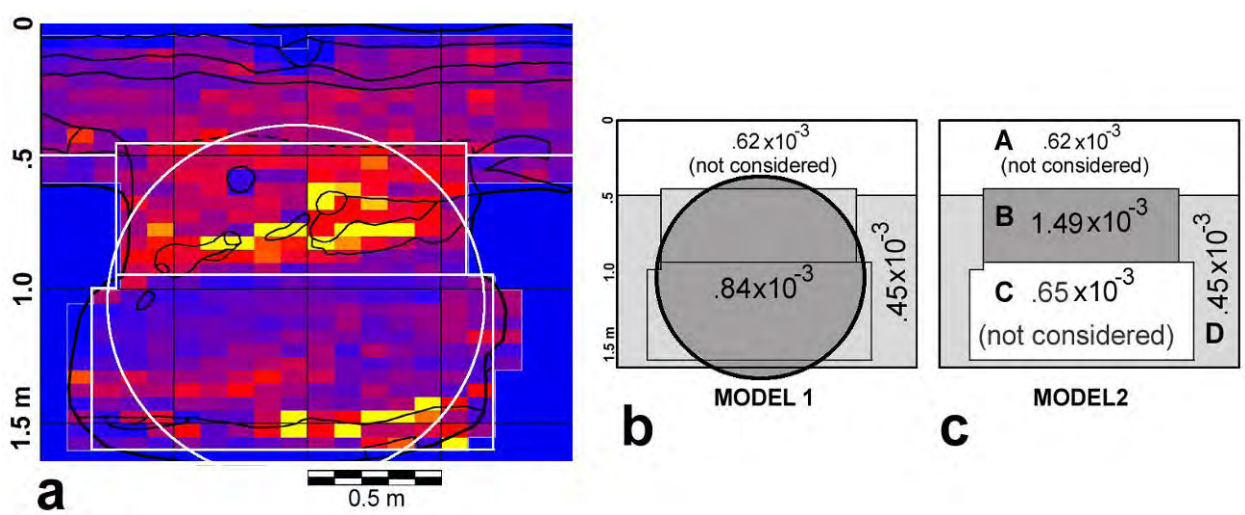

Figure 3.12. *Storage pit MS and models with a) showing MS2F measurements with stratigraphy (black) and simple structural models superimposed (in white), b) presents a simple spherical model with average MS values, and c) offers a model that recognizes the complexity of the pit's structure, with average MS values. All measurements in SI units.*

<u>*Model 2*</u>. Close examination of the profile MS measurements (Figure 3.12a) suggests problems with the foregoing model. The pit is actually composed of *two* units, Unit B of high MS at the pit's orifice, and Unit C of sediments below that generally exhibit low MS (a small pocket of higher MS near the pit bottom is not significant owing to its depth; Figure 3.12c). The average MS of Unit C is .65x10^{-3} SI, approximately the same as the near-surface unit A. As Unit C is deep and offers little magnetic contrast against the background (Unit D with .45 x 10^{-3} SI), it

is not here considered and Unit A is omitted again for reasons cited above. In this model the contrast is between Units B-D, and Unit B is modeled as a cylinder with height, h=.5m, radius, r= .65 m, Volume, $V=h\pi r^2$=.664 m^3, and depth of its center below the surface of .7 m. All relevant data are summarized in Table 3.3.

Table 3.3. *Data for layered storage pit Model 2.*
k_T=1.491x10^{-3} SI; k_B=.450x10^{-3} SI; Δk=1.041 x10^{-3} SI H=56,503; I=72.79^o; V=.664 m^3; d_1=1 m; d_2=1.5 m

Solving for d_1 gives:

$$F_1 = (2 \times .001041 \times 56{,}503 \times .664)/(4\pi 1^3) = 6.22 \text{ nT}$$

for d_2:

$$F_2 = (2 \times .001041 \times 56{,}503 \times .664)/(4\pi 1.5^3) = 1.84 \text{ nT}$$

and

$$F=F_1-F_2=4.38 \text{ nT}.$$

Correcting for the inclination angle with sin(I)F gives: sin(72.79^o)4.38 nT=4.18 nT. This model gives a much closer fit given the approximate values and volumes used here, and adding a small value to account for likely remanent magnetism within the pit puts the maximum closer to the realized MG value (Figure 3.11b).

Modeling pit magnetism two-dimensionally

Scollar (1990:423-439) presents an approach for the three-dimensional modeling of induced magnetic anomalies generated by archaeological features of arbitrary shape. This approach was later followed and elaborated by Eder-Hinterleitner et al. (1996) and Neubauer (2001). The basic idea divides an archaeological feature (the magnetic source) of arbitrary shape into a series of small cubes of equal size, each of which is treated as a dipole source. The magnetic effect of a cube can then be computed for a sensor located above the surface in *each* of a wide variety of sensor positions. The magnetic effect is then computed cube-by-cube over every cube within the arbitrary shape and summed to generate the shape of the magnetic anomaly recorded on the surface. This approach is complex mathematically and computationally. Following Eder-Hinterleitner et al. (1996:132-133; see also Scollar 1990:428), and similar to Eq. 1, the magnetic anomaly generated by a dipole source in any cube comprising an archaeological feature is calculated as:

$$F = HkVD \qquad \text{Eq. 2.}$$

where H is the ambient field strength, k is the MS contrast of the dipole source, V is its volume, and D represents a distance function between the position of the sensor and the position of the dipole source (cube). D is computed as follows:

$$D = \frac{x^2(3\cos^2 I-1) + z^2(3\sin^2 I-1) - y^2 - 6xz\sin I\cos I}{(x^2+y^2+z^2)^{\frac{5}{2}}} \qquad \text{Eq. 3.}$$

where x, y, and z are distances between the position of the sensor and the position of the dipole source on x (north-south), y (east-west), and z (depth) axes, and I is the inclination angle (Scollar

1990:428). The *x*-axis is assumed to be in the direction of the dipole (i.e., magnetic north); our profile face is aligned with geographic north where the declination angle of approximately 6° gives negligible effect. D can be described as "the influence of each dipole source on the measuring device [sensor]" (Eder-Hinterleitner et al. 1996:133).

In the context of our pit profile we are dealing with a two-dimensional face and we therefore need to work only with the two dimensions of *x* and *z*, since the profile face is oriented approximately north-south and distances on the *y*-axis (east-west) are therefore zero. This simplifies the expression to:

$$D = \frac{x^2(3\cos^2 I - 1) + z^2(3\sin^2 I - 1) - 6xz\sin I\cos I}{(x^2+z^2)^{\frac{5}{2}}}$$

Eq. 4.

Obviously, Eq. 2. must be computed twice, once for each sensor in a gradiometer, followed by calculation of their difference, or we can compute:

$$F = HkV(D_1 - D_2) \qquad \text{Eq. 5.}$$

where D_1 and D_2 represent the distance function applied to the bottom and top sensors, respectively.

Implementation of this model (Eq. 5) was greatly facilitated by GIS. It was accomplished in a series of modeling steps.

1. The top stratum that blankets a wide area of the site and covers the pit above about .55 m was removed from the raster representation of the MS2F profile because its uniform magnetism is not relevant to the problem (as before). This left a raster of 20 columns (for the 2 m profile width on the *x*-axis) x 21 rows (for its remaining depth on the *z*-axis from .55-1.55 m below the surface) with a spatial resolution of .1 x .05 m for the respective *x* and *z* axes (Figure 3.13g). All rasters in the following are of this dimension and resolution unless otherwise specified.
2. "Z_{BOTTOM}" and "Z_{TOP}" rasters were created with *each row* representing the distance below the top and bottom sensors, respectively (ranging from .825-1.825 m for the bottom sensor and 1.325-2.325 m for the top sensor; Figure 3.13a, b).
3. A separate raster was created for *each* possible horizontal (*x*-axis) position of the sensors (i.e., over every column or every .1 m) which held the distance to every other position (column), with distances northward positive and southward negative. Twenty such rasters were computed and named "X1-X20" based on the reference column; the one showing *x*-axis distances from the middle column at X11 (profile center) is shown in Figure 3.13c.
4. The distance function, D, was computed (Eq. 4) with $I = 72.79^o$ (as above), for each sensor using Z_{BOTTOM} and Z_{TOP} to yield D_1 and D_2. This had to be undertaken for *each* of the 20 "X" layers (each column) and for each sensor, creating distance influence layers "$D_1$1- $D_1$20" and "$D_2$1- $D_2$20". The per-cell distance influence, D_1, on the bottom sensor when it is centered over column 11 in the center of the profile is illustrated in Figure 3.13d while the distance influence, D_2, on the top sensor is given in Figure 3.13e. Their difference (D_1-D_2) is shown in Figure 3.13f.

5. The raster holding the raw MS values (Figure 3.13g) was converted to Δk contrasts with the background (Figure 3.13h) by subtracting the representative value of $.45 \times 10^{-3}$ SI for that unit (see Figure 3.12). *k* was then multiplied by the total magnetic field strength, *H*=56,503 nT, as above, and the volume of a cell, determined as V=.5 x .1 x .1 m = .0005 m^3. The result gives the magnetic moment H*k*V (Figure 3.13i). These calculations change only the values in the cells, not their relative magnitudes, so the mappings look the same and only the scales change (Figure 3.13g, h, i).
6. The result of Step 5 was then multiplied by the difference of the distance function computed for each sensor (D_1-D_2) for *each* of the 20 columns to yield the total magnetic contribution in nT on a per-cell basis. This created rasters "NT1-NT20" (NT11 is illustrated in Figure 3.13j).
7. For each raster NT1-NT20, the nT values in each cell of the profile were summed in each column to yield 20 rasters ("SUM1-SUM20") each containing *one* row and 20 columns (the result for column 11 is given in Figure 3.13k). This indicates the total contribution of *each column* in the profile to a MG at a particular *x*-axis position (and *z*-axis height) over the profile.
8. Finally, the individual sums per *x*-axis position were summed to yield the total anomaly strength in nT *due to induced magnetism* that should be recorded by a magnetic gradiometer at the surface in each position of the profile (Figure 3.13l). This profile is graphed in Figure 3.13m).

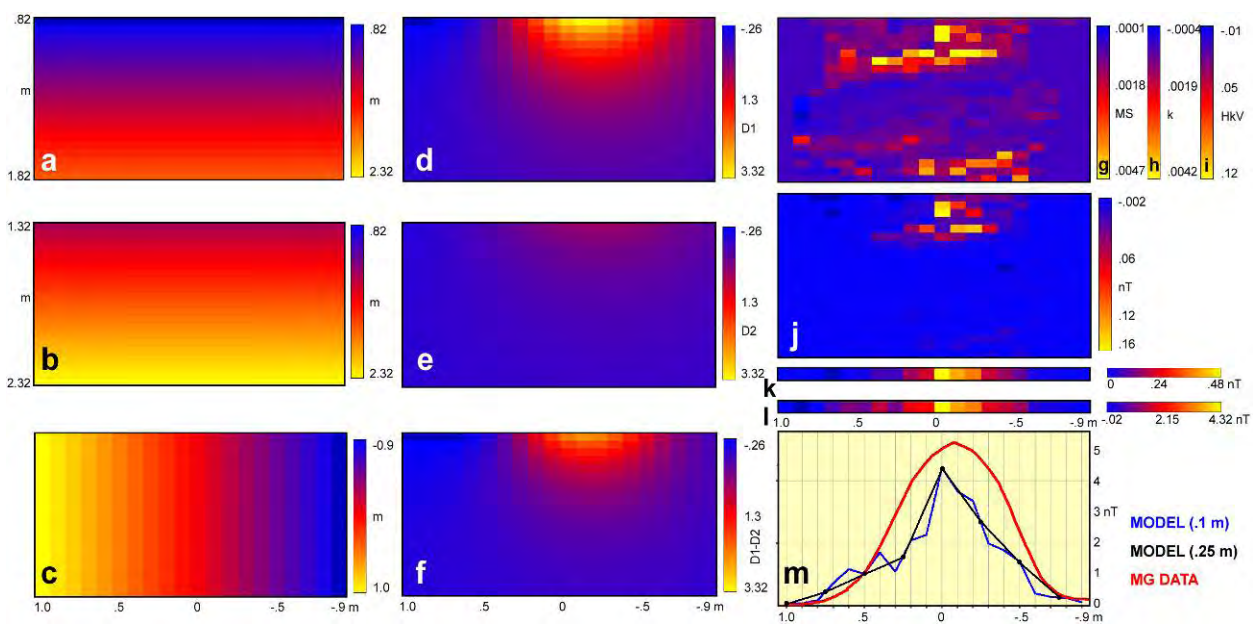

Figure 3.13. *Two-dimensional magnetic model by raster GIS: a) distance below bottom sensor for all sensor positions, b) distance below top sensor, c) horizontal distances from column 11, d) distance function (D_1) from bottom sensor (column 11), e) distance function (D_2) from top sensor, f) difference D_1-D_2, g) raw MS measurements, h) MS contrasts, k, i) magnetic moment HkV, j) contribution of nT per cell from position over column 11, k) sum of contribution of nT per column with sensor over column 11, l) total sum of nT contributions per column, m) graph of l. NOTE: c, d, e, f, j, k) are illustrated for central column 11 only.*

The graph in Figure 3.13m illustrates results expected by the model (blue) against the actual MG results recorded in 2001 (red). The fit seems only fair, however. We note the modeled maximum of 4.4 nT is somewhat lower than the observed of 5.2 nT, and this may be due to consideration of only induced magnetism, as explained earlier. There is also marked asymmetry and lack of "smoothness" in the model results compared to the actual. This may result from a number of factors.

a. *Sampling density*. The model employed a horizontal resolution of .1 m, but the MG survey utilized a sampling interval of .25 m. A third graph is therefore plotted in Figure 3.13m (in black) that simulates model results at this resolution and it is much smoother and more closely conforms with the realized MG data, although some skewness yet exists.
b. *Remanent magnetism*. It is obvious that burned earth from hearth cleanings exist and were dumped into the pit, although the volume of this material is undoubtedly low. Dipole alignments of this material cannot be predicted and they could add or detract somewhat from field strength recorded at the surface and alter the shape of the curve.
c. *Off-set between profile & transect*. The difference between the model and actual may also be due to an off-set between the location of the profile where MS was recorded and the actual position where the MG transect used in Figure 3.13m was walked. This transect was simply the closest to the profile locus, and with a half-meter between the 2001 transects there is considerable "wiggle room" compared to the line of the excavated profile. Given the great variation in storage pit content in terms of basket loadings of sediments and their magnetic compositions, evidenced by the difference between our 2012 profile (Figure 3.7) and the 2004 profile (Figure 3.6), the MG results at the surface could vary considerably between transect only a few decimeters apart.
d. *Lateral magnetic effects from y-axis not considered*. MS was recorded on only a single plane on the *x*-*z* axes at *y*=0. Obviously, MS occurring to the west or east of this plane (on the *y*-axis) was not measured and its effect was therefore not included in the model (Figure 3.13j illustrates the contribution of lateral magnetism on the *x*-axis from a single sensor position, and a similar result must also occur on the *y*-axis).
e. *"Averaging" not employed.* We note Eder-Hinterleitner et al. (1996) and Neubauer (2001) both utilize average magnetic contrasts within stratigraphic units in their modeling efforts, rather than the per-cell values of delta *k* employed here. This methodology undoubtedly introduces a smoothing or generalizing effect. This approach was not investigated here.

The asymmetry in the model results appears correct when one considers the distribution of the raw MS measurements (Figure 3.13g). The right (south) side of the pit is where most of the high MS contrasts exist, and this is reflected in the model.

Profile B: Fortification Ditch

The second type of archaeological feature investigated for its magnetic properties is a fortification ditch located on the outer periphery of the village (labeled "B" in Figure 3.2). The ditch in question is designated as "Ditch 4," and dates most likely to the late 15th century (Ahler 2005b). There is no visible evidence of this ditch on the surface and it was only discovered by magnetic gradiometry in 2002 as a mildly robust positive magnetic feature (Crawford and Ahler

2003). The positive anomaly was explained as a result of the ditch being sealed as the village contracted, most likely with local topsoil, including magnetically enriched settlement soil, and other sediments (Kvamme 2003c). The net result is a large concentrated volume of soils and sediments of higher MS than the surrounding natural matrix, causing a magnetic contrast.

Photo-mosaic and profile

A 2 x 5 m trench crossing this ditch at a right angle was excavated in 2002 subsequent to the MG survey, described by Crawford and Ahler (2003) as "Feature 205." They note (p. 97) the "feature fill was similar in color and texture to the surrounding matrix but contained large bones, sherds, fire-cracked rock, and other less blatant detritus of village activity such as clay mottles and charcoal flecks"—giving clear evidence of fill from village sediments. The ditch was shown to be 2.25 m wide with an ultimate depth below surface of 1.62 m. Several layers of "natural" sediments were encountered, including a thick one of light yellow-brown silt undoubtedly derived from parent C-horizon materials which appear identical (Figure 3.14a). This was interpreted by Crawford and Ahler (2003:98) as "spoil or backdirt removed from a nearby excavation by the villagers." Other lenses of dumped sediments were encountered through much of the trench, including ash, and bone, sherds, and fire-cracked rock were prevalent in the uppermost 20 cm, fell off in density between 20-40 cm, and "increased and decreased in density throughout the levels" (Crawford and Ahler 2003:98). The excavators concluded that the ditch was filled first with eroded sediments followed by "dumped trash and earthen fill" (Crawford and Ahler 2003: 111).

Strangely, there is no hint in the profile of a spoil pile on either side of the trench resulting from its excavation or were post holes observed on its interior side where a palisade once would have stood (Figure 3.14a), common features of fortification ditches (Crawford and Ahler 2003:110). Later excavations and analyses indicated that a broad outer zone of near surface soils and sediments had been stripped from the surface of Double Ditch for various constructions causing this upper zone to be removed from the profile. Consequently, the upper part of the profile seen in Figure 3.14 has been truncated or removed from the scene, leaving only bottom portions of the ditch.

Our mapping and photography of the re-excavated profile broadly agrees with the results of 2002 (Figure 3.14b, c). Some of the variations between the decade-apart results arise because our profile was cut back about 5-10 cm from the locus of the former face, which undoubtedly introduced the minor differences seen here.

The MS measurements

The MS mapping of the profile was undertaken with 10 cm horizontal and vertical sampling intervals owing to the profile's large size. MS properties of the fully exposed 5 m long profile were mapped with the KT-9 (Figure 3.15a, b) and the MS2F (Figure 3.15c, d). For comparison purposes, MS in a meter-wide segment of the ditch profile was also mapped by the MS2D at its deepest point (Figure 3.15e, f).

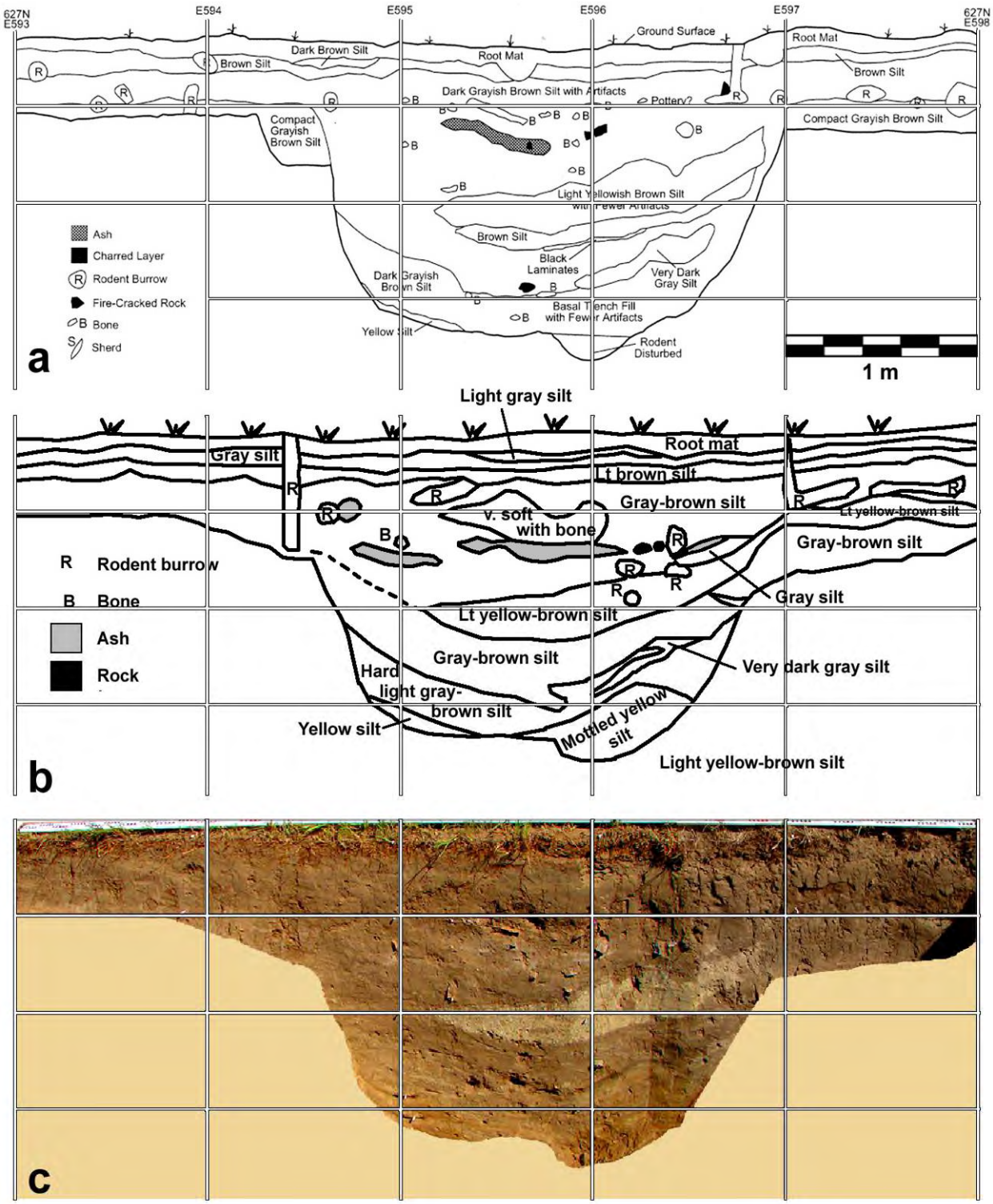

Figure 3.14. *Excavation profile through Ditch 4 showing observed stratigraphy as mapped in a) 2002, b) in 2012, and c) photographed in 2012. The 2x5 m profile lies on the north wall of the excavation at N627 in the Double Ditch local coordinate system, with east coordinates indicated. East is to the right.*

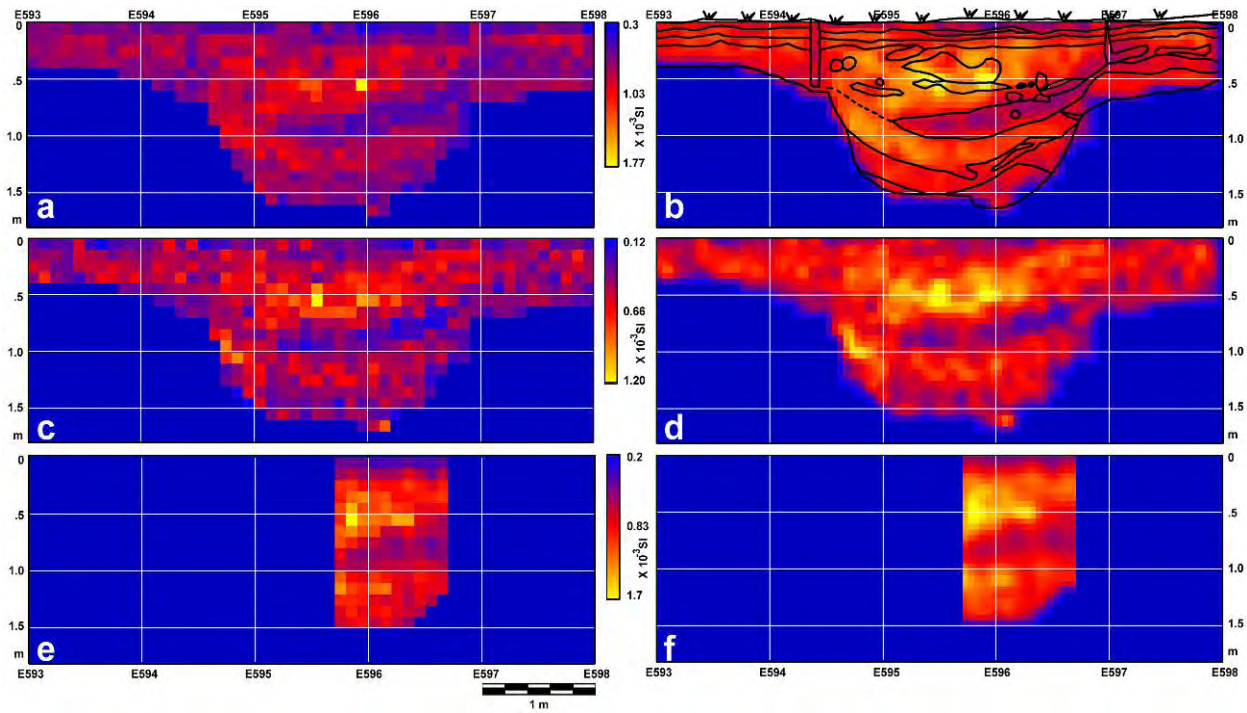

Figure 3.15. *MS mappings of the ditch profile: a) KT-9 raw data, c) MS2F raw data, e) MS2D raw data. Images in the right column have been resampled to 5 x 5 cm resolution and contrast-enhanced for improved visualization and correspond with images in the left column. The stratigraphic profile from 2012 is superimposed in b).*

The MS mappings in Figure 3.15 agree well with the visual mappings of stratigraphic changes and the photomosaic (Figure 3.14). Most apparent is the low MS in the "light yellow brown silt unit" that is so dominant in the photomosaic and represents a depositional unit derived from unmodified C-horizon material of generally low MS (typically about 0.4 x 10^{-3} SI) that was deposited by villagers as fill from some nearby excavation (Crawford and Ahler 2003:98). Immediately above this unit are zones and pockets of very high MS (1.2-1.8 x 10^{-3} SI) that correlate well with deposits of ash and fire-cracked rock (Figure 3.14). The raw magnetic profiles indicate decreased magnetism near the bottom of the ditch, which parallels the excavation report of lesser cultural material near the bottom (Crawford and Ahler 2003). The data also suggest somewhat elevated magnetism *above* the actual ditch compared to lateral areas to the right and left (Figure 3.15a, c). This may indicate upward migration of higher MS materials from bioturbation caused by rodents and insects. This observation has bearing on the mathematical modeling below. An interesting aspect of the MS mapping lies in its detail where the low MS characteristic of the loose fills of recent rodent work is clearly seen (e.g., at E594.5 in the KT-9 profiles, Figure 3.15a, b; compare Figure 3.14b). The profile section obtained from the MS2D sensor parallels well both of the other data sets.

Sensor differences

The relationships between the three MS sensors gives insights and parallel some of the previous findings. Data were extracted from the *N*=144 positions in which all three sensors were applied (i.e., confined to the MS2D survey of Figure 3.16e). As before, the MS2F measurements are significantly lower than those of the KT-9, with a mean difference of .264 x 10^{-3} SI

(Table3.4). Yet, the data from the common measurement points in the full profile (with *N*=484; Figure 3.15a, c) show a moderately strong correlation of *r*=.65, indicating parallel responses (Figure 3.16a). Returning to the common measurement space of all three surveys, the data in Table 3.4 indicate the MS2D measurements more closely parallel those of the KT-9 with only a small mean difference, and this view is supported by the scatterplots where the correlation between the MS2D and the KT-9 is much higher (*r*=.76) than the correlation between the MS2D and MS2F (with *r*=.62; Figure 3.16b, c). These findings make sense given the technical specifications of each device.

Table 3.4. *Descriptive statistics for the raw MS ditch measurements (x10^{-3} SI).*

Instrument	*N*	*Mean*	*s.d.*	*Min*	*Max*
MS2F	144	.479	.161	.14	1.20
KT-9	144	.743	.171	.30	1.77
MS2D	144	.780	.205	.20	1.47

The 15 mm diameter MS2F sensor receives 90% of the measured signal from within only 6 mm of its face (Bartington Instruments 2013). For the 65 mm diameter KT-9 sensor, 90% of its signal arrives within 20 mm of its face (Exploranium 1997), so this instrument offers a much wider and deeper sensitivity than the former. The MS2D possesses characteristics that are closer to those of the KT-9 with a coil diameter of 185 mm and 90% of its signal received within 60 mm (Bartington Instruments 2013). This causes closer descriptive statistics and a higher correlation with the KT-9 than occurs with the MS2F.

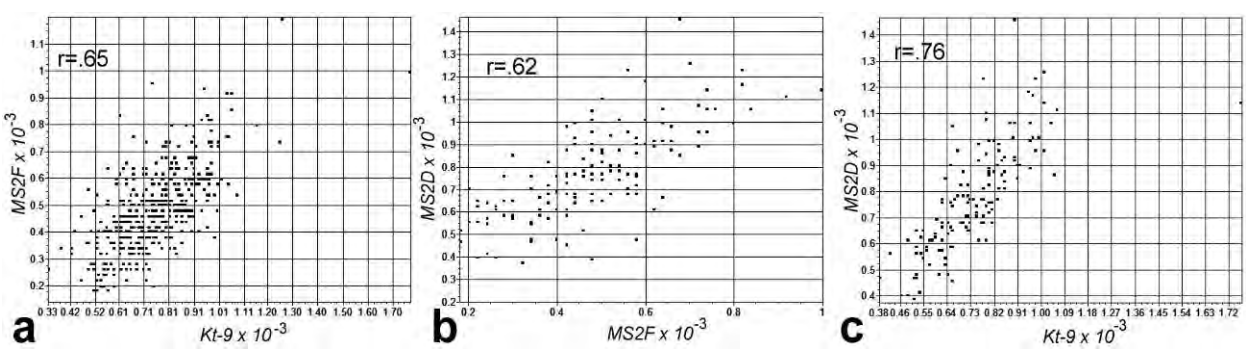

Figure 3.16. *Scatterplots showing MS response relationships between a) the MS2F and KT-9, b) the MS2F and MS2D, and c) the Kt-9 and MS2D.*

Modeling ditch magnetism two-dimensionally

The magnetic modeling approach elaborated by Eder-Hinterleitner et al. (1996) and Neubauer (2001), which breaks up a volume into numerous small cubes that are each treated as a dipole source, is again followed here, made operational through GIS processing. As before, the MS data utilized were from the MS2F sensor (Figure 3.15b). A simple model of the ditch feature was first constructed (Figure 3.17). The model recognizes two relevant units: the fill of the ditch itself, and sediments immediately over the ditch that may be magnetically enriched by biogenic activity, as discussed previously. Each of these units is compared to corresponding *lateral* units for magnetic contrasts. The average MS values of these units were computed by GIS. The background MS was found to be somewhat lower than background values taken near the previous pit area (Figure 3.12). The lower value of the top unit (.45 x 10^{-3} vs. .62 x 10^{-3} SI) is

explained by the ditch location at the periphery of the village where magnetic enrichment by human occupation can be expected to have been much less, with relatively few years of occupation before the village contracted in this area (Crawford and Ahler 2003). The slightly lower value of the bottom, C-horizon unit (.40 x 10^{-3} vs. .45 x 10^{-3} SI) may be due to simple changes in sediments or perhaps magnetic "pollution" in the area of the pit excavation, which is closer to the longer-settled village core where magnetic enrichment many be expected to be higher. Other units in the model (Figure 3.17), including the topmost turf and surrounding subsoil, are ignored.

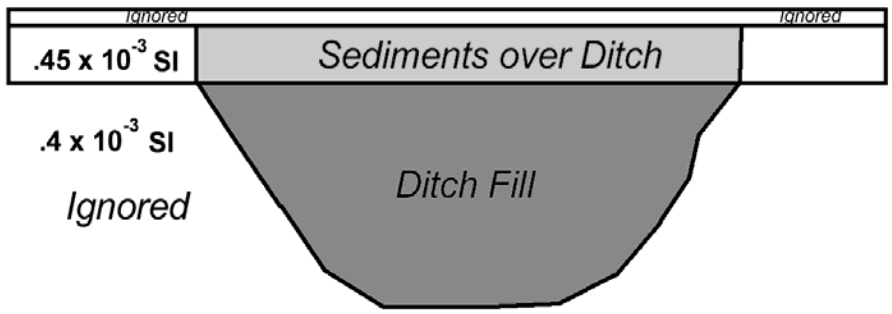

Figure 3.17. *Simple model of two ditch units (in gray) used for modeling, with background lateral MS values used as contrasts for each unit indicated.*

Using this model, *k*, the MS contrast of each dipole source (the cells in Figure 3.15b) was computed in each cell within the ditch and in the area of sediments overlying the ditch. Following Eq. 5, these data were multiplied by H=56,503 nT, the ambient field strength, V=.1^3=.001 m^3, the volume of each cell (dipole source), and the quantity (D_1-D_2), where D_i is the distance function between every possible location of a sensor and the center of the dipole source (Eq. 3). We note in the context of our ditch profile that we are dealing with a two-dimensional face and we therefore need to work only with the two dimensions of *y* and *z*, since the profile face is oriented approximately east-west and distances on the *x*-axis (north-south) are therefore zero. This greatly simplifies the expression to:

$$D_i = \frac{z^2(3\sin^2 I - 1) - y^2}{(y^2+z^2)^{\frac{5}{2}}} \qquad \text{Eq. 6.}$$

Equations 5-6 were applied cell-by-cell and then summed to yield the total anomaly strength in nT *due to induced magnetism* that should be recorded by a magnetic gradiometer at the surface in each position of the profile.

Magnetic gradiometry

The actual MG data recorded in 2002 in the vicinity of the fortification ditch are illustrated in Figure 3.18a, with the locus of the excavation profile indicated. This survey was conducted in transects separated by .5 m with data along transects sampled every .25 m. The magnitude of the MG data over the excavation profile is illustrated in red in Figure 3.18b, where the half-meter spacing between transects on the east-west axis should be apparent. The results of the model, at the MS cell resolution of 0.1 m, are shown in blue, and again illustrate significant variation and divergence from the actual data for all of the reasons cited previously. When these data are resampled and smoothed to a similar half-meter resolution, the agreement between the model and the data appears very close indeed.

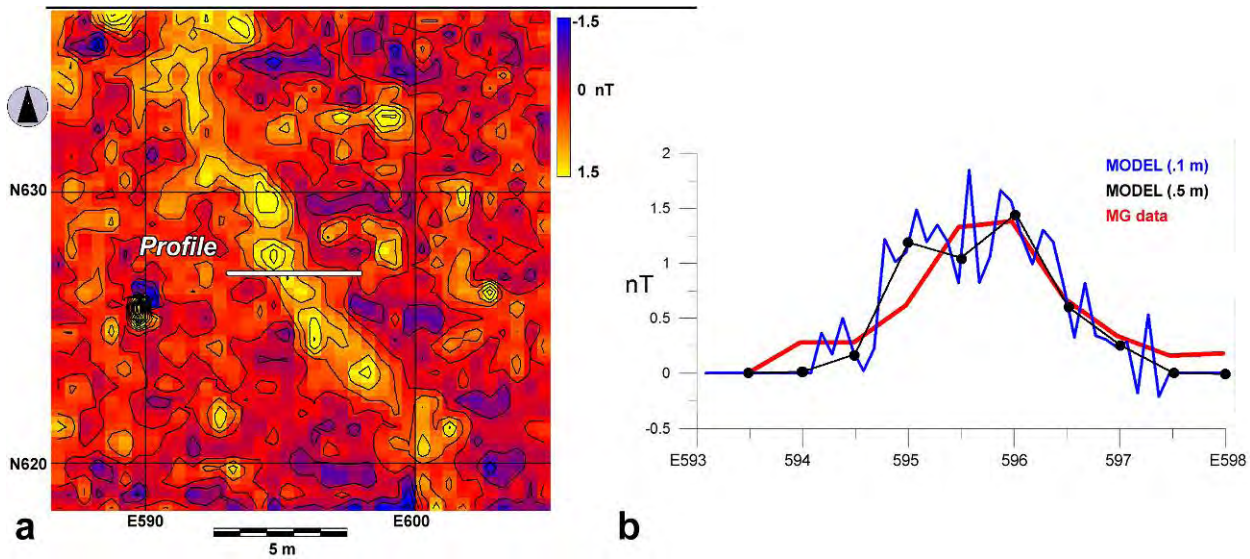

Figure 3.18. *MG data and mathematically modeled anomaly: a) segment from original MG survey conducted in 2002 with locus of excavation profile crossing ditch-caused anomaly (yellow), b) MG data over ditch profile and mathematical model at two spatial resolutions.*

Profile C: House floor

A third common archaeological feature in Northern Plains villages is the earthlodge or house. Plains lodges are large, often 15 m in diameter, and they contain many features including hearths and internal storage pits. Moreover, many houses were burned through acts of warfare, abandonment, or through accident. We therefore wished to examine archaeological magnetism within a house and selected one within the village core for re-excavation that showed evidence of its burning (labeled "C" in Figure 3.2).

Photo-mosaic and profile

A 1 x 2 m trench was excavated to below the floor level of the house in 2004. That excavation revealed a zone of charred “roof fall”—sediments that once formed a roof covering of the earthlodge that burned along with the house and fell to the floor. This burned unit was evident as “blotches of charcoal and patches of reddish scorched earth” lying directly on the house floor (Ahler 2005a:108). Within this unit the locus of a subterranean storage pit that reached nearly 2 m in depth was also discovered and excavated (Figure 3.19a). Immediately after the excavation two vertical soundings were made by Rinita Dalan with the Bartington MS2H probe, soon after the pit study described earlier (Ahler 2005a:110). These soundings were placed adjacent to the open excavation and showed moderately high magnetism (in arbitrary, uncalibrated MS units at that time) at depths that reflected the burned roof material sitting on the house floor (Figure 3.19a). The northern sounding (right, Figure 3.19a), however, also illustrates a massive MS spike near the base of the excavation in a “sterile light yellow” unit. Its source was unexplained in 2004. With the core holes placed 20 cm *behind* the profile, it was thought that the instrument recorded the high susceptibility of an unknown feature not seen in the profile, perhaps burned soil, a hearth, or nearby fire-cracked rock.

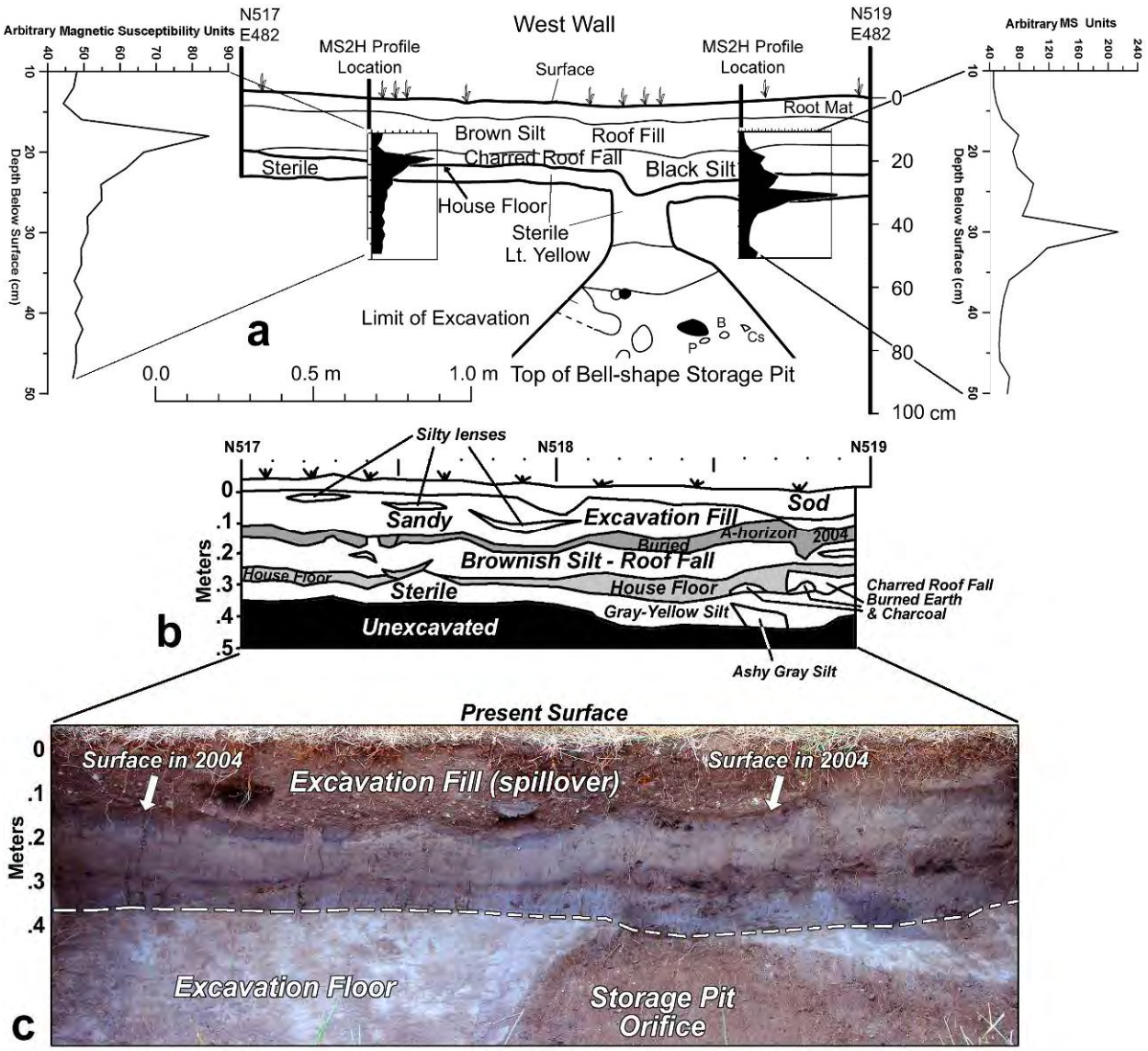

Figure 3.19. *Profiles of the house floor excavation: a) profile of 2004 with MS2H results superimposed, b) profile of 2012, and c) photomosaic from 2012. The .5x2 m profile lies on the west wall of the excavation at E482 in the Double Ditch local coordinate system, with north coordinates indicated. North is to the right.*

Our re-exposure of this excavation in 2012 revealed a very different profile because (1) we cut back the face about 5 cm to yield "clean" sediments, and (2) more than 10 cm of a sandy matrix that was used to back-fill the 2004 excavations was found to overly the original profile (Figure 3.19b, c). In other words, the original ground surface of 2004 now lies at an average depth of about 10 cm below the surface. The cutting back of the profile by 5 cm also reveals why the large magnetic "spike" was encountered near the floor of the earlier excavation. Several pockets of highly fired earth and a deposit of ashy silt (probably associated with fired earth) are now visible in the profile. The orifice of the storage pit, not re-excavated, is clearly visible in the excavation floor (Figure 3.19c).

The MS measurements

The MS2H results of 2004 are exciting because they indicate elevated magnetism associated with burned lodge roof materials that have fallen to the floor of the structure. More detailed, systematic, and higher resolution mapping of MS was therefore certain to yield additional insights. The profile MS mappings with the KT-9 Kappameter and the Bartington MS2F are shown in Figure 3.20a, c. Interpolated data sets (with a spatial resolution of .025 m) that are enhanced for contrast are given in Figure 3.20b, d. It is immediately apparent that both instruments yield very parallel results. Both indicate the dual levels of burned floor/roof fall of relatively high MS with the low MS of the sandy fill matrix above. They also reveal the significantly higher MS to the north (right) in the vicinity of the clearly burned sediments, charcoal, and ash (compare Figure 3.19b, c). In the contrast enhanced views individual pockets of high MS are visible, probably pointing to burned sediments. An important finding is that although the floor of the house lies at an elevation of about .3 m below the surface, and all burned roof material lies above this floor, the MS data indicate elevated MS on and *below* the level of the floor, suggesting the likelihood of very high temperatures that may have baked the sediments beneath.

Sensor differences

Statistically, histograms of the data from both instruments indicate bimodality, with one mode representing the zone of high MS associated with fired sediments, and the mode of low MS pointing to the sandy matrix fill (Figure 3.20e, f). As before, the KT-9 tends to yield significantly higher measurements with a mean of $.685 \times 10^{-3}$, compared to the MS2F with a mean of $.420 \times 10^{-3}$ SI. That responses are related is revealed by a high correlation of r=.87, although the scatterplot indicates considerable heteroscedasticity in higher measurements (Figure 3.20g).

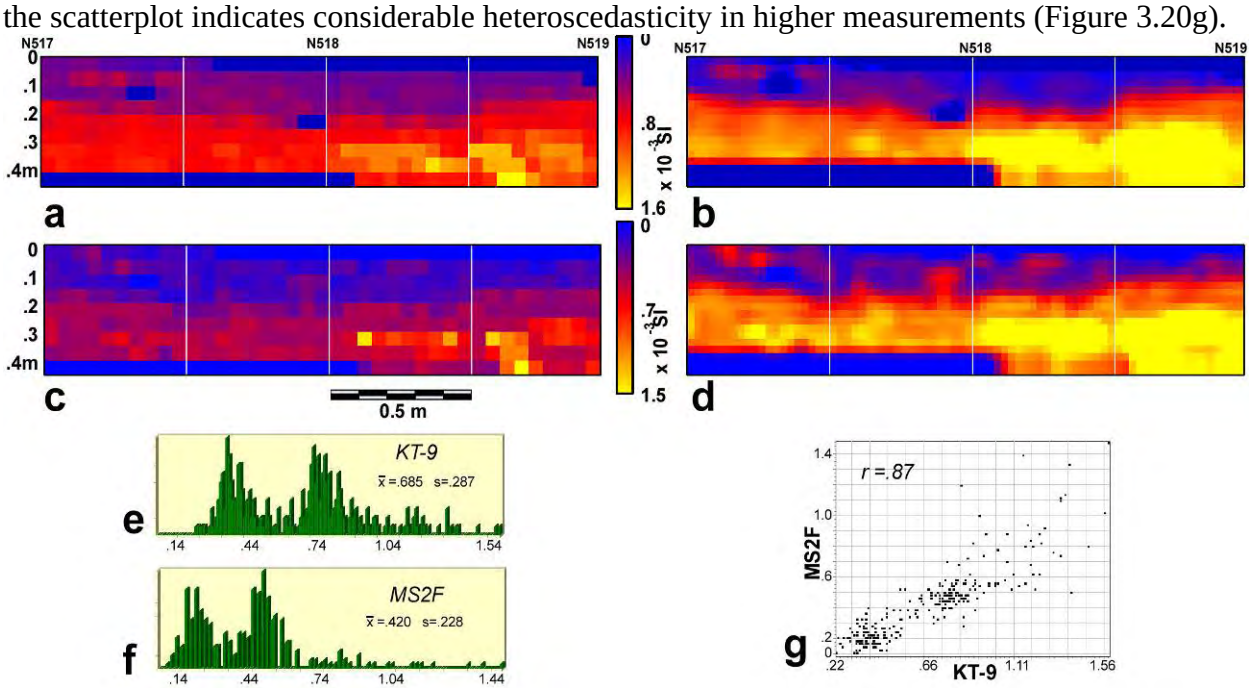

Figure 3.20. *MS mappings and related data of the house excavation profile: a) raw KT-9 MS (.05 m resolution), b) interpolated KT-9 MS (.025 m resolution), c) raw MS2F MS (.05 m resolution), d) interpolated MS2F MS (.025 m resolution), e) histogram and statistics for the KT-9 data, f) histogram and statistics for the MS2F data, g) scatterplot and correlation coefficient.*

Magnetic susceptibility and magnetic gradiometry

These MS mapping results may suggest that high levels of magnetism will be recorded by surface magnetometers over burned houses, yet this may not generally be the case. First, the MS indicated by the burned sediments is relatively low, with few measurements above $1x10^{-3}$. Moreover, as emphasized by Clark (2000:101), a deep pit of high MS might act as a large bar magnet, making it readily detectable, but a shallow "pit" (e.g., house floor) of equal volume mimics a series of *short* bar magnets in which the north and south poles are close together, so that they tend to cancel each other out resulting in a smaller signal perhaps detectable only at the edges of the feature. This is why a continuous layer of magnetically enriched topsoil (high MS) is undetectable. In the case of the house floor segment studied here, it lies only centimeters away from a very large storage pit that generates a pronounced MG anomaly that totally dominates any signal from other features, making something as subtle as a burned floor undetectable (Figure 3.21a, b). For these reasons, and because no lateral data on MS *outside* of the house floor are available, magnetic modeling is not here attempted.

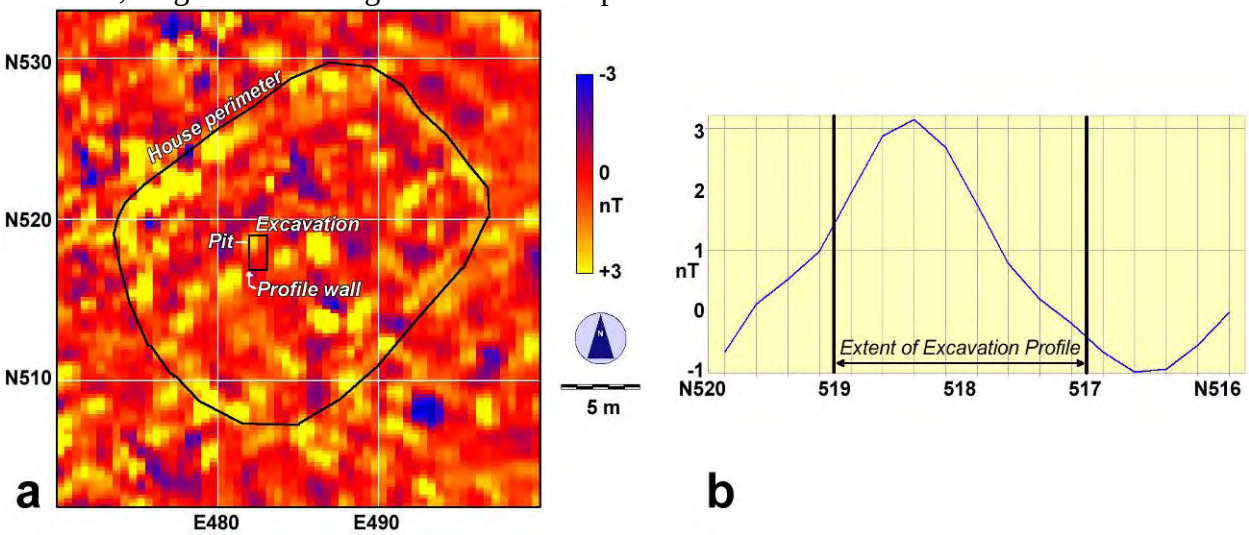

Figure 3.21. *MG data showing a) the entire house with the locus of the 2004 excavation, and b) the magnetic anomaly recorded along the line of the mapped profile, dominated by the anomaly generated by the storage pit.*

CONCLUSIONS

The MS mappings of archaeological profiles presented here offer unique views of magnetic variation across *profiles* of common features in Northern Plains archaeology: a subterranean storage pit, a fortification ditch, and a burned house floor. These features have parallels in many other archaeological culture areas across the continent. Findings indicate that variation in MS is complex, it appears to derive from many sources as suggested by that variation, and it offers new perspectives by revealing a dimension of the subsurface previously unseen. MS changes may well depict individual episodic events not normally visible or detected archaeologically. In other words, traditional drawn profiles of stratigraphy or even photography often do not reveal the subtle variations seen here magnetically, which may point to individual depositional actions. Moreover, the data suggest the complexity of archaeological magnetism. A MG at the surface records a simple sum of all sources of magnetism (induced and remanent) below the instrument to a typical effective depth of perhaps 1.5 m (Clark 2000:90). Anomalies

that are generated therefore represent a gross simplification of the complex variation that occurs below. In the case of the pit and ditch features examined here, the results are simple bell-shaped curves with highest magnitudes near the feature centers where the greatest volume of high MS deposits occur. Lower magnitudes are typical near feature peripheries where larger volumes of low MS materials, with smaller contrasts relative to the background, prevail.

Simple mathematical models gave insights that helped explain the results. By working with high spatial resolution models with .1 m sampling intervals, it is suggested that magnetic variation may be somewhat more variable than is typically found by MG measurements recorded on the surface, simply because sampling densities in field practice tend to be lower, which has the effect of "smoothing" the result. Clearly, pockets of high MS, particularly near the surface, have a large impact on surface MG. However, for these variations to be recorded, high sampling densities must be employed. At Double Ditch, quarter- or half-meter sampling was insufficient to detect such minor variations, but modeling shows that tenth-meter sampling may show such small variations pointing to local pockets of high MS materials, such as those occurring from hearth cleanings.

CHAPTER 4: IDENTIFICATION OF REMANENT ANOMALIES

As discussed in Chapter 1, anomalies in magnetometry data sets are of two types, remanent and induced, of which the former are generally *thermoremanent* (to distinguish them from other kinds of remanent anomalies which occur much less frequently; see Evans and Heller 2003). Thermoremanent anomalies are formed by intense burning, as occurs in hearths, kilns, or burned structures. Induced anomalies, on the other hand, occur because magnetizable materials are subjected to the Earth's inducing magnetic field. Anomalies arise from variations in magnetic compounds held within soils, sediments, rocks, and other materials, and by differences in their volumes and densities. Thermoremanent and induced anomalies can look much the same to a magnetometer, which makes distinguishing between them problematic, and doing so can be critical to archaeological interpretation. Knowledge of the locations of hearths (thermoremanent) versus storage pits (induced), for example, can indicate much about a site's layout and organization. For this reason, we investigate a methodology for discriminating between the two magnetic anomaly types.

METHODS

The basic idea behind our approach comes from a simple relationship. In magnetometry surveys the total magnetization, M_T, generated by a buried feature is simply the sum of any remanent component, M_R, plus the induced magnetization, M_I, due to the magnetic susceptibility inherent to the material (Linford 2006:2222):

$$M_T = M_R + M_I.$$

It follows, then, that to isolate the remanent component, M_R, one may subtract the induced component from the total to yield

$$M_R = M_T - M_I,$$

and we attempt just that. We employ a magnetic gradiometer (MG) to measure the total magnetization in an area, and then perform a follow-up survey with a magnetic susceptibility (MS) meter (usually the EM38B) to measure only the induced magnetic component. The differences in forms of magnetism measured by these instrument types are well understood (e.g., Desvignes and Tabbagh 1995:129-130). Based on the correlation between magnetometry and MS data sets owing to induced magnetic components common to both, we regress the gradiometry on the susceptibility data and utilize the residuals as a data set that more clearly points to remanent anomalies. In effect, what this accomplishes is a conversion of the MS data from SI units to equivalent nT and their subtraction from the total gradiometry to yield, at least partially, a remanent component. We recognize that this approach is neither an ideal nor a perfect solution. Linford (2006:2233), for example, notes that a correlation between EM38 MS data and conventional magnetometry "is complicated," in part owing to the different volumes of soil evaluated. Yet, we believe the approach is worth investigation and our results are at least interesting and show moderate to good indications of success in four distinct survey areas. Problems associated with the approach are discussed in detail.

One methodological problem of this correlation-based approach that must be considered up front arises from outliers or extreme measurements that typically occur in MG and MS data sets. They commonly arise from the presence of iron artifacts. In MG data sets they generate dipolar anomalies with large positive and negative poles (Kvamme 2006a; see Chapter 1). Their large values, and the fact that half of them are negative in value, upset and reduce correlations with other data sets, such as MS. A similar problem arises in MS data obtained with the EM38B, where large negative and more moderate positive values occur over shallow metal objects (Bevan 1998:31). The effect is much worse in MG data where there is lateral (horizontal) sensitivity; whereas, in MS data experience has shown this response generally occurs only when the instrument lies directly above or adjacent to a metal target. As noted in Chapter 1, when extreme measurements were field recorded with the MS2D sensor, a new measurement was obtained at an adjacent location unaffected by the iron object, so these data are "clean" in this regard.

To mitigate the negative effects of spurious and extreme measurements on data set correlations we first identified in each survey area all dipolar anomalies indicated by MG. Using GIS methods on the registered data sets we then digitized polygons to isolate these locations. All measurements within these locations, ranging from 2-10% of the survey areas, were then ignored in subsequent analyses and interpretations. In this way valid data plots, relationships, and correlations could be established between the MS and MG data permitting this study to be undertaken.

SURVEY AREAS AND DATA

To pursue our tactic for identifying remanent magnetic anomalies, we surveyed three distinct areas within Fort Clark State Historic Site and another area within the Double Ditch State Historic Site using a magnetic gradiometer and instruments for measuring MS, the EM38B and the MS2D. The areas were selected because they contain many archaeological features common to Northern Plains villages, including earthlodges, a log cabin, storage pits, and hearths.

At Fort Clark three 20 x 20 m survey areas, labeled A-C (Figure 4.1), were selected based on an initial MG survey that covered the entire village area (Wiewel 2014). Each area was surveyed with a Bartington Grad 601 dual-sensor magnetic gradiometer. Within areas A and B eight measurements were taken per meter along transects separated by 0.5 m (for 16 measurements/m^2). MS data were collected with the Geonics EM38B with one meter transect separation and two samples per meter (for 2 measurements/m^2). In Survey Area C identical survey parameters were employed, but with transects separated by only 0.25 m for both instruments, giving 32 measurements/m^2 for MG and 8 measurements/m^2 for MS. Area A was also surveyed with the Bartington MS2D with a sampling density of one measurement/m^2 to permit an examination of the utility of this instrument, with its lesser depth penetration, for this procedure.

Survey Area A

This area contains the remnants of an Arikara earthlodge west of the fortification ditch near the village perimeter (Figure 4.1). Magnetically, the lodge walls exhibit a ring of elevated magnetism associated with the typical surrounding earthen berm (formed by eroded roof sediments). A hearth lies near the center of the lodge, and numerous other unexplained anomalies are found in its interior and along its perimeter. Although the lodge contains several dipolar

anomalies, indicating ferrous metal artifacts and historic debris, they are comparatively few relative to other dwellings in the village.

Survey Area B

This area includes an earthlodge that lies close to the village plaza in an area that experienced greater use (Figure 4.1), evidenced in various geophysical data sets by different construction episodes and overlapping houses during the village's occupation (Wiewel and Kvamme 2013). The lodge lies buried beneath refuse, and no evidence of it is visible on the ground surface. It is therefore probably associated with the earlier Mandan occupation of the site. In the MG data it is defined by a cluster of dipolar anomalies that point to iron artifacts within a ring of enhanced magnetism.

Survey Area C

This area includes an Arikara log cabin dating to about 1860 that overlies an earlier circular earthlodge (Figure 4.1). The rectangular cabin exhibits an interior partition, and numerous dipolar anomalies that point to iron artifacts are associated with the structure (Wiewel and Kvamme 2013).

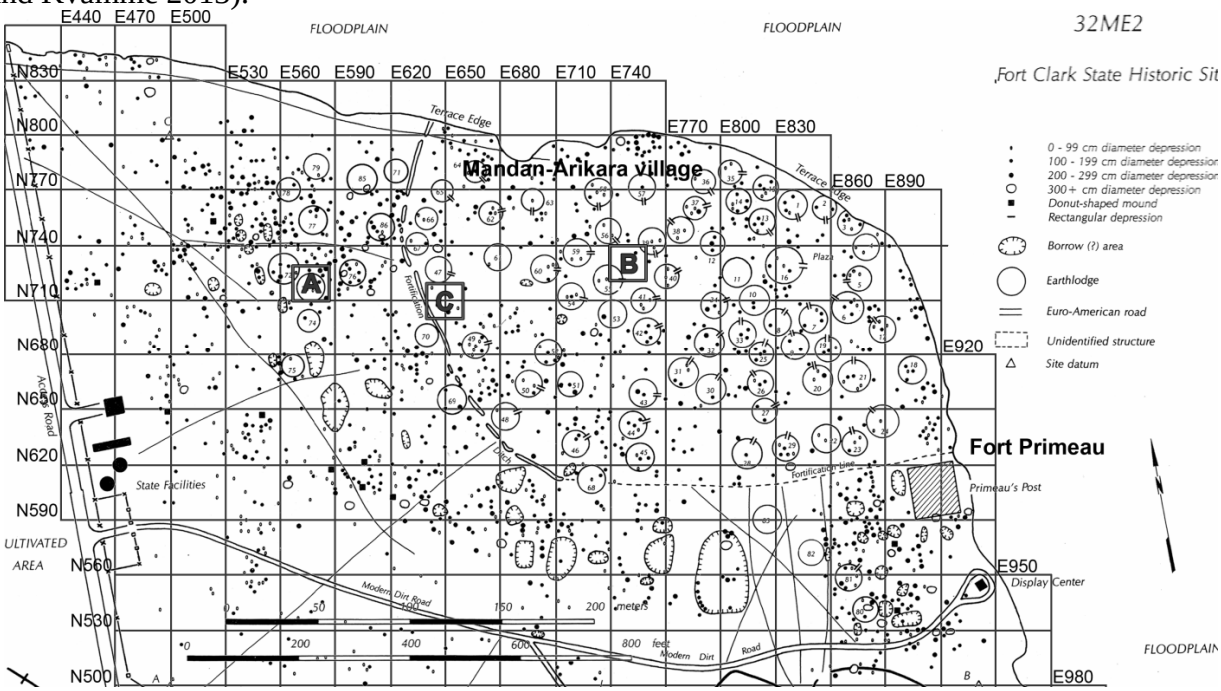

Figure 4.1. *Map of Fort Clark showing the locations of magnetic gradiometry and magnetic susceptibility surveys (adapted from Wood 1993:Figure 3). The grid illustrates 30 m blocks with coordinates indicated.*

Survey Area D

The fourth data set is from a 40 x 60 m block within the village core of Double Ditch (Figure 4.2). This area contains several circular earthlodges indicated by raised berms encircling the depressions of their floors, as well as depressions formed by earth borrowing pits used for lodge constructions (Kvamme and Ahler 2007). The former uniformly contain hearths while the latter do not, so this case well illustrates an example where the identification of thermoremanent anomalies is critical to interpretation. Numerous storage pits are also typically associated with

houses. Geophysical data were collected with a Geoscan Research FM36 magnetic gradiometer and a Geonics EM38B in 2004. Identical sampling strategies were employed for both instruments, with four measurements obtained per meter along transects and a 0.5 m transect separation (for 8 measurements/m^2). Significantly, based on the geophysical mappings, a coring program to validate the presence or absence of hearths within the surface depressions was undertaken by Ahler (2004) subsequent to the surveys, which permitted positive identifications of houses and borrow pit locations within this study area, offering a check on our methodology.

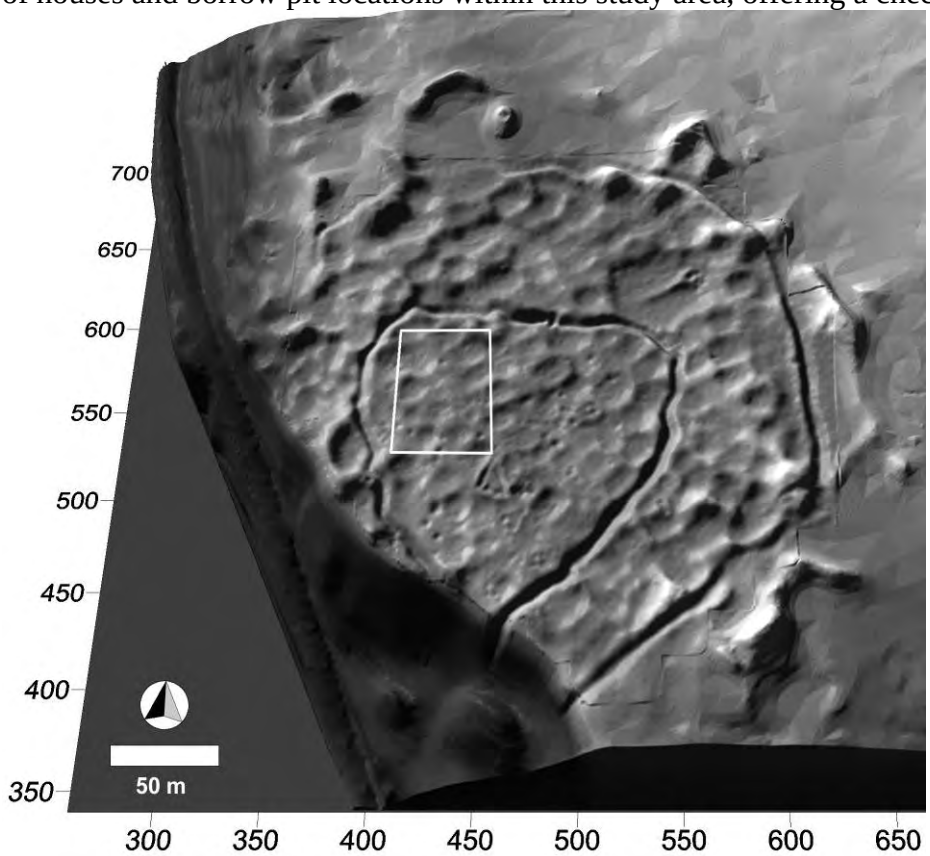

Figure 4.2. *Shaded digital elevation model of the Double Ditch site showing the location of the 40 x 60 m survey area. The two defensive ditches are readily visible as are numerous surface depressions pointing to the locations of former houses and borrow bits. The Missouri River lies to the west.*

RESULTS

In sections below the data are illustrated in grayscale in their "raw" form utilized in the regression analyses, in an interpolated form to improve visualization through reduced pixelation, and with "masks" that eliminate unanalyzed regions of dipolar anomalies visible in MG.

Survey Area A: Shallow Arikara Earthlodge on Village Periphery

Examination of the magnetic data from this earthlodge shows its perimeter to be clearly visible as a ring of elevated magnetism in the MG and MS datasets (Figure 4.3a, b). A small circular MG anomaly near the lodge center is a hearth based on its magnitude (approximately 12.5 nT) and location (Figure 4.3a). A broad area around the central hearth exhibits elevated MS (Figure 4.3b), probably caused by occupational activities that would have occurred near the hearth, including food preparation and cooking. These activities introduce organic materials which, combined with the burning of sediments near the hearth, serve to increase MS (see Introduction). Several circular MG anomalies are located near the earthlodge perimeter (Figure

4.3a). Prior excavations and geophysical investigations of similar lodges indicate they likely represent storage pits (Kvamme 2007; Kvamme and Ahler 2007). Storage pits are typically filled with settlement soils and midden materials which explain their visibility due to increased MS. Two obvious examples, one located near the lodge perimeter and the other on the lodge's exterior, are highly apparent in the MS image (gray arrows, Figure 4.3b) as are several others.

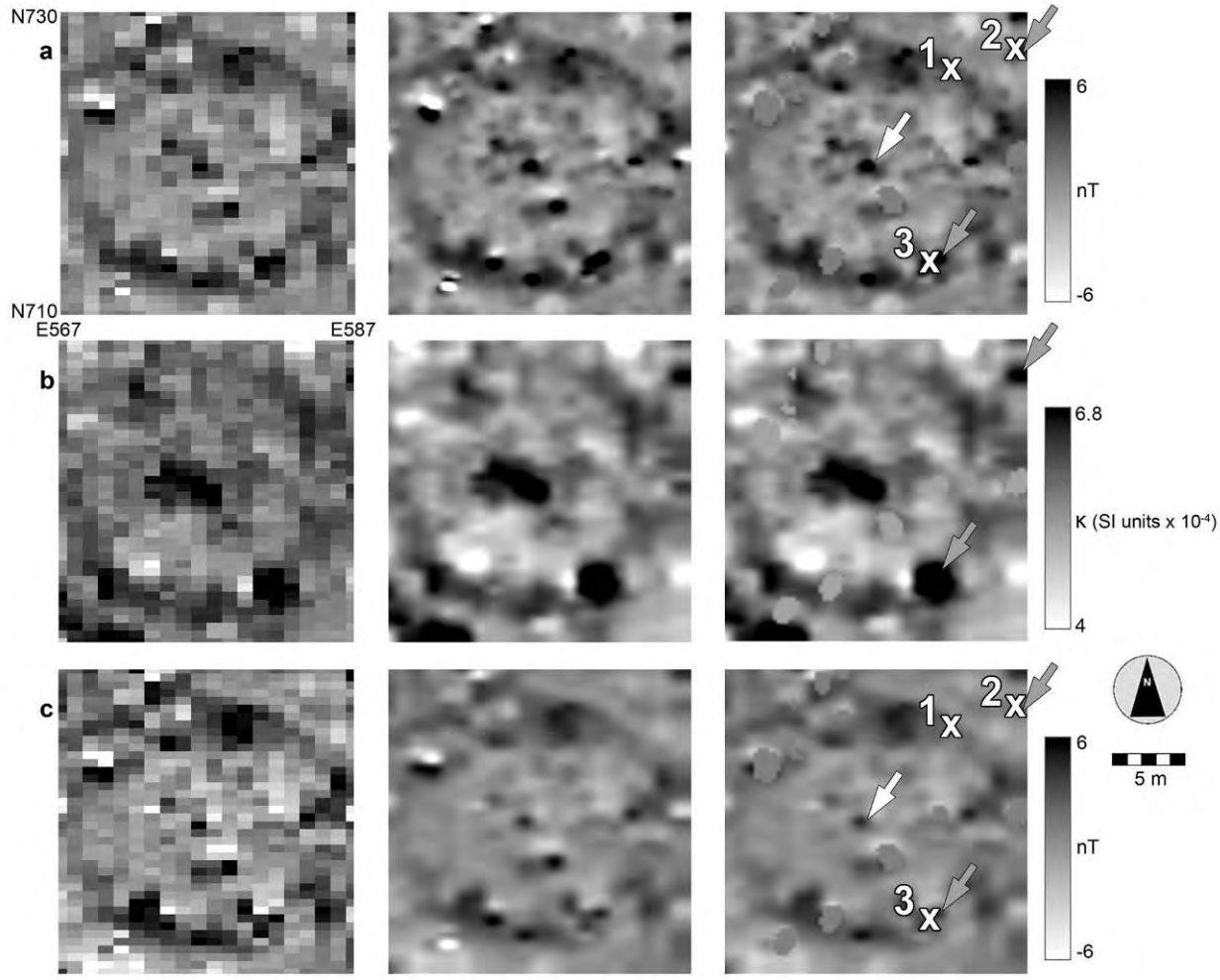

Figure 4.3. *Magnetic survey results of a shallow Arikara lodge in area "A" at Fort Clark: a) MG, b) MS (EM38B), and c) residual data. The left column shows the data at the 1 x 0.5 m resolution of the EM38B survey. The center column shows interpolated (smoothed) datasets. The right column illustrates the masked areas of dipolar anomalies excluded from the analysis. White arrows point to likely hearth features and gray arrows indicate storage pits. Numbers refer to measurement points discussed in the text.*

These obvious correspondences between the MG and MS data (Figure 4.3) together with their theoretical relationship suggest correlation, and this bears out quantitatively with a moderate value of r=0.458 (Figure 4.4). As described in the introduction, this relationship is due largely to the induced magnetic component, captured by both surveys. Some of the unexplained variance is therefore the result of remanence, theoretically captured only by the MG survey.

Yet, other factors also contribute to the lack of correlation seen here. One may result from deep storage pits, which often extend 1.5-2 m beneath the surface (Kvamme and Ahler

2007). A magnetic gradiometer, with its 1.5 m depth response (see Chapter 1), readily locates these features owing to the large volumes of magnetically susceptible materials they hold, while many of these features may lie beyond the range of MS instruments (here, the measurement depth of the EM38 is about 50 cm; see Chapter 1). Consequently, it is quite possible that some storage pits seen in MG may be less visible or invisible in MS surveys, although it is likely that near-surface elements of these pits will give some response in MS surveys. There is also the likelihood of upward migration of materials of higher MS through biogenic activity (rodent work, earthworms; see Introduction). The results shown in Figure 4.3a, b, however, suggest that many storage pits are indicated by the MS survey.

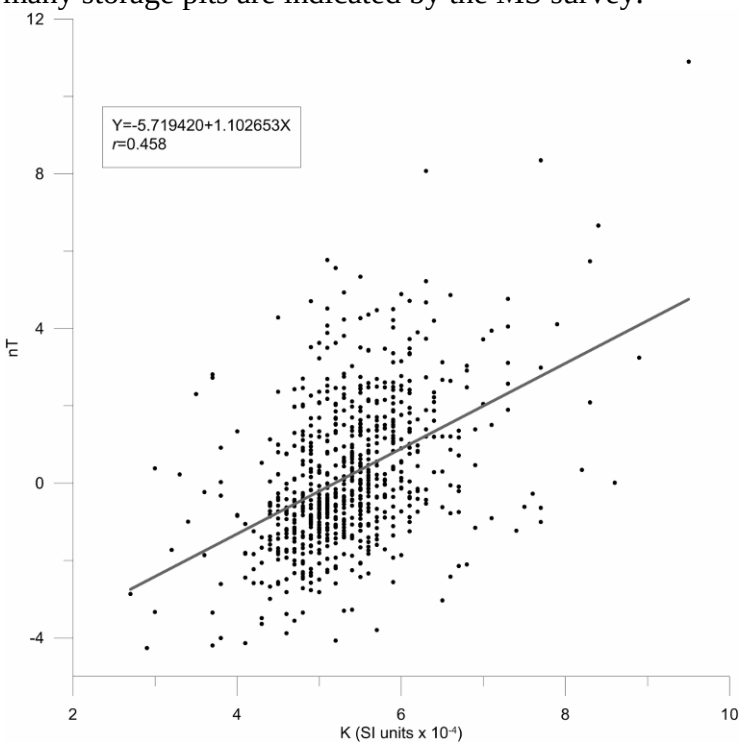

Figure 4.4. *Scatterplot illustrating the relationship between MS (EM38B) and MG data for Survey Area A.*

Some of the variation seen in Figure 4.4 may also be due to small off-sets in the placements of the two instruments during the field surveys, which causes magnetic properties to be measured at slightly different locations. Both instruments used to acquire these data perform at very fast survey rates of about one meter per second, which cause small variations in measurement loci as the instruments move over the ground. In other words, from one instrument to the next the locations at which measurements are actually acquired may vary from 10-20 cm. This can cause discrepancies in the loci of the magnetic responses actually measured (explored in detail in once case study below). In Chapter 2, a repeatability experiment comparing the results of two surveys made in the same area demonstrates significant variation from this factor alone.

The regression of the MG data on the MS data yielded the following function:

$$Y = -5.719 + 1.103 * X$$

where X is the MS measurement in SI units and Y is the corresponding MG measurement in nT. Our premise is that the residuals from this function will reflect, in part, remanent magnetism, where the residuals (R) are simply defined as the variation *not* modeled by the function (Hays 1988), or:

$$R = Y - (-5.719 + 1.103 * X).$$

Applying this function to the data in Figure 4.3b yields the resulting residual maps shown in Figure 4.3c.

The residual maps suggest the success of our tactic because many induced anomalies resulting from magnetically susceptible material appear to be reduced or eliminated (Figure 4.3c). For example, the perimeter of elevated magnetism surrounding the earthlodge in the raw MG and MS data, composed of mounded topsoil and therefore an induced anomaly, is much less visible (Figure 4.3c). In fact, at measurement locus 1 the MG measurement was 2.44 nT, while the residual is only 0.81 nT. Likewise, two inferred storage pits that yield induced anomalies of 4.89 nT and 12.86 nT at measurement loci 2 and 3, respectively, in the MG data, only return 1.36 nT and 4.13 nT in the residual data (Figure 4.3). Yet, the central hearth, an anomaly likely to exhibit remanent magnetism, remains visible in the residual data, although it appears much less robust. This result may be due to the lodge's occupation length. If the lodge was only used for a short period prior to abandonment, a possibility given its location near the periphery of the village and relatively few dipolar anomalies indicative of iron artifacts, the hearth may not have had adequate usage to develop strong remanent magnetism.

The remaining residual anomalies in Figure 4.3c probably point to a combination of several phenomena. Those within the lodge floor could point to auxiliary hearths where remanent magnetism is possible. Those along the lodge perimeter likely represent deep storage pits that generate induced anomalies, but which were undetected or only partially detected by the shallow-depth MS instrument.

A survey of the same area was also undertaken with the Bartington MS2D sensor, described in Chapter 2. As noted there, the MS2D illustrates a moderate correlation with the EM38B in a shallow site setting, so it is not surprising that the MS2D data exhibit a moderate, albeit lower, correlation with the MG data of *r*=.353 (Figure 4.5)

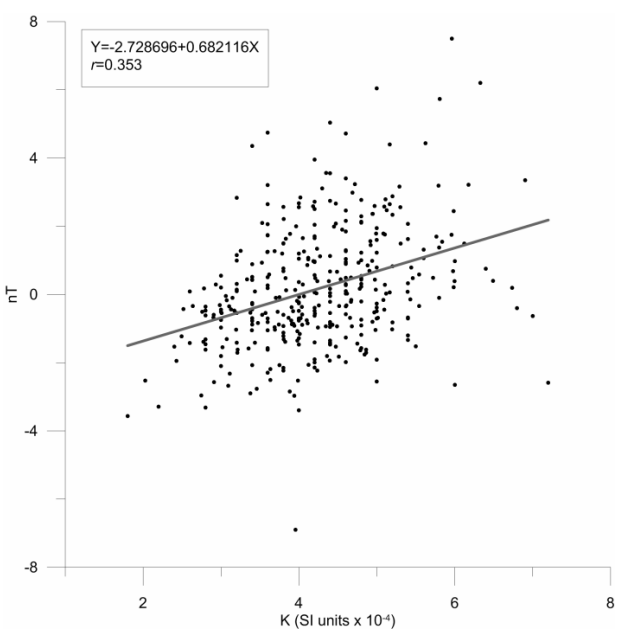

Figure 4.5. *Scatterplot showing the relationship between MS (MS2) and MG data for Survey Area A.*

This decreased correlation between MG and MS is likely due to the shallower measurement depth of the MS2D, only 10 cm (see Introduction). This may make it more difficult for it to detect deeper magnetic features, like storage pits. In fact, in the mapping of these data there is little indication of the storage pits along the lodge perimeter as seen in the MG data (Figure 4.6a, b). Since storage pits are deep features largely absent in the MS data, they tend to be more robustly indicated in the residual data (Figure 4.6c). The shallow mapping of the hearth area by the MS2D shows a broad area of enhanced magnetism like the EM38B results (Figure 4.3b), again pointing to the food preparation and cooking activities that likely took place. Yet, the shape of this area is strangely lobed, which may be a result of simple differences in magnetism between the near-surface prospecting depth of the MS2D versus the deeper focus of the EM38B. It also could be a result of the coarser sampling interval.

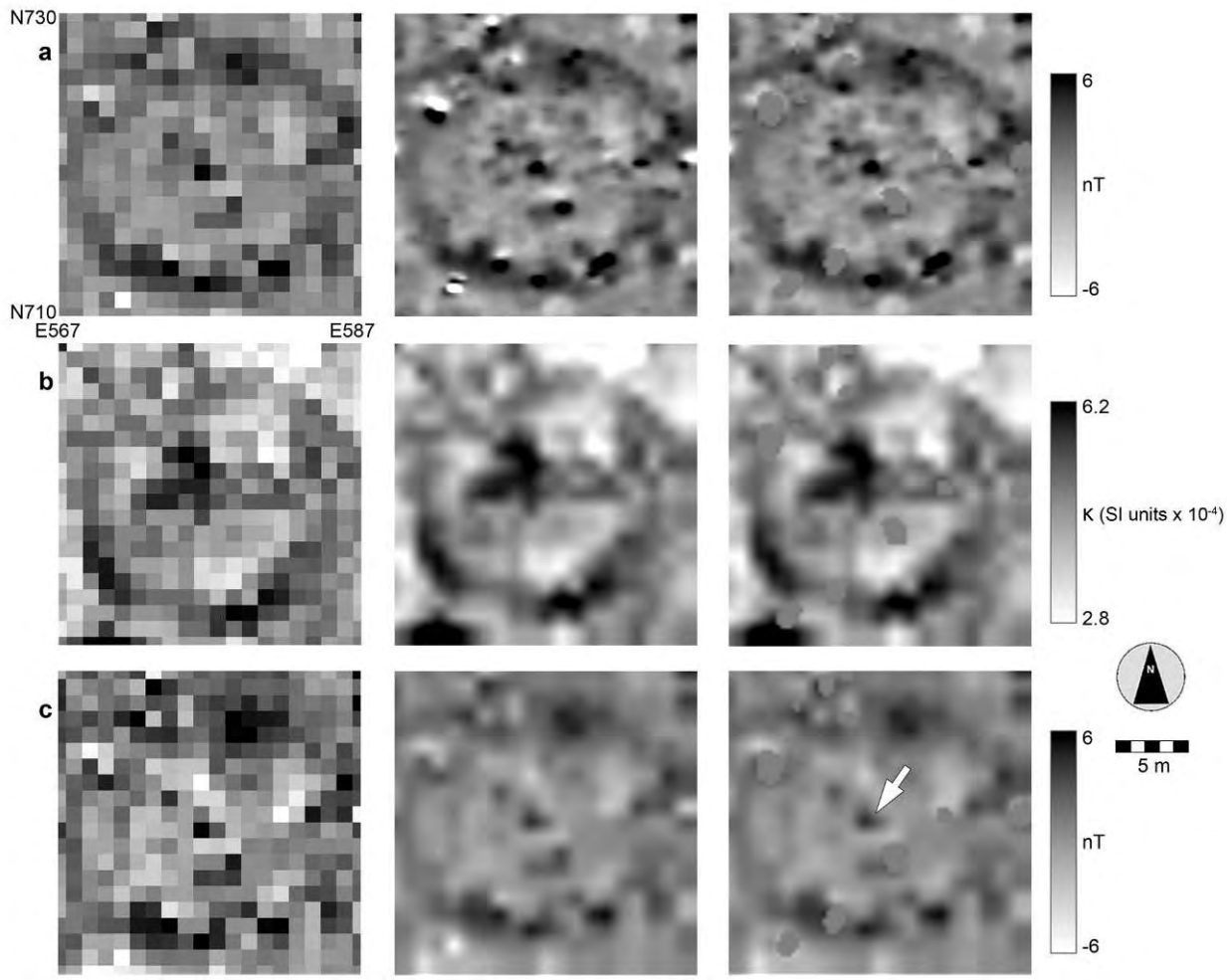

Figure 4.6. *Magnetic survey results at the shallow Arikara lodge in area "A" at Fort Clark: a) MG, b) MS (MS2), and c) residual data. The left column shows the data at the 1 m resolution of the MS survey. The center column shows interpolated (smoothed) datasets. The right column illustrates the masked areas excluded from the analysis. A white arrow points to a probable central hearth feature.*

Survey Area B: Buried Mandan Lodge in Village Core

This buried lodge was identified only after it was indicated in multiple geophysical data sets (Kvamme 2007:214-215). It probably represents a Mandan lodge from the site's early occupation. It lies close to the village center and exhibits little evidence on the ground surface, with a floor about a half-meter deep as indicated by soil cores. The archaeological features in this survey area are therefore near the prospecting limits of the EM38B, so this study represents a trial experiment to examine the performance of the regression approach at its limits. In this case the MG and MS data sets show only weak correlation (*r*=.24), as might be expected with the archaeological targets being at the limits of the EM38's range (Figure 4.7).

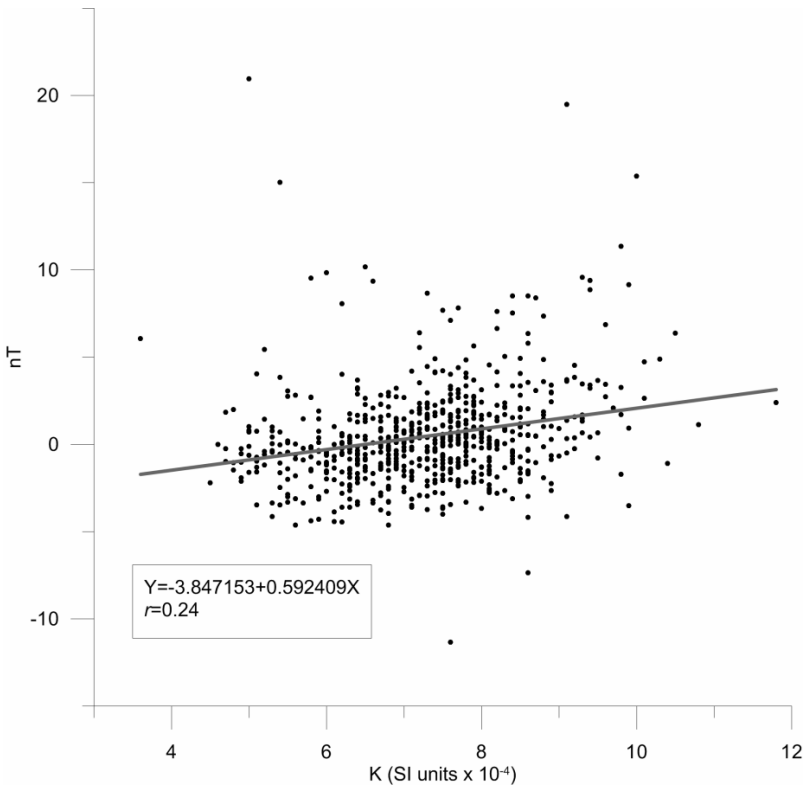

Figure 4.7. *Scatterplot showing the relationship between MS (EM38B) and MG data for Survey Area B.*

The MG data show a circular cluster of dipolar anomalies (Figure 4.8a). These anomalies result from iron artifacts and suggest the lodge depression was filled with refuse after its use ended. The lodge perimeter is mostly apparent in the MG data, but is extremely subtle in the MS data, probably owing to the depth issue (Figure 4.8a, b). Nevertheless, the regression approach seems to offer some success. In the residual data (Figure 4.8c) evidence of the perimeter ring is much reduced compared to the raw MG data. Additionally, a robust storage pit holding highly susceptible material (confirmed by coring; Ahler 2003:52-55; gray arrow, Figure 4.8b) appears to be largely regressed away in the residual image (Figure 4.8c). Finally, the central hearth, which is likeliest for high remanent magnetism, is the most robust anomaly in the residual image.

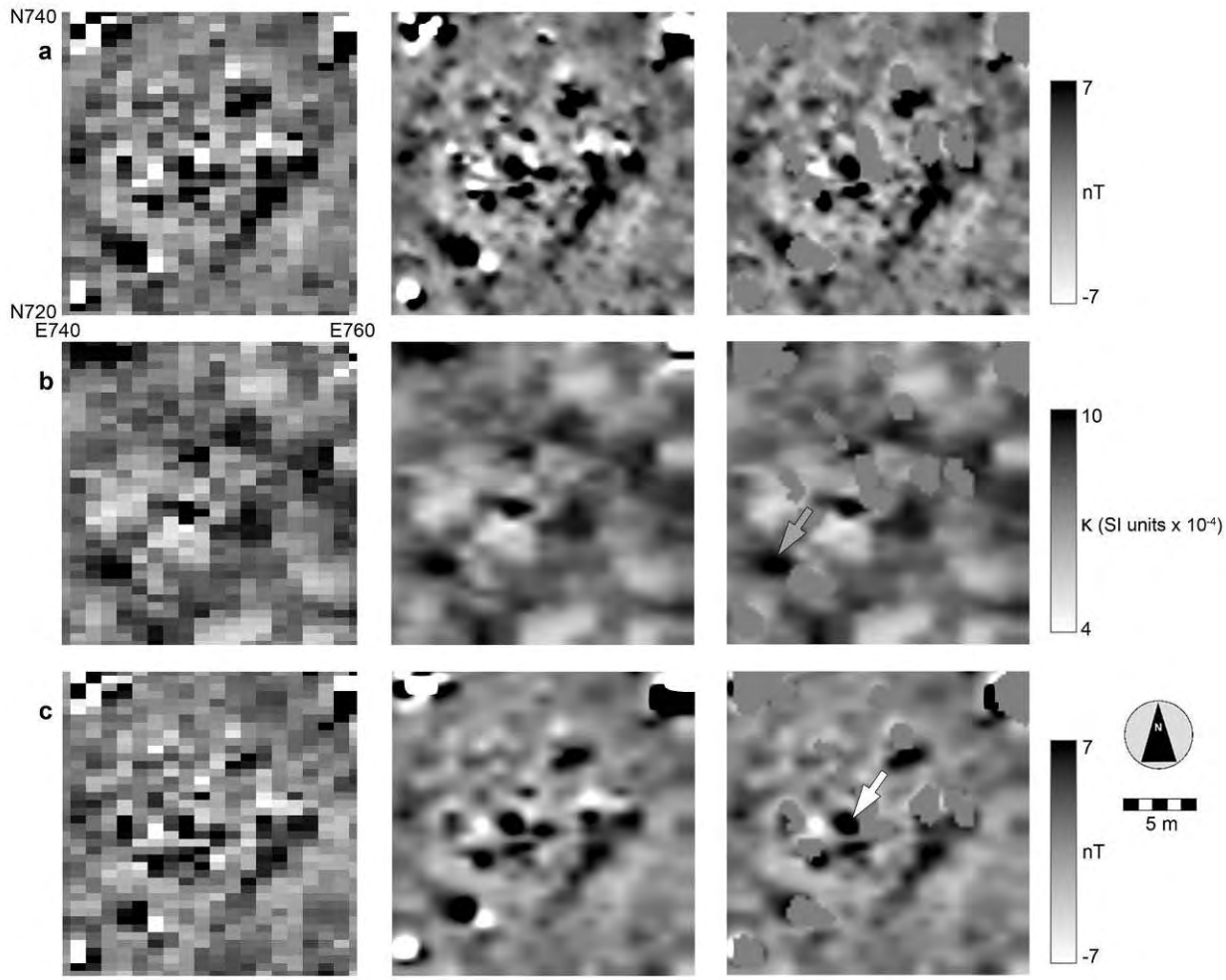

Figure 4.8. *Magnetic survey results of an earthlodge in area "B" at Fort Clark: a) MG, b) MS (EM38B), and c) residual data. The left column shows the data at the 1 x 0.5 m resolution of the MS survey. The center column shows interpolated (smoothed) datasets. The right column illustrates masked areas excluded from the analysis. A white arrow points to the central hearth and a gray arrow points to a storage pit, features confirmed by excavation or coring.*

Survey Area C: Shallow Arikara Log Cabin

The remains of this late-occupation (ca 1860) Arikara log cabin exist at a very shallow depth, generally less than 20 cm, making it ideal for MS and MG surveys. One of the striking findings of the geophysical surveys of this feature was the robustness of the magnetic data sets. Initially, we speculated that this signature might be due to burning, the use of a local stone with magnetic properties as foundation elements, and the presence of many ferrous artifacts (Wiewel and Kvamme 2013). Excavations in 2012 later revealed the presence of numerous metal artifacts which correspond with the dipolar anomalies as well as burned wooden planks and adjacent burned earth along the cabin perimeter (Mitchell 2012). Such burning increases MS and can also lead to remanent magnetism if the firing is hot enough and long enough (see Chapter 1).

The burned areas are indicated in the MG and particularly in the MS images, which clearly indicate the cabin's outline and an interior partition (Figure 4.9a, b). Elevated magnetism in these areas may also arise from microbial activity associated with the decay of wooden remnants (Aspinal et al. 2008:25). The many dipolar anomalies are also evident in the MG data. While the cabin probably had a fireplace its location remains uncertain. However, the excavations did reveal the presence of an earthlodge immediately below the site of the cabin by locating its central hearth (Figure 4.10). This hearth is located about 10 cm under the level of the cabin floor beneath the middle of the cabin's south wall. It is indicated by the larger magnetic anomaly in its vicinity (white arrows, Figure 4.9).

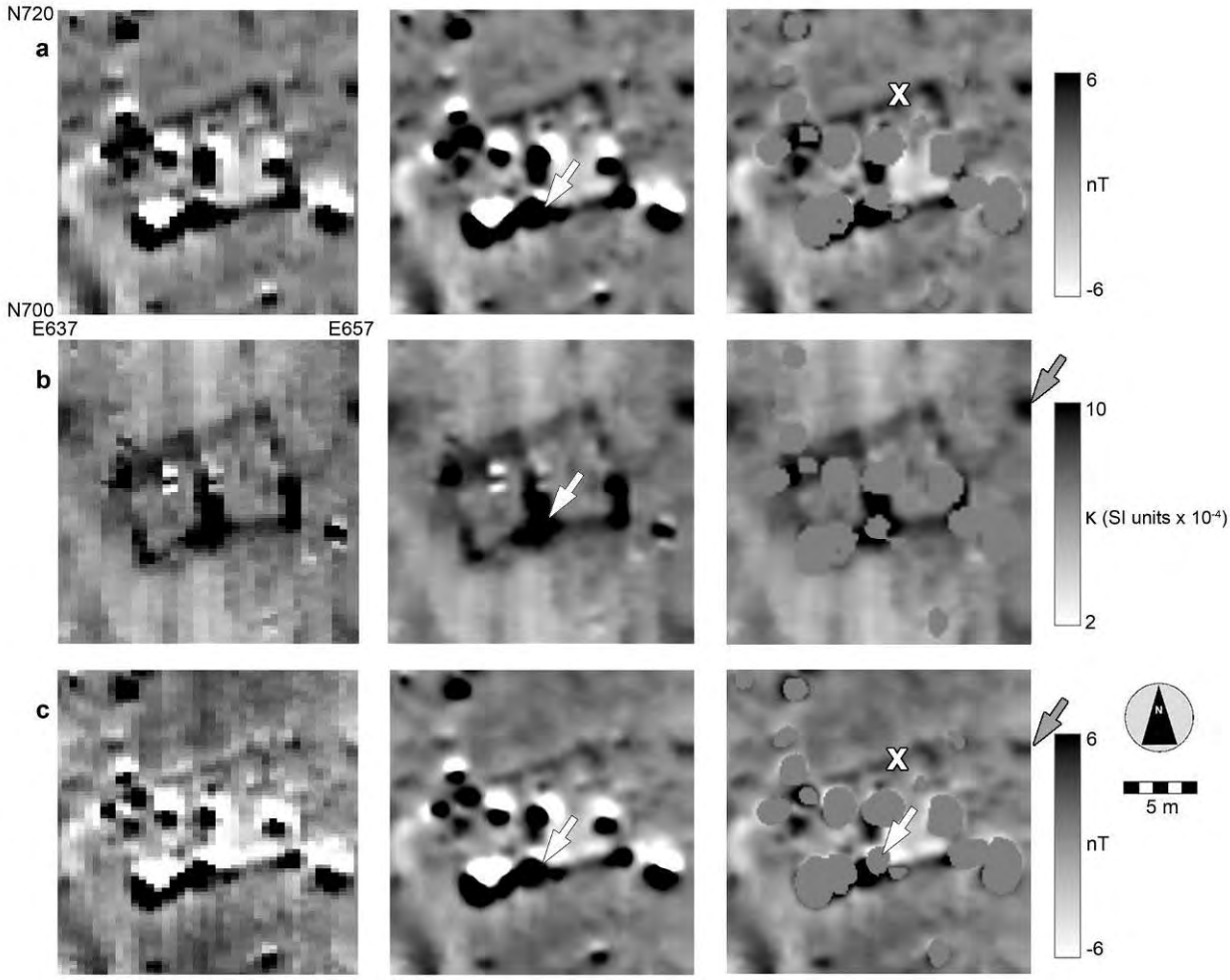

Figure 4.9. *Magnetic survey results in the vicinity of the Arikara cabin in area "C" at Fort Clark: a) MG, b) MS (EM38B), and c) residual data. The left column shows the data at the 0.25 x 0.5 m resolution of the MS survey. The center column shows interpolated (smoothed) data sets. The right column illustrates the masked areas excluded from analysis. The white arrow points to a known hearth, the gray arrow to a possible storage pit, and the "x" indicates a measurement point.*

Figure 4.10. *Large hearth from an earthlodge underlying the late Arikara log cabin. The far wall of the excavation unit is one meter in length.*

The MS (EM38B) and MG data indicate a moderate correlation of *r*=.43 (Figure 4.11). The regression function was employed to generate residual data, which is mapped in Figure 4.9c. Clearly, the outline of the cabin is much less apparent in the residual image, which suggests that the firing greatly increased the MS of the deposits and may not have been so intense as to produce strong thermoremanent magnetism. This outcome illustrates that this approach is able to reduce the magnitude of induced anomalies. For example, at the indicated measurement locus ("x" in Figure 4.9), the cabin wall measures 3.79 nT in the MG data, but only 1.87 nT in the residual data set. Some of this residual magnetism here may actually be thermoremanent from the firing.

A circular anomaly located near the edge of the survey area is visible in the MG and MS data sets (gray arrow, Figure 4.9). Its near-absence in the residual image, however, suggests that this anomaly is fully an induced magnetic feature, probably a storage pit. At the same time, the known hearth, a candidate for remanent magnetism, apparently remains a robust anomaly in the residual image (white arrow, Figure 4.9c), although, unfortunately, it is partially obscured by one of the dipolar anomalies resulting from the many iron artifacts. The dipolar anomalies, incidentally, are unaffected by the regression algorithm.

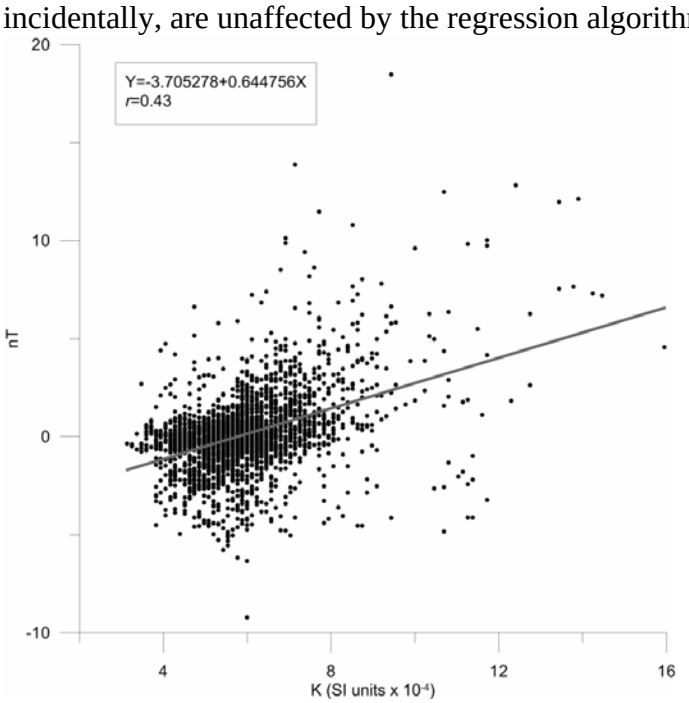

Figure 4.11. *Scatterplot showing the relationship between MS (EM38B) and MG data in Survey Area C.*

Survey Area D: Double Ditch Village Core

The village core area at Double Ditch is filled with numerous depressions in the surface that point to the loci of former lodges (Figure 4.2), but subsequent investigations also demonstrated the presence of earth borrowing pits which were undoubtedly employed to extract sediments for lodge coverings (the walls of each lodge were covered with approximately a quarter-meter of soil). The entire site area of Double Ditch was surveyed by MG between 2001-2004 (Kvamme and Ahler 2007; Kvamme 2008b). In 2004 a 40 x 60 m area was surveyed with an EM38B, permitting comparison of MS and MG data from this site and an investigation of possible thermoremanent anomaly distributions. The latter is important here because a lodge *must* possess a centrally-placed hearth, while none should be associated with a simple borrow pit. Importantly, a detailed examination of each surface depression in this survey area was made by Ahler (2004) through a soil coring program to establish which were lodges and which were borrowing areas, so validation of this study is possible.

A topographic mapping of the survey area reveals several large depressions in the surface which point to the loci of lodges or borrow pits (Figure 4.12a). The one in the northwest appears unusually large and therefore is likely a borrow pit. The MG data, extracted from the site-wide data set, reveal a plethora of rounded "point" anomalies approximately one meter in diameter that represent a combination of central hearths, auxiliary hearths, storage pits (for grain storage, about 1.5-2 m deep), and perhaps an occasional large rodent burrow (Figure 4.12b). These data underscore a fundamental problem inherent to MG data in Northern Plains archaeology: hearths and storage pits look much the same to a magnetometer. They differ only partially in one important way. Bales and Kvamme (2005) show that average *maxima* of anomalies known to represent hearths are significantly larger statistically than are the average maxima representing known storage pits, although the statistical distributions overlap greatly. In other words, a mid-magnitude anomaly could represent a small hearth or a large storage pit. Consequently, a method able to identify thermoremanent anomalies is much needed in these contexts. By superimposing the MG data over a Digital Elevation Model (DEM) of the region it appears that all of the surface depressions possess centrally located point anomalies that could represent hearths (white arrows, Figure 4.12d), but are they? Some, in fact, could represent the remnant "bottoms" of subterranean storage pits that were truncated by removal of their top portions through borrowing.

The MS data in the same region appear much different from the MG results (Figure 4.12c). They clearly show the general outlines of lodges or borrow pits that parallel the topography. This is made even clearer in Figure 4.12e. It appears that all of the surface depressions exhibit high values along their perimeters and low MS signatures near their centers. The low MS arises because in borrows the topsoil (high MS) was excavated away while in lodges the sod was typically removed from floor areas, with a similar effect (Kvamme and Ahler 2007). The high MS perimeter areas evidently arise from the low mounded berms composed of eroded roof sediments that surround most lodges and thin sheets of settlement soils between the lodges, invisible to MG. Some of the larger areas of high MS may simply represent a broad distribution of surface midden deposits. Significantly, the MS data also illustrate numerous small, circular, point anomalies like the gradiometry, most of which probably represent storage pits given their numbers and primary distributions along depression perimeters (a well-known distributional pattern in Mandan villages; Bales and Kvamme 2005; Kvamme 2007).

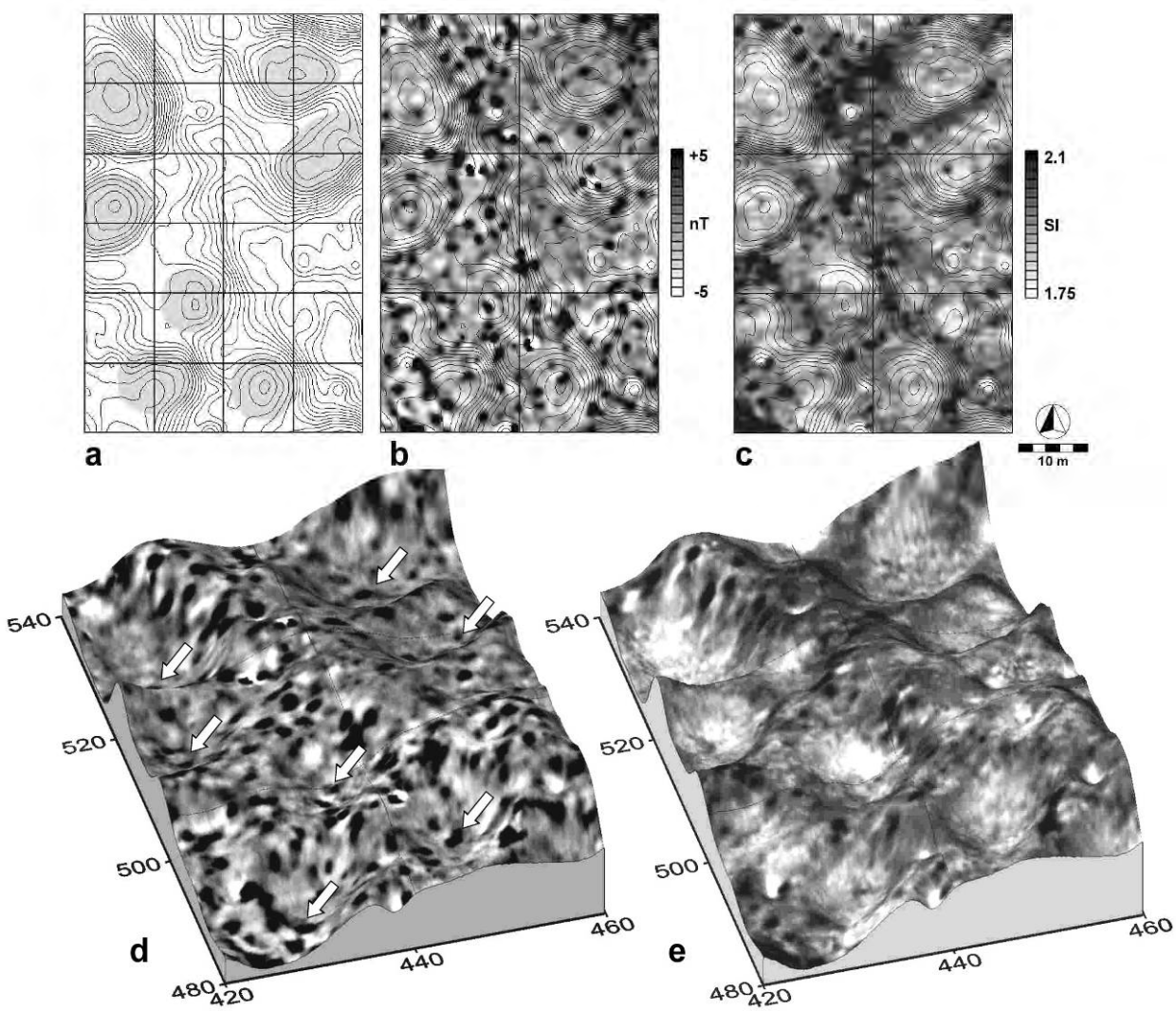

Figure 4.12. *The Double Ditch survey area showing a) the topography (5 cm contours) with depressions shaded, b) the MG, c) MS data, d) MG over topography, and e) MS over topography. White arrows in d point to anomalies central to surface depressions.*

A plot of the MS and MG data again reveals a moderate correlation of *r*=.4 (Figure 4.13). A regression model was fit to the data and residuals were computed. Figure 4.14a shows a stack of the relevant layers of information, beginning with MG (top), then MS, followed by the residual data and a shaded DEM. White arrows point to more robust anomalies in the residual data, likely hearths, that line up with depression centers in the DEM. Other anomalies in the residual data appear much less robust when compared to the original MG data (compare Figures 4.14b, c), and possibly signify such induced anomalies as storage pits.

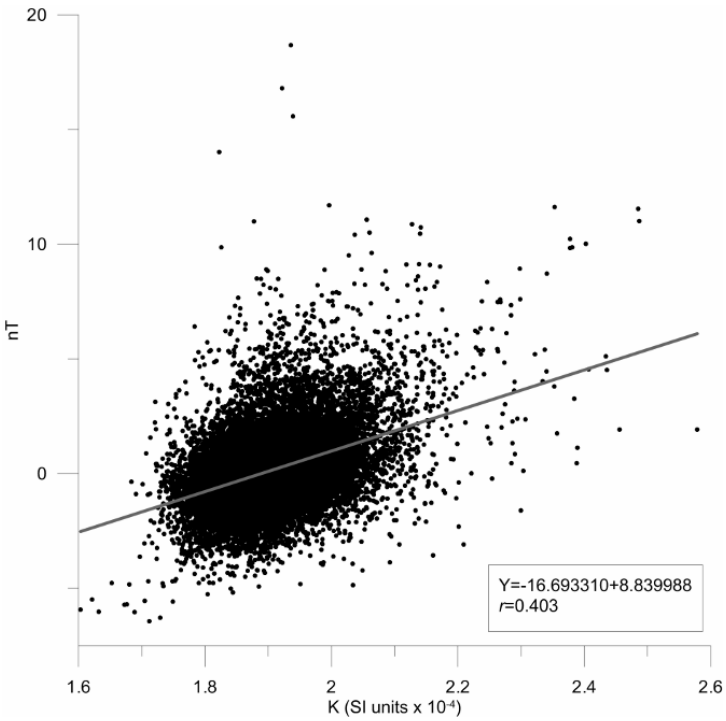

Figure 4.13. *Scatterplot showing the relationship between MS (EM38B) and MG data in the survey area at Double Ditch.*

Figure 4.14b shows the raw MG data with 5 cm contour lines superimposed. As noted, prominent point anomalies lie near the center of every depression, and these are circled. In the regression residual data set (Figure 4.14c), it is obvious that most of the point anomalies appear to be less robust and, indeed, some nearly disappear altogether. If the assumptions of our regression methodology are on-track, these anomalies of reduced magnitude may represent induced anomalies originating from such features as subterranean storage pits while remanent anomalies may retain their values.

The reduction in anomaly magnitudes is made more apparent by focusing on those of largest magnitude. Anomalies in the original MG data greater than 5 nT are illustrated in Figure 4.14d. There are a total of 76, representing primarily a combination of hearths and storage pits. In the residual data set the same tactic yields a total of 51 (Figure 4.14e). Significantly, four of the seven depressions indicate robust central anomalies (circled). Indeed, in the soil coring program conducted by Ahler (2004), each of these anomalies represent hearths, and these depressions are classified as lodges (Labeled "L"; Figure 4.14e). The remaining depressions lack central anomalies in the residual data set and, indeed, coring indicated that none of the many MG anomalies in these places were hearths. They were therefore classified as borrow pits (labeled "B"; Figure 4.14e). The remaining anomalies in this figure likely represent deep storage pits that were only partially detected or undetected owing to the limited depth range of the EM38B. This idea was more fully explored in Chapter 2. A few may represent auxiliary hearths.

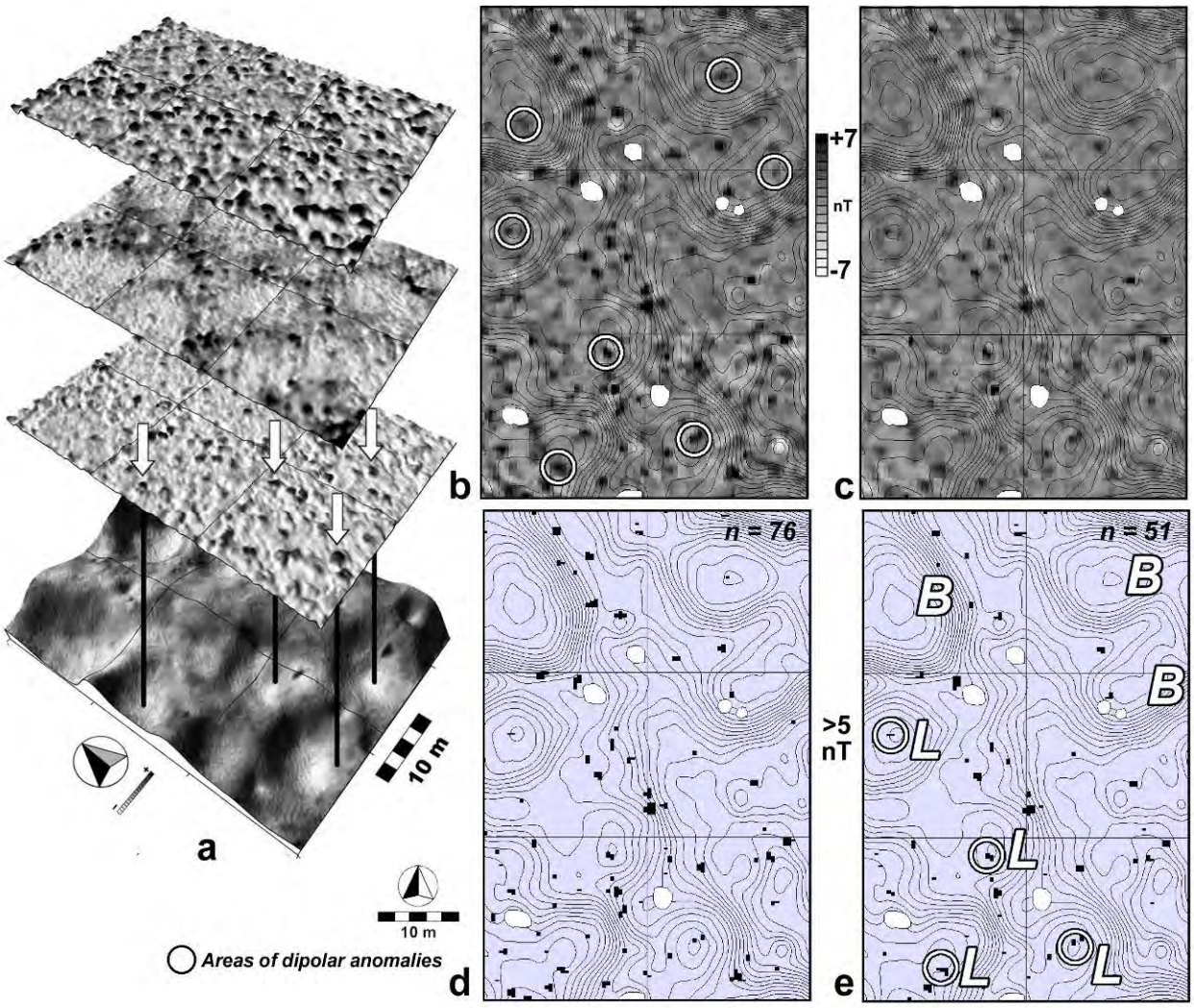

Figure 4.14. *Results of the regression at Double Ditch: a) super-positioning (from top) of MG, MS, residuals, and DEM (arrows point to anomalies central to depressions), b) MG (with anomalies central to depressions circled), c) residual data, d) MG anomalies > 5 nT, and e) residual anomalies > 5 nT, with anomalies pointing to hearths circled. "L" and "B" refer to lodge and borrow locations as determined through field coring. b-e) show 5 cm elevation contours and white zones indicating regions of dipolar anomalies in MG that were not analyzed.*

A close examination of the data within one of the earthlodges gives more detailed insights. In the MG data (Figure 4.15a) prominent anomalies are interpreted as hearths (H) or storage pits (S), with only the central hearth validated. The maximum of each anomaly is also reported. The MS data (Figure 4.15b) well reveal the floor area with a lack of any anomalies while along the lodge perimeter many of the anomalies interpreted as representing storage pits are indicated. The residual data are given in Figure 4.15c along with the maximum for each anomaly. Two patterns are apparent. First, anomalies interpreted or known to represent hearths and which might exhibit thermoremanence all maintain their magnetic magnitudes. The anomalies classified as storage pits, made apparent by induced magnetism, all show reductions in magnitude, with several showing a substantial decrease.

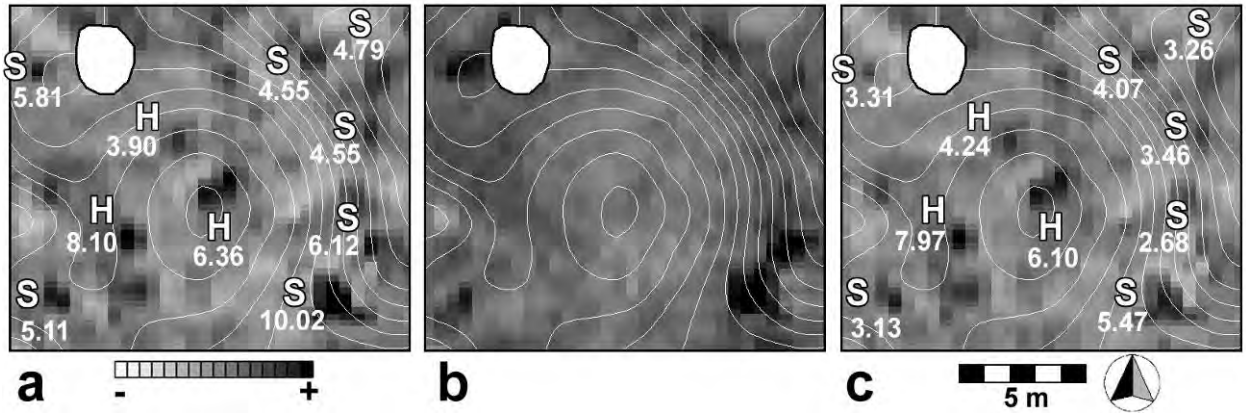

Figure 4.15. *Data from a single earthlodge at Double Ditch: a) MG, b) MS, c) residual data. Selected anomalies are interpreted as hearths (H) or storage pits (S), with the central hearth confirmed by coring. Numbers represent magnetic measurements in nT. The white region was unanalyzed owing to the presence of a large dipolar anomaly.*

DISCUSSION

The results of this investigation into the use of a regression of MG on MS data, and the plotting of residuals to aid in the identification of thermoremanent anomalies has shown moderate success. Anomalies representing hearths were generally indicated more robustly, while such induced anomalies as storage pits were reduced in magnitude. A clear shortcoming of this approach lies in sites that contain numerous iron targets that generate large dipolar anomalies which obfuscate other patterns which might occur. Another is archaeological deposits that lie at great depth beneath the surface, beyond or near the detection limits of MS instrumentation. Our study of the deep Mandan lodge, with its floor at 50 cm below the surface, was near the limits of MS detection and gave a relatively poor result. The effects of sensing depth were also illustrated in the study of the near-surface Arikara lodge. The correlation between MG and MS from the deeper-sensing EM38B (about 50 cm below surface) was r=.46 compared to only r=.35 for the shallow-sensing MS2D (about 10 cm). The reduced correlation of the latter led to a weaker result.

In all four of the case studies low to mid-range correlations occurred between the MG and MS data. This means that only a small part of the variation in MG lies in common with the MS data, which should result from correspondences between induced anomalies. These moderate to weak correlations caused poor regression models, with the resulting partial or moderate successes illustrated here.

In the foregoing, and also in Chapter 2, much emphasis was placed on the lack of depth penetration of MS instrumentation, and this factor is likely a chief reason for some of the moderate correlations with the MG data seen here. Half-meter MS detection versus one and a half-meters for MG represents an immense hurdle when the data sets are compared. There are also some differences in the lateral sensitivities between the instruments.

Another problem area was mentioned earlier, and it may not be so trivial. Minor placement differences as the instruments are recording during rapid surveys can significantly reduce correlations. This was forcefully demonstrated in Chapter 2 where repeat surveys with the *same* instrument yielded moderate correlations (r) of only .54-.56. At Double Ditch, we were able to examine this phenomenon further.

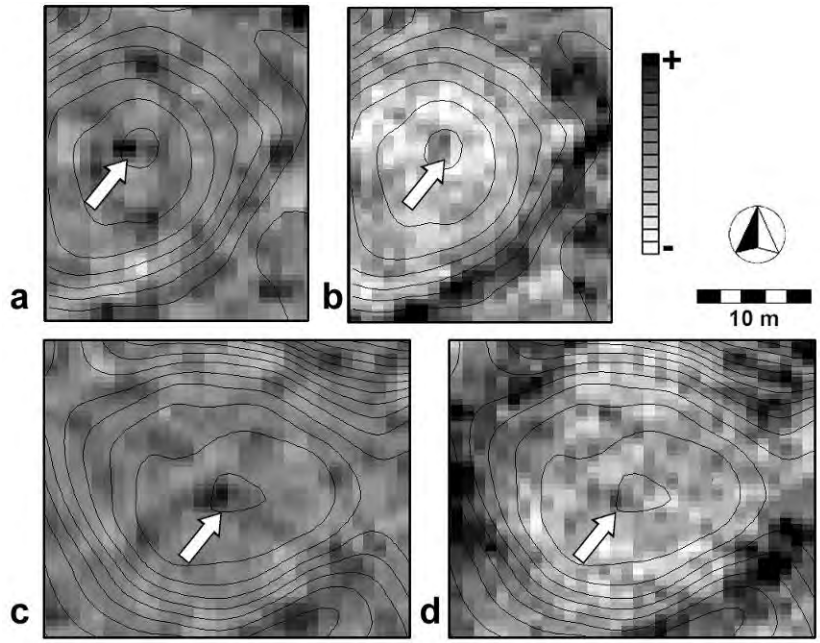

Figure 4.16. *Examples of variations in survey locations at Double Ditch where significant anomalies (arrows) are slightly off-set by one transect (column) reducing data correspondences and comparability: a) MG in lodge, b) MS (EM38B) in same lodge, c) MG in borrow pit, d) MS in same borrow pit.*

Close inspection of the Double Ditch MG and MS data, which were acquired at a common sampling density of .5 x .25 m, reveals small and subtle shifts between prominent anomalies (Figure 4.16). In one of the lodge locations an anomaly representing the central hearth in the MG data is off-set one column and row in the MS data (Figure 4.16a, b; columns are .5 m wide; rows are .25 m). Likewise, an anomaly within a borrow pit is off-set one column between the data sets (arrows, Figure 4.16c, d). With transects running along columns, such off-sets can easily occur because even a slight shift of a few centimeters in where a transect is walked can cause measurements to "skip" into the next column of data. While seemingly a trivial matter for visualization and interpretation purposes, quantitatively these data shifts serve to reduce the correlation between the data sets and therefore the strength of the modeling approach advocated here. One of the improvements that must be achieved to further pursue this regression approach is a closer spatial correspondence between the data sets, which may be obtained by greater care in surveys or through the use of advanced computer-based image registration methods (Burrough and McDonnell 1998).

CHAPTER 5: MAGNETIC VARIATIONS IN HUNTER-GATHERER CAMPS

Geophysical surveys of ephemeral hunter-gatherer sites are rare because they usually lack architectural remains and such ground disturbances as ditches and storage pits that are the typical targets of geophysical surveys. In one study of hunter-gatherer camps, however, Jones and Munson (2005) illustrate the value of magnetometry for locating hearths. The potential of MS mapping in hunter-gatherer sites has not been previously evaluated to our knowledge. In contrast, extensive multi-instrument geophysical surveys, including MS surveys, have been carried out in permanent village sites associated with agricultural peoples throughout the world (Atalan Çayirezmez et al. 2008; Buteux et al. 2000; Williams et al. 2007; see papers in Johnson 2006). Our own work at several Plains Village period (A.D. 1000-1886) sites in the Northern Great Plains has yielded a better understanding of their organization and complexity (Kvamme 2003c; Wiewel and Kvamme 2013). This work has almost always concentrated on the village core where the greatest density of human activities occurred and topographic expressions of features like houses, fortification ditches, and storage pits are evident. An important shortcoming of this focus is that much less is known about activities that occurred near the periphery of these sites.

One use of outlying areas surrounding permanent Northern Plains villages was as a temporary camping location for nomadic hunter-gatherer groups, who often visited for trading purposes. Nomadic tribes, including Dakota, Lakota, and Crow, are known to have visited Fort Clark frequently during the mid-nineteenth century. Ample documentation relates that these groups camped along the margins of the site, perhaps as far away as Chardon Creek which was some distance away from the Mandan-Arikara village and Fort Clark itself (Wood 1993; Figure 5.1). Identification of these locations is important for several reasons. Despite Fort Clark's documented significance as a center of exchange among Euroamerican traders, sedentary agriculturalists, and nomadic hunter-gatherers, virtually all archaeological research has focused on the trading posts or the village itself. Little research has been conducted on the hunter-gatherer camps which constitute an important aspect of the site's history and one that is not well understood archaeologically.

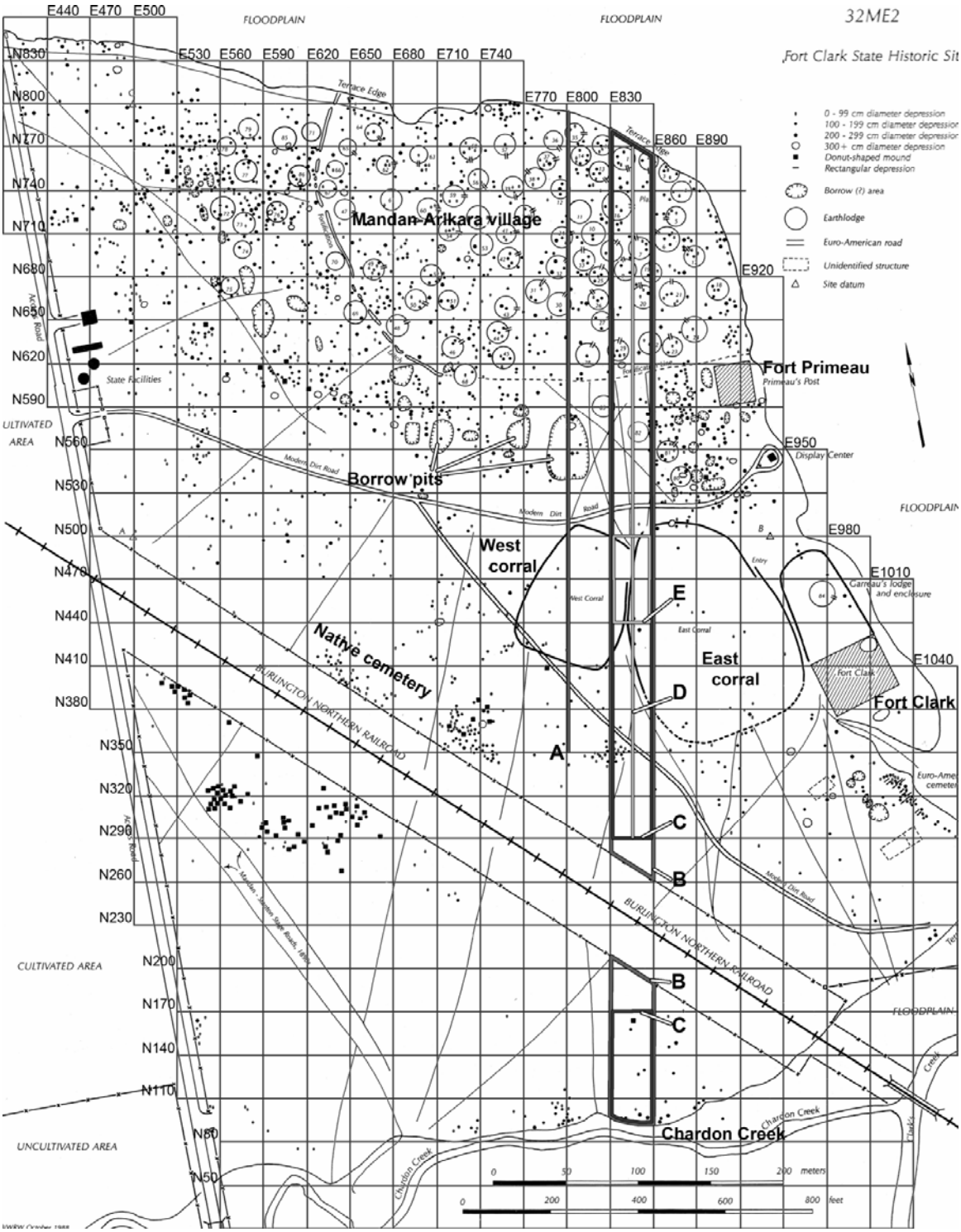

Figure 5.1. *Map of the Fort Clark State Historic Site and vicinity to the south showing the locations of magnetic susceptibility and magnetometry surveys performed to identify areas possibly utilized by nomadic hunter-gatherers while visiting the site for trading purposes (adapted from Wood 1993:Figure 3). The grid illustrates 30 m blocks with metric coordinates indicated. In the 19th century the Missouri River flowed immediately to the north and east of the mapped space.*

BACKGROUND INFORMATION

Historical documents in the form of artistic depictions and written accounts are one potential source of evidence detailing the location of nomadic hunter-gatherer camps at Fort Clark. No illustrations of these camps at Fort Clark are known to exist. Yet, the well-known artists George Catlin and Karl Bodmer, who wintered at Fort Clark in different years (1833 and 1834, respectively), portrayed remarkably similar and informative scenes of the two nearest American Fur Company trading posts, Fort Pierre and Fort Union (Catlin 1973 [1844]:Plates 3 and 85; Ruud 2004:Tableaus 10 and 28). Each image shows the trading posts situated in an open plain near the Missouri River. Surrounding the posts are many tipis of nomadic groups visiting for purposes of trade.

Given Bodmer's role as a scientific illustrator or documentary artist in the Maximilian expedition and Catlin's proclivity for employing greater artistic license (Wood et al. 2002), one might expect Bodmer's two images to provide a more accurate portrayal of Fort Pierre and Fort Union. The most significant difference between the two pairs of images is in the number of tipis, with Catlin showing many more in his illustrations. Still, Catlin's (1973 [1844]:209) writings corroborate his depictions when he states: "I made a painting […] shewing [*sic*] an encampment of Sioux, of six hundred tents or skin lodges, around the Fort, where they had concentrated to make their Spring trade." Despite the possibility of Catlin's exaggeration, at least one relevant observation can be made based on the four illustrations. That is, nomadic hunter-gatherers who visited the trading posts camped in a clustered pattern, with many groupings of tipis—perhaps family or clan groups—located a considerable distance from the posts.

Maximilian's account provides further support for this observation and offers additional insight regarding the location of nomadic encampments at Fort Clark. When he arrived at Fort Clark in June 1833, Maximilian (2010:199) notes: "Behind the fort were seventy leather lodges of the Crows" about 300 paces from the Mandan village. The expedition returned to Fort Clark in November 1833 after having traveled upriver to the American Fur Company's Fort McKenzie in present-day Montana. Maximilian (2012:52) states that during his absence, "Two hundred tents of Yanktonais [Dakota] had camped on the prairie behind Fort Clark and stayed there three to four days." Combined, these historical documents provide a starting point for our geophysical investigations and a reference for the types of features one would expect to identify.

A number of circumstances limit the utility of geophysical investigations in hunter-gatherer contexts. Specifically, the types, densities, and frequencies of human behaviors that leave behind archaeological evidence are relatively rare. Dwellings are generally in the form of tents or other ephemeral structures, and constructions that disturb the earth (ditches, pits, long-term architecture) generally are absent. Yet, even in short-lived camps, other human behaviors like cooking and the use of fire remain frequent, and refuse was commonly abandoned. At Fort Clark we may presume that nomadic tribes visited the site throughout its nearly 40 year history (from about 1822-1861). Consequently, many of the potential camp sites may have been occupied repeatedly. This suggests that at potential camp sites many activities may have actually taken place in a cumulative sense. Their net effect is therefore likely an accumulation of magnetic enhancements resulting from numerous hearths, a general enrichment of the site soils through many burning events, and the cumulative deposition of organic wastes that promote increased magnetic susceptibility (see Chapter 1; Kvamme 2006a). Moreover, as Fort Clark was an important trading center, many metal artifacts were traded (mostly of iron), and these too would have accumulated in the soil through loss or discard. We may therefore assume that MS

and magnetometry surveys will indicate hearths, ferrous metal artifacts, and anthropogenic enhancements to the soil resulting from cooking and other fires, food waste, and other occupational activities.

SURVEY AREAS

We anticipated that over time nomadic camp activities at Fort Clark would leave characteristic signatures of magnetic anomaly clusters and increased magnetism isolated from the Mandan-Arikara village and the Fort Clark trading post itself. To evaluate this assertion, a series of MS and magnetometry surveys were undertaken in the open spaces south of the village and west of the trading post. This is the approximate area referred to by Maximilian (2010:199), "about 300 paces from the Mandan village," although a historically documented Native cemetery located in the open area further to the west would certainly have been avoided. The following geophysical surveys were undertaken and are illustrated in Figure 5.1.

Survey A

A MS survey using the Bartington MS2 system with the “D” surface scanning probe of a 440 m long transect was performed north of the railroad tracks, running north-to-south (N-S) from N350-N790 along the E802.5 line, with samples taken every 5 m (Figure 5.1). Typically, two or more measurements less than 25 cm apart were taken at each location (the instrument was zeroed before each measurement) and then averaged. Uncharacteristically high measurements (data spikes) caused by the presence of metal artifacts were avoided by the repeated measurements and are not generally included. These data were converted to volume susceptibility following the procedure described in the operation manual (see Chapter 1; Bartington Instruments 2013).

Survey B

A Bartington MS2 survey with the "D” surface scanning probe was undertaken in a 30 x 690 m area in 5 m sample intervals oriented in a N-S column between N80-N770 and between E830-E860 (Figure 5.1). The six measurements taken across the 30 m wide survey area (with 5 m separation) were averaged to produce a single transect of data centered on the E845 line. This survey extended south of the railroad tracks to the edge of Chardon Creek.

Survey C

A magnetic gradiometry survey, performed with a Bartington Grad601 dual-sensor system (see Chapter 1), covered the same area described in "B" with 8 samples per meter and 0.5 m between transects (16 measurements/m^2).

Survey D

A MS survey of a single 480 m N-S transect along the E844.5 line was conducted with 0.5 m sampling using the Geonics EM38B (Chapter 1; Figure 5.1). Due to the long length of this transect and this instrument’s tendency to “drift” after initial zeroing, the data were de-sloped by subtracting an observed linear trend. The data were scaled from their native ppt to SI units (see Chapter 1) through a zero-intercept regression against a nearby data set calibrated to SI units.

Survey E

A MS survey of a 30 x 60 m area was performed along the N-S column from N440-N500 between E830-E860 using the Geonics EM38B with two measurements per meter and 1 m transect separation (Figure 5.1). The measurements were converted to SI units using procedures described in the operating manual (see Chapter 1; Geonics 2003:13).

RESULTS

Surveys A and B: Linear MS Transects with Bartington MS2D

Surveys A and B represent two transects of Bartington MS2D data only a short distance apart that extend across the village to the railroad tracks to the south and beyond in the case of Survey B (Figure 5.1). Survey A includes measurements taken along a single line while Survey B represents an average of six transects taken across a 30 m wide space. Both transects are informative and offers insights regarding the enhancement of soil MS caused by human activity across the site. The highest MS values are found between approximately N600-N800 and correspond to the core area of the Mandan-Arikara village (Figure 5.2). In fact, this area of the site includes some of the most densely packed lodges. Because this region would have experienced the most intense and long-term use, including food storage in large subterranean storage pits, frequent cooking, food disposal, fire-building and other occupational activities, the high MS values are not surprising. This pattern of high susceptibility in the core village area and relatively lower susceptibility south of the village is expected. However, the MS data point to additional localized areas of high susceptibility far outside the village.

For instance, the data clearly illustrate increased susceptibility values between approximately N450-N575 on Survey A's E802.5 line (Figure 5.2a). These measurements correspond to two features visible on the ground surface (Figure 5.1). The northernmost feature (centered on N560) is a large borrow pit. Why this feature exhibits high susceptibility is not clear, although many collapsed storage pits surround the borrow pit. The high susceptibility values may somehow derive from the storage pits, especially if they were filled with magnetically enriched midden materials after their regular use for food storage ended. The second feature, a probable horse corral, appears to relate to high susceptibility values between N460-N500. The feature consists of a low oval-shaped earthen embankment. A soil chemistry analysis performed in the 1980s demonstrated high concentrations of phosphorus and total carbon within the corral areas, argued to be the result of accumulated animal waste (Wood et al. 2011). Similarly, increased MS in this area is likely caused by a combination of animal waste and the mounded soil encircling the corrals. The significant rise in MS south of the N410 line (Figure 5.2a), clearly outside of the corral space (Figure 5.1), is associated with few visible surface features and may indeed point to a region of magnetic enrichment resulting from past human activities, such as those that might occur in hunter-gatherer camps.

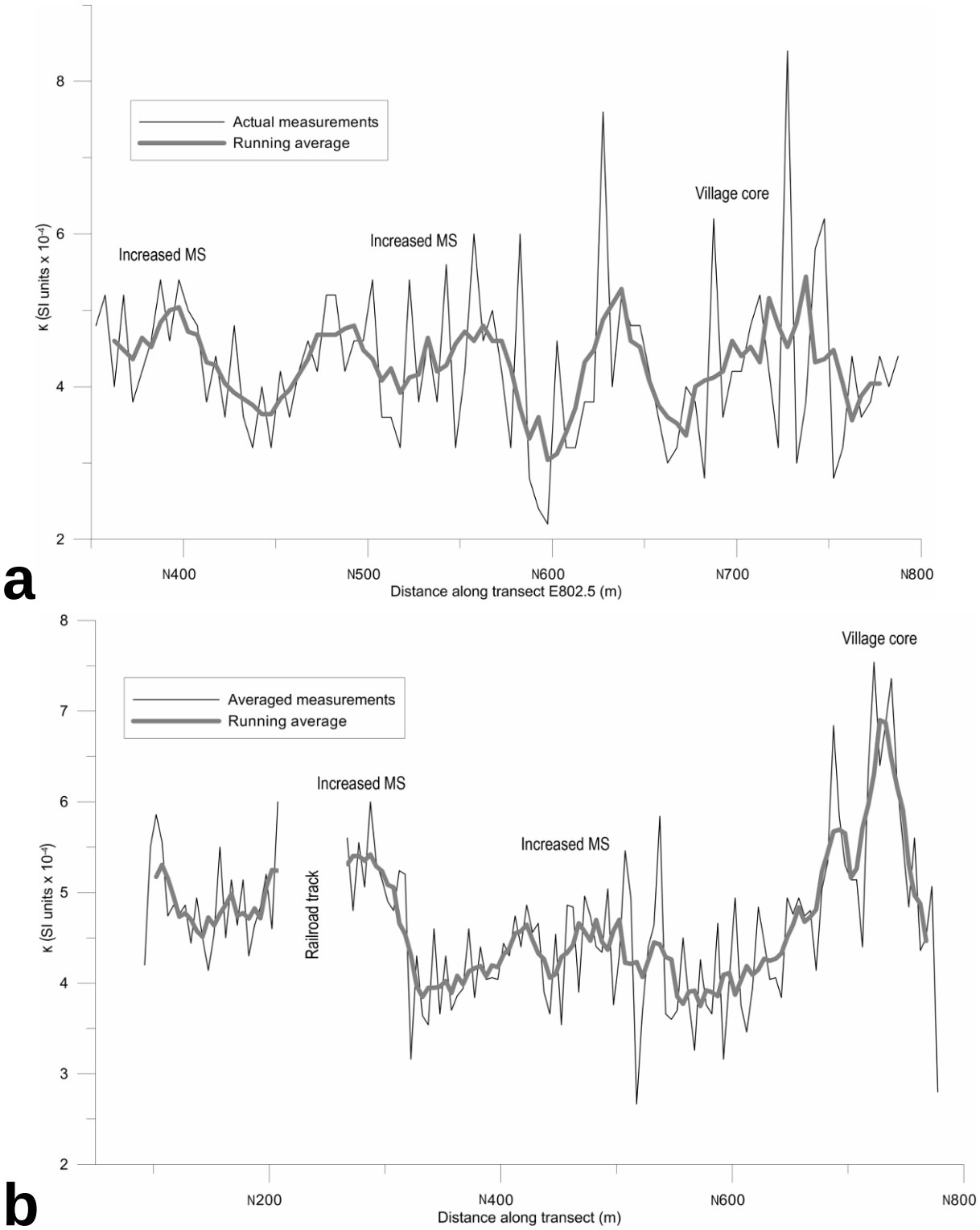

Figure 5.2. *MS transect data collected by the Bartington MS2D along a) the E802.5 N-S transect (Survey A), and b) the E845 N-S transect (average of six transects across 30 m wide Survey B). The plots include actual values as well as a running average of seven measurements. North is to the right*

The MS measurements shown in Figure 5.2b, which represent the average of six transects between E830-E860 (Survey B), mirror these interpretations. Specifically, we see very high MS in the village core (north of N600) and a region of elevated susceptibility south of the village core (between about N400-N500) that relates to the corrals as this transect passed over these features (Figure 5.1). More importantly, this transect, like the previous, exhibits elevated MS far to the south, an exciting finding given our belief that these areas of the site were utilized by nomadic groups who regularly visited Fort Clark. In Figure 5.2a, the high values are centered on N400, an open area south of the corrals with some topographic features visible on the ground surface. The second transect (Figure 5.2b) shows a similar result, with an even larger increase in MS measurements south of N300.

Unfortunately, a railroad track cuts through this area of the site which prevented data collection over an approximately 60 m area. Yet, MS values remain very high south of the railroad track near Chardon Creek despite its considerable distance from the Native village. We believe this area along the creek would have been the prime camping spot for hunter-gatherer groups visiting the site for any extended period for several reasons. In particular, it is close to fresh water, it likely contained good pasture as it does today as it is far from the Mandan-Arikara village where overgrazing was likely, it offers good shelter from winds and storms with a protective terrace edge, and it is away from the village burial ground (Figure 5.1) which may have made camping near the village less desirable.

It may be of some significance that the MS measurements south of the railroad tracks are likely *reduced* in magnitude by the much thicker vegetation in this un-mowed hayfield, which caused an increased distance between the MS2D sensor and the soil (areas north of the railroad track are mowed). As related in the Chapter 1 and demonstrated in Chapter 2, contact with the soil is crucial to surveys utilizing the MS2D since the response falls off rapidly with depth. Specifically, the response is only 50 percent at 1.5 cm and 10 percent at 6 cm from the sensor's surface (Bartington Instruments 2013). Despite our attempt to flatten the vegetation during the survey through simple foot-stomping, we strongly believe the thicker vegetation nevertheless had the effect of reducing the measurements. Thus, the greater thickness of the vegetation cover likely led to decreased measurements overall. Although this pasture is used for cattle grazing, we do not believe the higher levels of cattle waste could conceivably increase MS through organic enrichment (see Introduction), as it does not explain the similar increase in MS also seen immediately north of the tracks.

Survey C: Magnetic Gradiometry Transect

Some of the MS findings are clarified by the results of a magnetic gradiometry survey along the same N-S transect of Survey B (Figure 5.3). For instance, the high MS measurements seen in Figure 5.2b from approximately N600-N770 correspond with the village core where earthlodges, hearths, and storage pits are common. Additionally, many of the largest data values in Figure 5.2b are caused by ferrous metal, evidenced by numerous dipolar magnetic anomalies in the gradiometry data. South of about N600 the magnetic gradiometry data are relatively less variable with fewer dipolar anomalies. However, the low mounded edges of the corrals beginning at about N510 are visible as arcing anomalies of slightly elevated magnetism, probably due to mounding of surface soils, with values between about 1-1.5 nT. Linear negative anomalies, about -0.5 nT in strength, parallel these berms and correspond with trails incised into the surface, which causes an increased ground-to-sensor distance and a decrease in apparent magnetism.

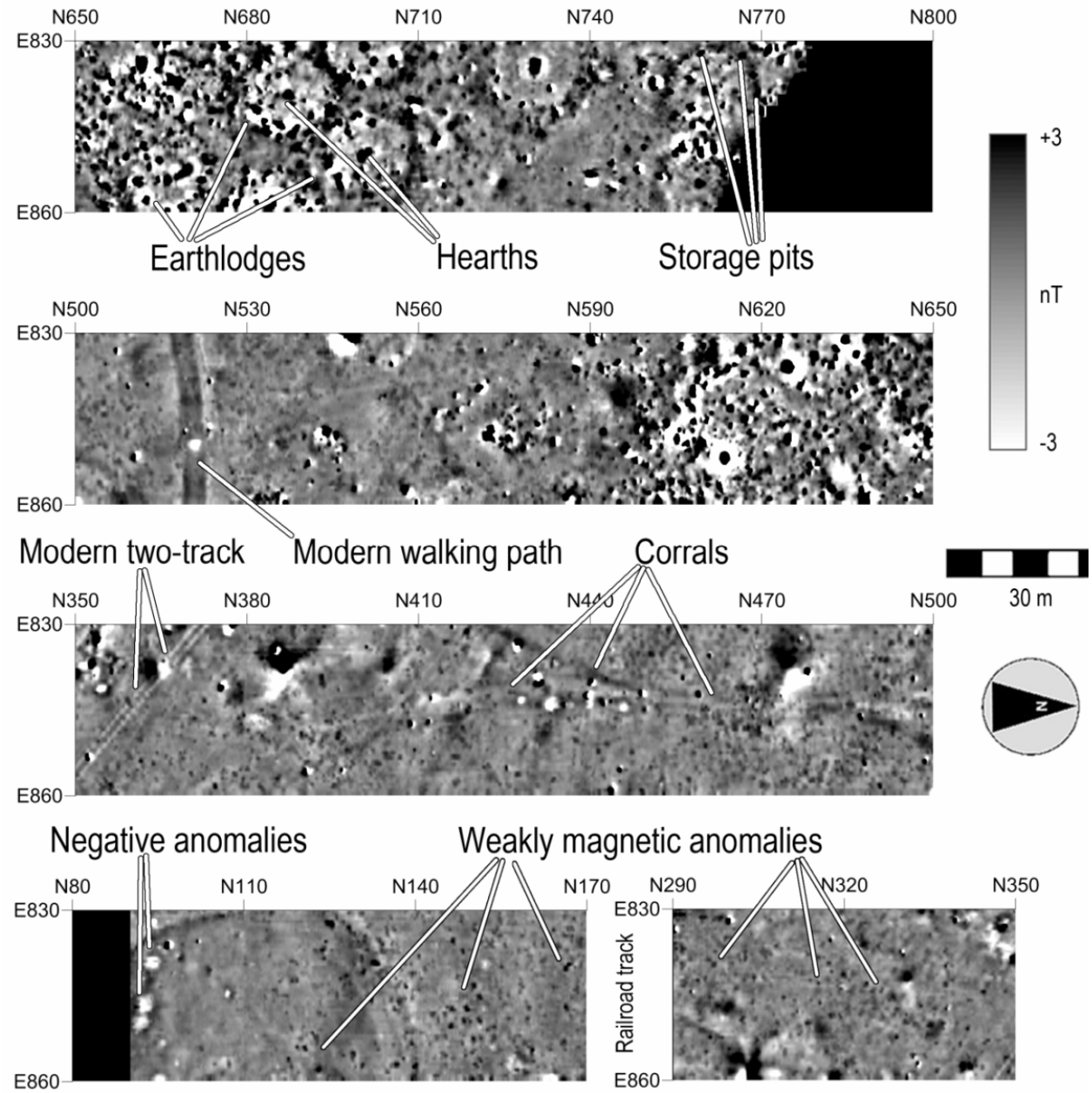

Figure 5.3. *Magnetic gradiometry data along N-S transect between E830-860 showing a sampling of anomalies related to known archaeological features as well as unexplained anomalies that may be indicative of nomadic hunter-gatherer campsites (Survey Area C).*

Of most importance are numerous clusters of weakly magnetic anomalies toward the southern edge of the survey area (Figure 5.3). Anomalies of this type are not unique to this area as similar ones can be seen across much of the N-S transect. However, the clustered patterning of these anomalies south of the railroad track and immediately to the north (around N320) perhaps indicates an anthropogenic cause. Most have magnetic values between 2-5 nT and are possibly caused by a build-up of small and weakly burned hearths through time, as would be likely in successive hunter-gatherer camps. Moreover, some of these anomalies are dipolar, indicating the

presence of metal and therefore human activity (Figures 5.3 and 5.4). Additionally, several large negative anomalies correspond with surface depressions along the edge of Chardon Creek. They may represent archaeological features (perhaps unfilled storage pits), but other explanations are possible (e.g., former animal burrows or tree throws). Coring or test excavations will be necessary to clarify these interpretations.

An enlarged view of the magnetic gradiometry data south of the railroad track (one segment of Survey C) is shown in Figure 5.4. These data are overlaid on an elevation model to illustrate the correspondence between magnetic and elevation data. Topographically, the ground surface exhibits little change except near Chardon Creek where it slopes abruptly toward the creek. Near the middle of the survey area, a series of weakly positive and negative parallel, linear, magnetic anomalies are apparent (indicated by a black arrow in Figure 5.4). These anomalies are perhaps naturally caused, such as the remnants of a filled paleochannel or a thin layer of overbank sediment. Alternatively, they may indicate an historic trail or even a cattle or buffalo trail that crossed the creek near the survey area. No evidence of trails is visible on the ground surface in the survey area today, however (Figure 5.1). Interestingly, the clusters of magnetic anomalies that we believe indicate hearth features of nomadic hunter-gatherer campsites are located well away from the creek edge. In fact, the area buffering the creek (within approximately 30 m) exhibits considerably fewer anomalies in comparison. This may indicate a preference for locating camps away from the creek edge or its use for other purposes (e.g., gardening). Alternatively, a flash flood event may have scoured away deposits containing archaeological evidence, or perhaps high levels of recent sedimentation buried archaeological features more deeply in this area, making magnetic anomalies weaker or invisible.

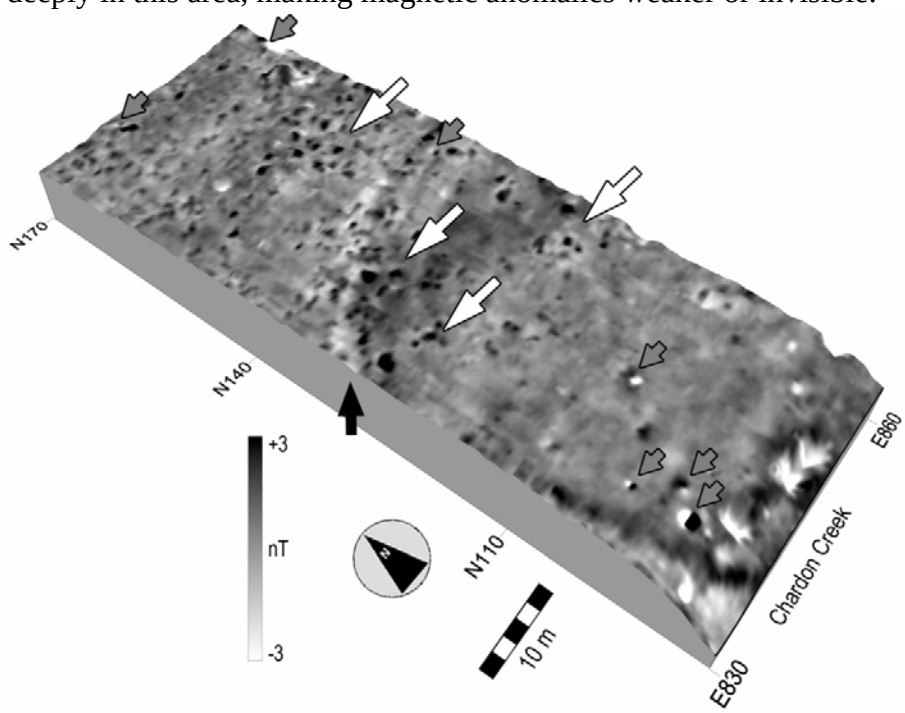

Figure 5.4. *Close-up details of the magnetic gradiometry data overlaid on an elevation model (Survey Area C south of the railroad track). White arrows point to clusters of magnetic anomalies, perhaps indicating hearth features. Gray arrows indicate dipolar magnetic anomalies indicative of iron artifacts while an unusual linear anomaly is noted with a black arrow.*

Survey D: Linear MS Transect with Geonics EM38B

In general, the MS data collected with the EM38B along the E844.5 N-S transect parallel the Bartington MS2D measurements (Figure 5.5). For instance, the village core exhibits higher MS values on average than other areas along the transect. Subtle increases in MS also point to other prominent features like the corrals (between approximately N400-N500). Significant differences are apparent, however. One obvious difference is the large data spikes (extreme values) caused by metal, particularly within the village core, a finding that parallels the magnetic gradiometry data (Figure 5.3). In the slow Bartington MS2D surveys with manual recording, extreme measurements or data spikes were avoided simply by sampling to the left or right when they were encountered, and thus they are generally absent in the data. This was not possible in the EM38B surveys with their rapid pace and automated data logging which recorded all measurements on the fly without the possibility of editing.

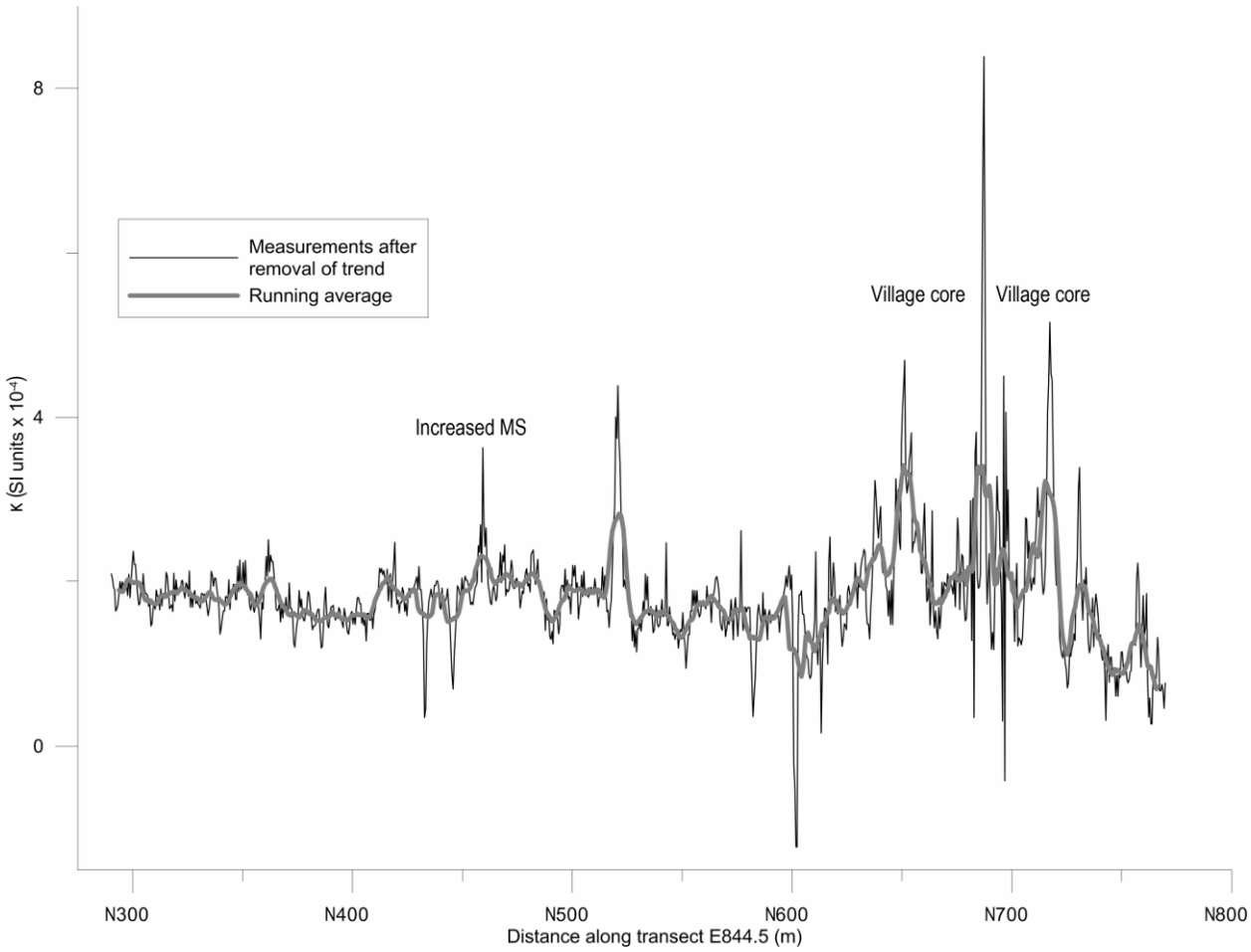

Figure 5.5. *MS data collected by the Geonics EM38B along the E844.5 N-S transect (Survey Area D). The plot illustrates the "de-trended" data as well as a running average of 15 measurements.*

More importantly, the increase in susceptibility values visible in the MS2D data sets toward the southern end of the transect is not as strongly evident in this case, although a mild increase to the south is noted. The reasons for this difference are unclear. One possible explanation arises from dissimilar survey methods. MS2D measurements were averaged across six transects, each separated by 5 m, to produce the plot in Figure 5.2b. In contrast, Figure 5.5 is derived from survey with the EM38B along a *single* transect. It is possible that this single transect simply missed some areas of magnetic enrichment a short distance away. More likely, the varied responses are due to differences in sensing depths between the two instruments. The MS2D response curve is very shallow, less than 10 cm, with 50 percent of the signal received from the top 1.5 cm (Bartington Instruments 2013). The in-phase component of the EM38B yields a weighted average of MS through a depth of about 50 cm, with peak sensitivity at about 20 cm depth and much less sensitivity below 10 cm (Dalan 2006a:Figure 8.7). The high MS shown at shallow near-surface depths by the MS2D on the south ends of the transects (Figure 5.2) is consistent with the presence of recent hunter-gatherer camps. That similarly high MS is not indicated by the EM38B may therefore be due to its lack of response to very shallow depths which is further reduced by being averaged with the remaining volume through a depth of 50 cm.

Survey E: MS Survey with Geonics EM38B in 30 x 60 m Area

The MS data acquired by the EM38B in the 30 x 60 m block are less informative regarding the possibility of hunter-gatherer encampments (Figure 5.6). Compared to the magnetic gradiometry results, these data offer less detail, due in part to a lower sampling density (0.5 x 1 m versus 0.5 x .125 m). Still, there are subtle indications of the mounded berm that surrounds the corrals, shown as higher MS. Other point anomalies with high MS values correspond with anomalies in the gradiometry data. Two large MS anomalies do fall near the center of the survey area which are more weakly indicated in the gradiometry data as small clusters of positive anomalies. Their very high susceptibilities suggest unusual activity that caused high MS, such as extensive dispersal of fired soils, concentrated cooking areas, or an unusual magnetic enrichment from organic matter from corral-related activities. It cannot be certain that these anomalies were generated by hunter-gatherer activities, however. Similar surveys should be extended to the south to provide a better assessment of potential activity areas and encampments. Note that with the wider transect spacing of the EM38B survey, the iron object that generated the large dipolar anomaly seen in the gradiometry data at about N480 apparently was not traversed and is therefore not visible (Figure 5.6).

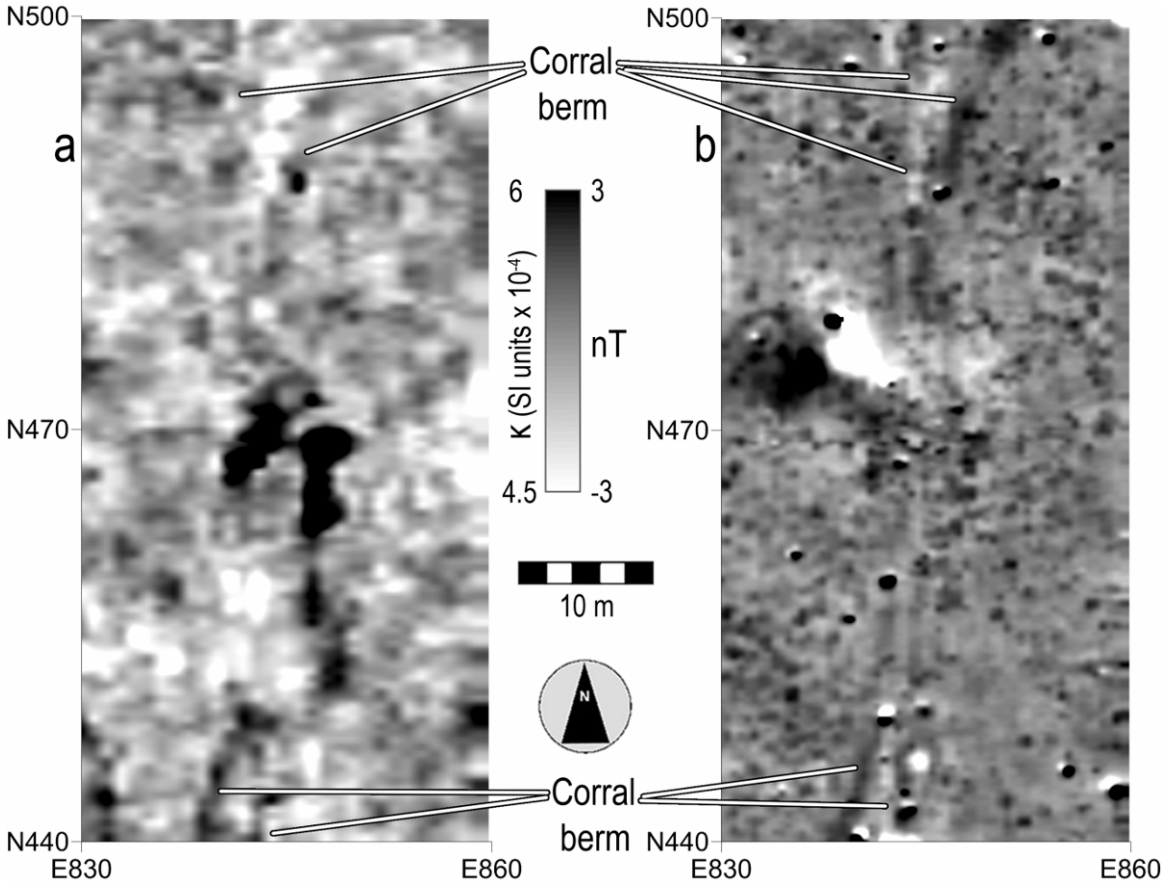

Figure 5.6. *MS (a) and magnetic gradiometry (b) data collected along the N-S transect (Survey Area E) between N440-N500.*

DISCUSSION

Prior to this research no archaeological evidence existed concerning the locations of likely nomadic hunter-gatherer camps at the Fort Clark State Historic Site, aside from brief descriptions in Maximilian's (2010, 2012) journal entries. Our findings offer additional lines of evidence that could point to their locations. From a magnetic standpoint, the village periphery, and even regions much beyond such as the Chardon Creek area, seem very active indeed, with enhanced MS and magnetic gradiometry anomalies similar to those found in portions of the village. These anomalies occur despite a near-absence of surface-visible features common to the village and trading post areas, such as clear depressions over former houses, a defensive ditch, and collapsed storage pits. As hunter-gatherer camps did not possess such features, we must infer that these magnetic anomalies derive from other activities and archaeological features common to hunter-gatherer camps, such as cooking, fire building, processing of food, and the accumulation of refuse. Many of the visible magnetic anomalies illustrated here likely arise from these factors.

It seems clear that the Geonics EM38B offers advantages over the Bartington MS2D for MS surveys. It is much faster, permitting transects of hundreds of meters to be walked in minutes compared to hours. The greater speed also permits more data to be recorded per unit time and therefore higher sampling densities or spatial resolutions: two measurements/m were commonly

acquired with the EM38B compared to one every 5 m for the MS2D. The greater speed and higher sampling rate of the EM38B permitted high resolution survey of a 30 x 60 m area in a relatively short span of time (Figure 5.6). The EM38B also permits much deeper prospecting, to 50 cm, compared to the shallow sensing of the MS2D, of less than 10 cm. Yet, our work at Fort Clark suggests high MS occurs at extremely shallow depths that was detectable by the MS2D but not the EM38B (compare Figures 5.2 and 5.5). Moreover, the EM38B is highly susceptible to drift, especially with temperature changes, forcing the need to estimate corrections (Figure 5.5). Measurements with the MS2D, on the other hand, may be corrected by zeroing prior to each reading (see Chapter 1). At Fort Clark we feel that the MS2D gave superior results because more variations in MS were recorded that appear to occur at extremely shallow depths and may be due to recent hunter-gatherer occupations. At other sites this circumstance may not be true and the greater prospecting depth of the EM38B together with its greater speed or sampling rate may prove of more importance.

Although our results are not conclusive, we believe magnetic gradiometry and magnetic susceptibility methods are suitable for locating ephemeral hunter-gatherer sites. Considering our findings, surveys of large areas with course sampling using the Bartington MS2D can be useful as a prospecting technique to pinpoint areas that can be investigated further. In fact, we consider our geophysical surveys an initial step that should lead to more extensive geophysical and archaeological work in this area of the site. More importantly, we hope our work will encourage similar research at other village sites along the Missouri River in North and South Dakota. Since these sites served as hubs of trade in a vast network (Swagerty 1988; Wood 1980), such an undertaking is necessary to better comprehend the complexity of intertribal trade relations prior to and at the advent of Euroamericans.

CHAPTER 6: CONCLUDING SUMMARY

This report attempted to increase understanding of archaeological magnetism, its causes, and how it may be measured to improve our interpretations not only of the magnetic record, but of our cultural past. It did so by examining four research topics with a wide variety of instruments for recording aspects of archaeological magnetism. Data were gathered at the Double Ditch and Fort Clark State Historic Sites, in North Dakota, two sites that hold a variety of prehistoric and historic cultural features ideal for these studies.

The first focus, in Chapter 2, was on instrumentation, specifically the utility of the two technologies for the field recording of near-surface magnetic susceptibility (MS). The twin-coil EM38 by Geonics Ltd., an electromagnetic induction device, was examined because these instruments have not been greatly used for this purpose. These data were compared against near-surface measurements of volume MS acquired with a single-coil Bartington MS2D field sensor, a long-accepted standard for the field recording of MS. Multiple surveys of areas and linear transects over a variety of archaeological features were undertaken with *both* instruments at Fort Clark. Statistical analyses and visual comparisons of the mapped data were made to yield assessments of the performance of these instruments in archaeological field contexts. The MS2D posed limitations that included a very slow rate of data acquisition and limited penetration depth (less than 10 cm), generally regarded as a disadvantage when considering large areas and often-deeper features. The EM38B, with its many times greater speed of survey and larger depth penetration (to about 50 cm), was shown to equal or surpasses the MS2D in data quality (especially in contexts where archaeological features were deeper), which make it preferable as a field instrument in many survey settings

Chapter 3 examined how the archaeological record forms magnetic anomalies that are commonly recorded in magnetometry surveys. It also investigated the utility of several hand-held instruments for recording MS in the vertical dimension, on bare-earth archaeological profiles or through down-hole sensing. In this study several excavations were made to expose sections, or profiles, across major archaeological feature types that occur in the Northern Great Plains (and elsewhere): a subterranean storage pit, a fortification ditch, and a house floor. To reduce project costs, previously excavated trenches across these features were re-opened in the Double Ditch State Historic Site, in central North Dakota. MS was recorded across the faces of the exposed profiles every 5-10 cm (depending on the sizes of the profiles) to reveal, in detail, the magnetic stratigraphy. These data could then be compared against magnetometry findings previously recorded at the surface. Visual comparisons alone suggested much about the "how and why" of anomaly formation at the surface. Nevertheless, simple and complex mathematical models, aided by GIS, quantitatively indicated how subsurface magnetism should express anomalies at the surface. Comparisons against the actual magnetometry showed moderate to excellent correspondences permitting better realization of relationships between subsurface magnetism and anomalies recorded by magnetometry.

Chapter 4 confronted a common problem in the interpretation of magnetometry data in large surveys, particularly in the Northern Plains. Typically, hundreds or even thousands of anomalies are roughly circular in shape, 1-3 m in diameter, and approximately of the same magnitude. Excavations have revealed they are typically generated by two cultural feature types. One is by hearths, which form thermoremanent anomalies, and the other occurs over abandoned cache pits filled with magnetically enriched soils that cause induced anomalies. Anomalies from both feature types, of course, look the same to a magnetometer, making site interpretation

difficult. Yet, distinguishing between hearths and storage pits is critical to understanding site structure and organization in any region. This study was carried out over a variety of house features at the Fort Clark and Double Ditch State Historic Sites using magnetometry and MS field surveys. As magnetometry quantifies the *sum* of remanent and induced magnetism while MS surveys are sensitive only to the latter, regression methods were employed where the *residuals* were argued to show magnetic anomalies resulting primarily from remanent magnetism, generally hearths. The remaining anomalies were induced anomalies and most often represented storage pits. While this pioneering study was only moderately successful (owing to correlations between the magnetometry and MS data typically less than r=.5), we believe it is a beginning and have identified avenues for improvements. Validation was offered because in several instances hearths and storage pit locations were known and model predictions were generally correct.

The final case study in Chapter 5 addressed a shortcoming in archeo-geophysics by focusing on hunter-gatherer camps (something rarely undertaken owing to a lack of major ground disturbances made by these societies that are the primary targets of geophysics). This was particularly important in this project because of our lack of knowledge about early Native interactions with fur trading centers in the Northern Plains generally, and specifically at the well-documented Fort Clark State Historic Site. Historically, nomadic Dakota and Crow groups visited Fort Clark for purposes of trade. A likely camping spot was along nearby Chardon Creek, some distance away from the Mandan-Arikara village which dominates the site, but eye-witness accounts also relate nomadic camps closer to the village. These camps form a crucial aspect of the history of the site that is not well understood and archaeological investigation has been nearly absent. MS and magnetometry surveys were performed that indicate anthropogenic enhancements to the soil—increased MS—likely from cooking fires, food waste, and other occupational activities. These results give a fuller idea of spatial and organizational aspects of Fort Clark's history and suggest that much more might be learned in this way about hunter-gatherer camping locations and activities.

ACKNOWLEDGEMENTS

We are indebted to Fern Swenson, Deputy State Historic Preservation Officer and Director of the Archaeology and Historic Preservation Division of the State Historical Society of North Dakota (SHSND) for access to Fort Clark and Double Ditch and general support in all aspects of the project, particularly in providing power equipment for the excavations and back-filling at Double Ditch. Tim Reed of the SHSND helped relocate one of the excavations from 2004 by total station. Jo Ann Kvamme and Margaret S.Patton, staff and graduate student, respectively, from the University of Arkansas, served as field crew. Dr. Kacy Hollenback, of Southern Methodist University, and Fern Swenson assisted with fieldwork at Double Ditch. Erik Holland of the SHSND generously provided camping space on a nearby property during the fieldwork at Fort Clark. Lee Alderin provided access to his leased property for our magnetic surveys of potential hunting-gathering camps. This report was developed under a grant from the National Park Service and the National Center for Preservation Technology and Training. Its contents are solely the responsibility of the authors and do not necessarily represent the official position or policies of the National Park Service or the National Center for Preservation Technology and Training.

REFERENCES CITED

Ahler, Stanley A., ed. (2003). *Archaeological Investigations at Fort Clark State Historic Site, North Dakota: 1968 through 2003 studies at the Mandan/Arikara village*. PaleoCultural Research Group, Flagstaff, Arizona. Submitted to the State Historical Society of North Dakota, Bismarck.

Ahler, Stanley A. (2004). Artifact densities, spatial patterns, and settlement dynamics. In *Archaeological Investigations During 2003 at Double Ditch State Historic Site, North Dakota*, edited by S.A. Ahler, pp. 295-314. Unpublished report by PaleoCultural Research Group, Flagstaff, Arizona, submitted to the State Historical Society of North Dakota, Bismarck.

Ahler, Stanley A. (2005a). Pit excavations. In *Archaeological Excavations During 2004 at Double Ditch State Historic Site, North Dakota*, edited by S. A. Ahler, pp. 77-137. Unpublished report by PaleoCultural Research Group, Flagstaff, Arizona, submitted to the State Historical Society of North Dakota, Bismarck.

Ahler, Stanley A. (2005b). Summary and conclusions. In *Archaeological Excavations During 2004 at Double Ditch State Historic Site, North Dakota*, edited by S. A. Ahler, pp. 327-336. Unpublished report by PaleoCultural Research Group, Flagstaff, Arizona, submitted to the State Historical Society of North Dakota, Bismarck.

Aspinal, Arnold, Chris Gaffney and Armin Schmidt (2008). *Magnetometry for Archaeologists*. AltaMira Press, Lanham, Maryland.

Atalan Çayirezmez, Nurdan, Ertepinar Kaymakçi, Pinar, and Geoffrey D. Summers (2008). Remote sensing methods at Kerkenes: combining geophysical and other methods. *Journal of the Earth Sciences Application and Research Centre of Hacettepe University* 29:87-100.

Bales, Jennifer R., and Kenneth L. Kvamme (2005). Geophysical signatures of earthlodges in the Dakotas. In *Plains Earthlodges: Ethnographic and Archaeological Perspectives*, D.C. Roper and E.P. Pauls, eds., University of Alabama Press, Tuscaloosa, pp. 157-183.

Bartington Instruments (2013). *Operation Manual for MS2 Magnetic Susceptibility System*. Bartington Instruments. Electronic document http://www.bartington.com/operation-manuals.html, accessed April 1, 2013.

Benech, C., and E. Marmet (1999). Optimum depth of investigation and conductivity response rejection of the different electromagnetic devices measuring apparent magnetic susceptibility. *Archaeological Prospection* 6:31–45.

Bevan, Bruce W. (1998). *Geophysical Exploration for Archaeology: An Introduction to Geophysical Exploration*. Midwest Archeological Center Report No. 1, U.S. National Park Service, Lincoln, Nebraska.

Bowers, A.W. (1949). *A History of the Mandan and Hidatsa.* Unpublished Ph.D. dissertation, Department of Anthropology, University of Chicago.

Breiner, S. (1973). *Applications Manual for Portable Magnetometers*. Geometrics, Sunnyvale, California.

Burger, H. Robert, Anne F. Sheeehan, and Craig H. Jones (2006). *Introduction to Applied Geophysics: Exploring the Shallow Subsurface*. W.W. Norton, New York.

Burrough, Peter A., and Rachael A. McDonnell (1998). *Principles of Geographical Information Systems, 2nd edition*, Oxford University Press

Buteux, Simon, Vince Gaffney, Roger White, and Martijn van Leusen (2000). Wroxeter Hinterland Project and geophysical survey at Wroxeter. *Archaeological Prospection* 7:69-80.

Catlin, George (1973 [1844]). *Letters and Notes on the Manners, Customs, and Conditions of the North American Indians, Vol 1*. Reprinted by Dover Publications, New York.

Clark, Anthony (2000). *Seeing Beneath the Soil: Prospecting Methods in Archaeology, revised edition.* Routledge, London.

Clark University (2013). IDRISI Selva GIS and Image Processing Software. http://www.clarklabs.org/products/idrisi.cfm.

Clay, R. Berle (2006). Conductivity survey: a survival manual. In *Remote Sensing in Archaeology: An Explicitly North American Perspective*, edited by Jay K. Johnson, pp. 79-108. University of Alabama Press, Tuscaloosa.

Cole, M.A., N.T.Linford, A.W.Payne, and P.K.Linford (1995). Soil magnetic susceptibility measurements and their application to archaeological site investigation. In *Science and Site: Evaluation and Conservation*. J. Beavis ad K. Baker, eds., Bournemouth University School of Conservation Sciences Occasional Paper 1, pp. 144-162.

Crawford, George T., and Stanley A. Ahler (2003). Fortification trench investigations. In *Archaeological Investigations During 2001 and 2002 at Double Ditch State Historic Site, North Dakota*, edited by S.A. Ahler, pp. 95-114. Unpublished report by PaleoCultural Research Group, Flagstaff, Arizona, submitted to the State Historical Society of North Dakota, Bismarck.

Dalan, Rinita A. (2006a). Magnetic susceptibility. In *Remote Sensing in Archaeology: An Explicitly North American Perspective*, edited by Jay K. Johnson, pp. 161-203. University of Alabama Press, Tuscaloosa.

Dalan, Rinita A. (2006b). A geophysical approach to buried site detection using down-hole susceptibility and soil magnetic techniques. *Archaeological Prospection* 13:182-206.

Dalan, Rinita A. (2008). A review of the role of magnetic susceptibility in archaeogeophysical studies in the USA: recent developments and prospects. *Archaeological Prospection* 15:1-31.

Dalan, Rinita, and Dean Goodman (2007). Imaging buried landforms using down-hole susceptibility and three-dimensional GPR visualization software. *Archaeological Prospection* 14:273-280.

Desvignes, Guy, and Alain Tabbagh (1995). Simultaneous interpretation of magnetic and electromagnetic prospecting for characterization of magnetic features. *Archaeological Prospection* 2:129-139.

Eder-Hinterleitner, A., W. Neubauer, and P. Melichar (1996). Reconstruction of archaeological structures using magnetic prospection, In *Interfacing the Past, Computer Applications and Quantitative Methods in Archaeology CAA95, Vol 1*, edited by Hans Kamermans and Kelly Fennema, pp. 131-137, *Analecta Praehistorica Leidensia* 28.

Evans, Michael E., and Friedrich Heller (2003). *Environmental Magnetism*. Academic Press, Amsterdam.

Exploranium (1997). *User's Guide, KT-9 Kappameter, Rev. 1*. Exploranium, Mississauga, Ontario.

Fogel Aaron (2005). Investigating a Mississippian Mound Top Structure Utilizing Archaeogeophysics and Archaeology: a Three-Dimensional Application of Down-Hole Susceptibility Technology. Unpublished M.A. thesis, University of Mississippi, Oxford, Mississippi.

Gaffney, Chris, and John Gater (2003). *Revealing the Buried Past: Geophysics for Archaeologists*. Tempus, Stroud, Gloucestershire, England.

Gaffney, C., G. Hughes, and J. Gater (2004). Geophysical surveys at King Lobengula's Palace KoBulawayo, Zimbabwe. *Archaeological Prospection* 12:21-49.

Geonics Ltd. (2003). *EM38B Ground Conductivity Meter, Dual Output Version, Operating Manual*. Geonics Limited, Mississauga, Ontario.

Hays, W. L. (1988). *Statistics, 4th edition*. Holt, Rinehart and Winston, New York.

Heller, Andrew R. (2009). *New Interpretations of the Fort Clark State Historic Site Based on Aerial Color and Thermal Infrared Imagery*. Unpublished M.A. thesis, Department of Anthropology, University of Arkansas, Fayetteville.

Hunt, William J., Jr., ed. (2003). *Archeological Investigations at Fort Clark State Historic Site North Dakota: 1973-2003 Studies at the Fort Clark and Primeau Trading Posts*. PaleoCultural Research Group, Flagstaff, Arizona. Submitted to the State Historical Society of North Dakota, Bismarck.

Johnson, Jay K., ed. (2006). *Remote Sensing in Archaeology: An Explicitly North American Perspective*. University of Alabama Press, Tuscaloosa.

Jones, Geoffrey, and Gene Munson (2005). Geophysical Survey as an approach to the ephemeral campsite problem: case studies from the Northern Plains. *Plains Anthropologist* 50:31-43.

Kvamme, Kenneth L. (1999). Recent directions and developments in geographical information systems. *Journal of Archaeological Research*, 7(2):153-201.

Kvamme, Kenneth L. (2001). *Final Report of Geophysical Investigations Conducted at the Mandan/Arikara Village, Fort Clark State Historic Site (32ME2), 2000*. Submitted to the PaleoCultural Research Group, Flagstaff, Arizona, and the State Historical Society of North Dakota, Bismarck.

Kvamme, Kenneth L. (2003a). Geophysical surveys as landscape archaeology. *American Antiquity* 68:435-457.

Kvamme, Kenneth L. (2003b). *Geophysical Findings at the Double Ditch State Historic Site (32BL8), North Dakota, 2002*. Submitted to PaleoCultural Research Group, Flagstaff, Arizona, on file at the State Historical Society of North Dakota.

Kvamme, Kenneth L. (2003c). Multidimensional prospecting in North American Great Plains village sites. *Archaeological Prospection* 10:131-142.

Kvamme, Kenneth L. (2006a). Magnetometry: nature's gift to archaeology. In *Remote Sensing in Archaeology: An Explicitly North American Perspective*, edited by Jay K. Johnson, pp. 205-233. University of Alabama Press, Tuscaloosa.

Kvamme, Kenneth L. (2006b). Data processing and presentation. In *Remote Sensing in Archaeology: An Explicitly North American Perspective*, edited by Jay K. Johnson, pp. 205-233. University of Alabama Press, Tuscaloosa.

Kvamme, Kenneth L. (2006c). Integrating multidimensional geophysical data. *Archaeological Prospection* 13:57-72.

Kvamme, Kenneth L. (2007). Geophysical mappings and findings in Northern Plains village sites. In *Plains Village Archaeology: Bison-hunting Farmers in the Central and Northern Plains*, edited by Stanley A. Ahler and Marvin Kay, pp. 210-221. University of Utah Press, Salt Lake City.

Kvamme, Kenneth L. (2008a). Remote sensing: archaeological reasoning through physical principles and pattern recognition, In *Archaeological Concepts for the Study of the Cultural Past*, A.P. Sullivan III, ed. , pp. 65-84, University of Utah Press, Salt Lake City.

Kvamme, Kenneth L. (2008b). Archaeological prospecting at the Double Ditch State Historic Site, North Dakota, USA. *Archaeological Prospection* 15:62–79.

Kvamme, Kenneth L., and Stanley A. Ahler (2007). Integrated remote sensing and excavation at the Double Ditch State Historic Site, North Dakota. *American Antiquity* 72(3):539-561.

Linford, Neil (2006). The application of geophysical methods to archaeological prospection. *Reports on Progress in Physics* 69:2205-2257.

Maximilian, Prince of Wied (2010). *The North American Journals of Prince Maximilian of Wied*, edited by Stephen S. Witte and Marsha V. Gallagher, Vol. 2. University of Oklahoma Press, Norman.

Maximilian, Prince of Wied (2012). *The North American Journals of Prince Maximilian of Wied*, edited by Stephen S. Witte and Marsha V. Gallagher, Vol. 3. University of Oklahoma Press, Norman.

Mitchell, Mark D. (2012). Interim Report on Phase 1 Fieldwork, Geophysical Survey and Limited Archaeological Testing at Fort Clark State Historic Site (32ME2). PaleoCultural Research Group, Broomfield, Colorado.

Neubauer, Wolfgang (2001). *Magnetische Prospektion in der Archäologie.* Österreichischen Akademir der Wissenschaften, Vienna.

Payne, A. (1996). The use of magnetic prospection in the exploration of Iron Age hillfort interiors in southern England. *Archaeological Prospection* 3:163-184.

Ruud, Brandon K., ed. (2004). *Karl Bodmer's North American Prints*. University of Nebraska Press, Lincoln.

Scollar, Irwin (1990). *Archaeological Prospecting and Remote Sensing.* Cambridge University Press, Cambridge.

Swagerty, William R. (1988). Indian trade in the Trans-Mississippi West to 1870. In *Handbook of North American Indians*, vol. 4, edited by Wilcomb E. Washburn, *History of Indian-White Relations*, pp. 351-374. General editor, William C. Sturtevant. Smithsonian Institution, Washington.

Wiewel, Adam S. and Kenneth L. Kvamme (2013). The nineteenth-century Mandan/Arikara village at Fort Clark: results from a multi-instrument remote sensing investigation. In *Children of Mother Corn: The Sahnish in Archaeology, History, and Ethnography*, edited by Kacy L. Hollenback and Richard A. Krause. *Memoir, Plains Anthropologist, in press*.

Williams, Patrick Ryan, Couture, Nicole, and Deborah Blom (2007). Urban structure at tiwanaku: geophysical investigations in the Andean Altiplano. In *Remote Sensing in Archaeology*, edited by James R. Wiseman and Farouk El-Baz, pp. 423-441. Springer, New York.

Wood, W. Raymond (1980). Plains trade in prehistoric and protohistoric intertribal relations. In *Anthropology on the Great Plains*, edited by W. Raymond Wood and Margot Liberty, pp. 98-109. University of Nebraska Press, Lincoln.

Wood, W. Raymond (1993). Integrating ethnohistory and archaeology at Fort Clark State Historic Site, North Dakota. *American Antiquity* 58:544-559.

Wood, W. Raymond, Joseph C. Porter, and David C. Hunt (2002). *Karl Bodmer's Studio Art: The Newberry Library Bodmer Collection*. University of Illinois Press, Urbana.

Wood, W. Raymond, William J. Hunt, and Randy H. Williams (2011). *Fort Clark and its Indian Neighbors: A Trading Post on the Upper Missouri.* University of Oklahoma Press, Norman.